



British Geological Survey



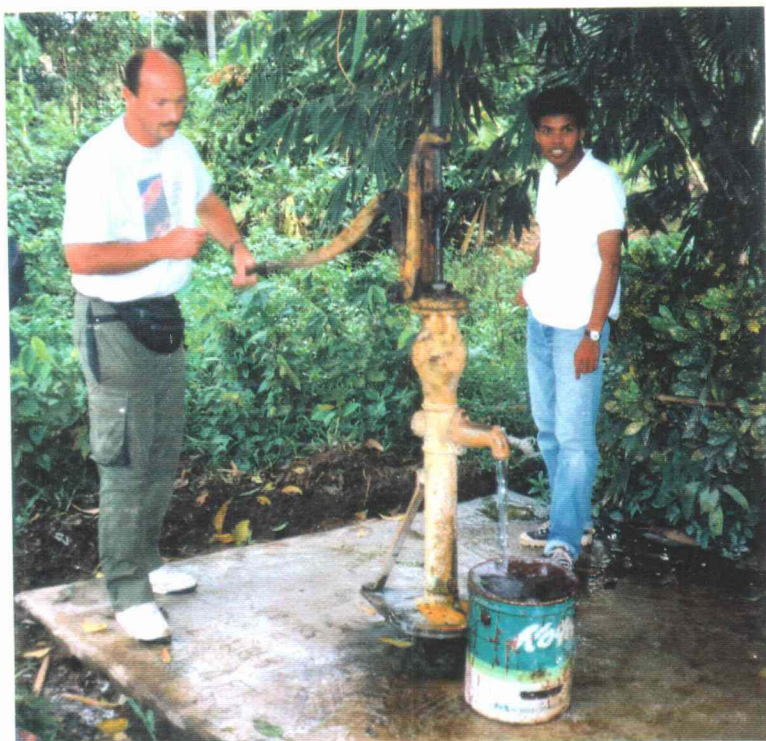
TECHNICAL REPORT WC/94/79
Overseas Geology Series

HYDROGEOCHEMISTRY OF ARSENIC IN AN AREA OF CHRONIC MINING-RELATED ARSENISM, RON PHIBUN DISTRICT, NAKHON SI THAMMARAT PROVINCE, THAILAND : PRELIMINARY RESULTS

F M FORDYCE¹, T M WILLIAMS¹, A PAIJITPRAPAPON² AND P CHAROENCHAISRI²

¹ British Geological Survey, Minerals and Geochemical Surveys Division, Keyworth, Nottingham, UK

² Department of Mineral Resources, Environment Division, Bangkok, Thailand



Natural
Environment
Research
Council

International Division
British Geological Survey
Keyworth
Nottingham
United Kingdom NG12 5GG



British Geological Survey

TECHNICAL REPORT WC/94/79

Overseas Geology Series

HYDROGEOCHEMISTRY OF ARSENIC IN AN AREA OF CHRONIC MINING- RELATED ARSENISM, RON PHIBUN DISTRICT, NAKHON SI THAMMARAT PROVINCE, THAILAND : PRELIMINARY RESULTS

F M FORDYCE¹, T M WILLIAMS¹, A PAIJITPRAPAPON², AND
P CHAROENCHAISRI²

¹ British Geological Survey, Minerals and Geochemical Surveys Division, Keyworth, Nottingham, UK

² Department of Mineral Resources, Environment Division, Bangkok, Thailand

A report prepared for the Overseas Development Administration under the
ODA/BGS Technology Development and Research Programme, Project 92/6

ODA classification :

Subsector: Geoscience

Theme: G2 - Identify and ameliorate minerals-related and other geochemical toxic hazards

Project title: Environmental impact of gold and complex sulphide mining

Reference number: R5553

Bibliographic reference :

Fordyce F M and others 1995. Hydrogeochemistry of arsenic in an area of chronic mining-related arsenism, Ron Phibun District, Nakhon si Thammarat Province, Thailand : preliminary results
BGS Technical Report WC/94/79

Keywords :

Mining, arsenic, hydrogeochemistry, toxicology, mine drainage, Thailand

Front cover illustration :

Hand-pumping deep aquifer groundwater from a village well in Ron Phibun District prior to collecting a water sample

© NERC 1995

Keyworth, Nottingham, British Geological Survey, 1995

EXECUTIVE SUMMARY

Approximately 50% of all naturally occurring elements can be toxic to plants, animals or humans if ingested in excess. Arsenic, a particularly toxic metalloid element, can be assimilated by humans through several pathways including drinking water, consumption of contaminated plant or animal tissues and inhalation of As-bearing particulates from the atmosphere. Arsenic exists in two common states in nature, the As(III) state is considered to be an order of magnitude more toxic than the As(V) state. The effects of acute As poisoning include gastrointestinal irritation, depressed nerve response and cardiovascular failure. Several additional disorders are known to occur in response to prolonged exposure to enhanced environmental As levels, the most common of which are skin lesions, hyper-pigmentation, skin cancer, and a range of internal carcinomas (mainly of the liver, bladder and kidneys).

This report outlines the results of a collaborative study of mining-related arsenic contamination undertaken by the British Geological Survey (BGS) and the Government of Thailand Department of Mineral Resources (DMR) in Ron Phibun District, Nakhon si Thammarat Province, southern Thailand. Health problems attributable to As toxicity in the area were first recognised in 1987 when a resident was diagnosed as suffering from arsenical skin cancer. Subsequent investigations by the Government of Thailand Department of Health have confirmed that the main cause of exposure is contaminated groundwater, in which As concentrations of up to 100 times the WHO interim As guideline (10 µg/l) occur. In 1988, the population 'at risk' was estimated to number 15 000, with over 1000 recorded cases of deleterious skin disorders attributable to chronic arsenism.

Ron Phibun District is located 800 km south of Bangkok in peninsular Thailand. The District lies in the Main Range Province of the South-east Asian 'tin belt', a zone of tin (Sn) and tungsten (W) mineralisation related to Triassic granitoid intrusions implaced in a Cambro-Ordovician sedimentary sequence. Primary Sn-W-As mineralisation and alluvial 'placer' tin deposits have been mined in the district for approximately 100 years, although only two dredging operations are currently active. This activity has left a legacy of physical disturbance and a range of mining-related waste products including (i) high-grade arsenopyrite waste piles derived from mineral separation activities at bedrock mining sites, (ii) waste from two ore dressing plants near Ron Phibun town, (iii) disseminated waste from small-scale panning and flotation activities undertaken by local villagers. Of these sources, the arsenopyrite waste piles have, to date, generally been considered to form the most likely source of surface and groundwater As contamination and a proposal to seal this material in an impermeable landfill has been developed by the Thai authorities. The potential cost of this plan is, however, considerable and the precise importance of the waste piles as a regional contaminant source has not yet been established.

In 1994, preliminary geochemical and hydrogeochemical sampling was carried out in the Ron Phibun area by the BGS (in collaboration with DMR) as part of a more extensive ODA-funded study of toxic trace element dispersal around mine sites in tropical countries (ODA Project R5553). The project forms part of the ODA/BGS Technology Development and Research (TDR) programme of international aid. The main aims of the project are (i) to establish the geological, climatic and technological controls on the release of potentially harmful elements (PHE's) during mining with particular reference to As; (ii) to model PHE dispersal and bioassimilation pathways and (iii) to formulate practical, cost effective pollution abatement and site remediation methods.

Mineralogical studies of high-grade arsenopyrite waste from two former bedrock mining localities were undertaken to assess the potential of this material as a source of surface and groundwater As contamination. X-ray fluorescence (XRF) data for the waste suggest that the total As content may be as high as 30%. Examination of different grain size and density fractions of the waste material showed that primary sulphides such as arsenopyrite hold only a small component of the total As burden, with the majority of the As residing in secondary

arsenate minerals, notably scorodite ($\text{FeAsO}_4 \cdot 2\text{H}_2\text{O}$). These secondary phases are relatively insoluble and are considered likely to release As into natural waters extremely slowly.

A hydrogeochemical survey of surface waters within and downstream of the bedrock and alluvial mining areas was undertaken, involving the collection of water from some 25 sampling sites. The bedrock mining areas were found to be characterised by acid waters pH (<6), sulphate (SO_4) anion domination and high levels of trace metals such as Al, Cd and Zn (maximum = 10507 $\mu\text{g/l}$, 247 $\mu\text{g/l}$ and 4193 $\mu\text{g/l}$ respectively). Values for Al and Cd significantly exceed the WHO guideline levels of 200 $\mu\text{g/l}$ Al and 5 $\mu\text{g/l}$ Cd. The high levels of trace metals in these waters reflect increased element mobility in acid conditions and breakdown of soluble sulphate and carbonate minerals. The levels of trace metals decline as the pH of surface waters rises downstream of the bedrock mining area (due to buffering over alluvium and carbonate lithologies). In contrast, As concentrations in the headwaters of the mine impacted Hai Ron Na catchment are low (66-208 $\mu\text{g/l}$) relative to the sub-regional average. These results support mineralogical evidence acquired for the bedrock mining areas which suggests that the As in high-grade mine waste is not readily soluble. The highest As concentrations (maximum 583 $\mu\text{g/l}$) in surface waters occur 2-7 km downstream of the bedrock mining area. It is possible that these high values are associated with another source of As related to the alluvial mineral deposits. However, As concentrations in surface waters draining the alluvial mining areas outwith the Hai Ron Na catchment are relatively low (< 100 $\mu\text{g/l}$).

Groundwater hydrogeochemistry assessments were carried out at house-hold wells supplied by water from a shallow alluvial aquifer (<15m) and at DMR borehole pumps which extract water from a deeper (>15m) carbonate aquifer. Highest total As concentrations (maximum = 5114 $\mu\text{g/l}$) in shallow wells were recorded in villages in the Hai Ron Na catchment and Ron Phibun town. Sixteen of the 23 shallow wells sampled contained As levels above the 10 $\mu\text{g/l}$ WHO guideline. In contrast, only two of the 13 deeper boreholes had As concentrations above this threshold. While there is no clear relationship between total As concentration and pH conditions, analytical As speciation determinations show a marked increase in As(III) concentrations in the reducing environment prevalent in some of the deeper boreholes. The increased As(III) levels (maximum = 39% total As) in some boreholes is of concern, as As(III) is considerably more toxic than As(V).

Soil XRF data indicate the presence of up to c. 5000 $\mu\text{g/g}$ As in alluvial soils in the Hai Ron Na catchment, whereas soils to the east of Ron Phibun town yielded <100 $\mu\text{g/g}$. Sequential extraction data show that only 20% of the total As burden is bound to crystalline Fe-oxides. The remainder is assumed to be held as detrital sulphides suggesting that the soils overlying both bedrock and alluvial mining areas may hold a substantial reservoir of arsenopyrite. Further investigations are required to confirm the presence of arsenopyrite in the soils of the alluvial plain. If proved, these soils could constitute a major potential source of As in the area.

Given the relatively low concentrations of As recorded in the headwaters of the Hai Ron Na (close to the bedrock mining area), it is difficult to envisage that the high-grade As-rich waste piles constitute the principal source of surface and groundwater contamination because surface drainage is the only plausible mechanism by which recharge water from the bedrock mining area could be carried to the shallow or carbonate aquifers of the alluvial plain. It would appear from the high As values recorded in the vicinity of the ore dressing plants (and nearby small-scale prospecting activities) that waste from these activities probably constitutes a major source of As contamination. Further investigations are, however, required to evaluate fully the influence that these sources exert on local geochemical conditions. The contribution of alluvial deposits to As contamination is less clear. High As values were recorded in alluvial soil in the Hai Ron Na catchment but further soil studies are required to determine the extent of As contamination in the area. It is possible that As mobility is significantly enhanced in the Fe-poor alluvial material in the absence of scavenging by Fe-oxides. Detailed investigations into the mineralogy and multi-element chemistry of the alluvium are required to confirm these findings.

The epidemiological data collected by the Thai authorities for Ron Phibun District indicate a district-wide skin lesion incidence of > 20%, rising to over 90% in the immediate vicinity of Ron Phibun town. These incidence levels appear to be consistent with epidemiological data from other parts of the world where similar problems occur. Data obtained in this study show that shallow groundwater concentrations in the most contaminated wells fall within the 4000 - 6000 µg/l range generally considered likely to induce visible arsenism symptoms in a majority of the population. However, many of the wells in Ron Phibun area contain 100 - 200 µg As and considerable uncertainties exist in the interpretation of exposures of this magnitude. 'Secondary' factors, which are relatively unimportant at very high (> 1000 µg/l) As concentrations, become critical in areas with water supply concentrations of < 200 µg/l As. In assessing As toxicity at Ron Phibun, it is vital that these secondary influences, including As speciation, effects of other trace elements, population behavioural patterns and alternative (ie. non water) exposure pathways are evaluated. Such factors may be of fundamental importance in the derivation of a toxicologically acceptable threshold for potable water in the area.

Any future strategy for improved pollution control at Ron Phibun should account for the following characteristics of the site:

- (i) Intense acid mine drainage is not a major factor controlling As mobility.
- (ii) Dissolved Fe concentrations are lower than those normally associated with mine drainage.
- (iii) Arsenic is the principal aqueous contaminant, occurring primarily as oxyanionic species which are mobile over a wide pH range therefore conventional decontamination methods involving pH regulation are inappropriate.
- (iv) The suitability of physical removal and containment; bioremediation and chemical removal techniques should be investigated.

CONTENTS

1.	INTRODUCTION	1
1.1	Background	1
1.2	Arsenic geochemistry and toxicology	2
1.2.1	Physical chemistry & geochemistry	2
1.2.2	Hydrogeochemistry	3
1.2.3	Soil chemistry	5
1.2.4	Toxicology and human exposure	5
1.3	Ron Phibun District	8
1.3.1	History of the As toxicity problem	8
1.3.2	Physiography	8
1.3.3	Geology	11
1.3.4	Mineralisation and mining	11
1.3.5	Hydrogeology	13
1.4	Previous investigations	15
1.4.1	Medical and epidemiological studies	15
1.4.2	Geological and geochemical studies	17
1.4.2.1	Contaminant sources	17
1.4.2.2	Surface waters	17
1.4.2.3	Groundwaters	18
1.4.2.4	Sediment and soils	19
1.4.3	Problem alleviation	19
2.	CURRENT INVESTIGATION	20
2.1	Waste characterisation	20
2.1.1	Tailings characteristics	20
2.1.2	High grade waste characteristics	23
2.1.3	General mineralogical observations	25
2.2	Hydrogeochemistry	27
2.2.1	Methodology	27
2.2.2	Surface waters	29
2.2.2.1	pH, Eh and conductivity	29
2.2.2.2	Total arsenic	33
2.2.2.3	Analytical As speciation	33
2.2.2.4	Major anions	33
2.2.2.5	Major cations	36
2.2.2.5	Minor and trace elements	36
2.2.3	Groundwaters	37
2.2.3.1	pH, Eh and conductivity	37
2.2.3.2	Total arsenic	39
2.2.3.3	Analytical As speciation	41
2.2.3.4	Major anions	44
2.2.3.5	Major cations	44
2.2.3.5	Minor and trace elements	46
2.3	Geochemical modelling	47
2.3.1	Methodology	47
2.3.2	Modelled As speciation	48
2.3.3	Modelled surface water hydrogeochemistry	50
2.3.4	Modelled groundwater hydrogeochemistry	51

2.4	Arsenic pedogeochemistry	53
2.4.1	Methodology	53
2.4.2	Results	53
3.	DISCUSSION	54
3.1	Mechanisms of surface and groundwater contamination	54
3.1.1	High grade waste piles	54
3.1.2	Alternative sources of As contamination	55
3.2	Toxicological aspects of arsenic contamination at Ron Phibun.	56
3.3	Mitigation potential	58
3.3.1	Physical removal of arsenopyrite waste	59
3.3.2	Bioremediation	59
3.3.3	Chemical removal	59
4.	CONCLUSIONS and FUTURE PRIORITIES	60
5.	ACKNOWLEDGEMENTS	61
6.	REFERENCES	62
	APPENDIX 1: List of Arsenic Minerals	65

LIST OF FIGURES

- Figure 1. Eh-pH diagram for the system As-S-O-H.
- Figure 2. Sources and pathways of As to man via the food chain.
- Figure 3. Map of the granite provinces of South-east Asia showing the location of Ron Phibun District.
- Figure 4. Location of the fourteen village areas in Ron Phibun District.
- Figure 5. View from arsenopyrite waste pile 6 in the Ron Na-Suang Chan Mountains across Ron Phibun town and the alluvial plain.
- Figure 6. The geology of Ron Phibun District.
- Figure 7. Surface water pH values recorded at sites RPW1-26 in Ron Phibun District, August 1994.
- Figure 8. Groundwater flow paths in Ron Phibun District.
- Figure 9. XRD trace of the < 20 μm fraction of tailings sample RPT2.
- Figure 10. XRD trace of the < 10 μm fraction of tailings sample RPT1A.
- Figure 11. Magnified photograph of (a) scorodite and sulphur grains and (b) arsenopyrite from tailings sample RPT1A.
- Figure 12. Photograph and sketch of selected grains and coatings from tailings sample RPT1A.
- Figure 13. 'Piper diagram' showing major cation, anion and TDS characteristics of Ron Phibun surface waters.
- Figure 14. Arsenic concentrations in surface waters recorded at sites RPW1-26 in Ron Phibun District, August 1994.
- Figure 15. Shallow groundwater pH values recorded at sites RPSW1-23 in Ron Phibun District, August 1994.
- Figure 16. Co-variation of redox parameters and borehole depth in the carbonate aquifer at deep groundwater sites RPDW1-13, Ron Phibun District.
- Figure 17. Arsenic concentrations in shallow groundwaters recorded at sites RPSW1-23 in Ron Phibun District, August 1994.
- Figure 18. Arsenic concentrations in deep groundwaters recorded at sites RPDW1-13 in Ron Phibun District, August 1994 and location of soil samples RPS1-4.
- Figure 19. 'Piper diagram' showing major cation, anion and TDS characteristics of Ron Phibun shallow groundwaters.
- Figure 20. 'Piper diagram' showing major cation, anion and TDS characteristics of Ron Phibun deep groundwaters.

- Figure 21.** Eh-pH diagram for the system Mn-O-H.
- Figure 22.** Modelled As speciation in surface drainage samples RPW 2, 11 and 17 and deep groundwaters RPDW 1 and 7.
- Figure 23.** Modelled Fe speciation in surface drainage samples RPW 2, 11 and 17 and deep groundwaters RPDW 1 and 7.

LIST OF TABLES

- Table 1. Average As contents of certain media.
- Table 2. Arsenic concentration in selected normal adolescents and shallow well waters in Ron Phibun District.
- Table 3. Prevalence of clinical symptoms of arsenism in selected members of the population in Ron Phibun District, 1994.
- Table 4. Arsenic contamination in selected surface waters in Ron Phibun District (monitored by DMR between 1992 and 1994).
- Table 5. Arsenic concentrations in selected shallow groundwaters in Ron Phibun District (monitored by DMR between 1991 and 1994).
- Table 6. Grain size and gravimetric partitioning of As in Ron Phibun tailings sample RPT2.
- Table 7. Grain size and gravimetric partitioning of selected trace elements in Ron Phibun tailings sample RPT2.
- Table 8. List of mineral phases identified by electron microprobe analysis from tailings sample RPT1A.
- Table 9. Practical detection limits for all elements and ions determined in water samples.
- Table 10. Physio-chemical data for surface water samples RPW1 - RPW26, Ron Phibun District.
- Table 11. Physio-chemical data for shallow groundwater samples RPSW1 - RPSW23, Ron Phibun District.
- Table 12. Physio-chemical data for deep groundwater samples RPDW1 - RPDW13, Ron Phibun District.
- Table 13. Pearson correlation matrix of determinands in surface waters, Ron Phibun District.
- Table 14. Pearson correlation matrix of determinands in shallow groundwaters, Ron Phibun District.
- Table 15. Pearson correlation matrix of determinands in deep groundwaters, Ron Phibun District.
- Table 16. Results of sequential extraction of As in soils from Ron Phibun District.

1. INTRODUCTION

1.1 Background

Under certain circumstances, several naturally occurring elements can be harmful to plants, animals or humans. These **potentially harmful elements** (PHE's) include toxic metals (and metalloids) such as Cd, Pb and Hg, which have no clear biological function. In addition, some 30 elements (for example As, Cu, Zn and Se) are considered essential for human and animal health in small doses, but can be toxic in excess. The human body is exposed to PHE's via several pathways including, inhalation from the atmosphere, ingestion of drinking water, soil ingestion and consumption of plant or animal tissues which have accumulated PHE's through the food chain. The adverse effects of toxic levels of PHE's in humans have been well documented (eg. Mertz, 1987) and include carcinogenesis, skin diseases, neurological problems, bone disorders and the malfunction of several vital organs.

A diverse range of PHEs (including As, Sb, Pb, Zn, Cd, Cu, Ni, Co, Cr, U) are routinely enriched in areas of metalliferous mineralisation and are subject to mobilisation and dispersal by mining and mineral processing activities. The toxicological risk associated with elevated concentrations of these elements in the environment is dependent on several factors, including their chemical form, the precise exposure pathway and the dose received. The mobility and bioavailability of PHEs is also influenced by ambient environmental or physiographical factors such as climate, pH/Eh regime (of soil or water) and the type of vegetation cover.

In 1992 the British Government Overseas Development Administration (ODA) provided funding for a detailed investigation of the geochemical impacts of gold and complex sulphide mining in tropical regimes (Project R5553) as a part of a long-standing ODA-British Geological Survey (BGS) Technology Development and Research (TDR) programme of international aid. The main aims of the project are: (i) to establish the geological, climatic and technological controls on the release of PHE's during mining with particular reference to As; (ii) to model PHE dispersal and bioassimilation pathways and (iii) to formulate practical, cost effective pollution abatement and site remediation methods.

During the period 1992-1994, case-studies of some 50 gold and base metal mining operations in a variety of geological/metallogenic settings were undertaken in Malaysia, Zimbabwe and the Philippines. In 1994 the project was extended to include an area of As contamination associated with former Sn-W mining at Ron Phibun, southern Thailand. Preliminary geochemical sampling at Ron Phibun was undertaken during August 1994 in close liaison with staff of the Government of Thailand, Department of Mineral Resources

(DMR). This report details the results of this preliminary survey and highlights the extent of the problem at Ron Phibun with particular emphasis on (i) the distribution and geochemistry of As in surface drainage, shallow groundwaters and deep groundwaters, (ii) toxicological implications and (iii) possible options for site remediation.

1.2 Arsenic Geochemistry and Toxicology

1.2.1 Physical Chemistry and Geochemistry

Arsenic is a naturally occurring element present in rocks, soils, water, the atmosphere, plants, animals and man. A metalloid (semi-metal) element of Group V of the periodic table, As occurs at a relatively low average crustal abundance of 1800 µg/kg, ranking 51st of all naturally occurring elements (Greenwood and Earnshaw 1984). Table 1 lists some average As concentrations in various media.

Table 1. Average As contents of certain media.

Media	Average As µg/kg	Reference
Basaltic Rocks	1500	Royal Society of Chemistry, 1982
Gabbroic Rocks	1400	“
Granitic Rocks	1500	“
Shale	13000	“
Sandstone	1000	“
Phosphate Rocks	21000	“
Soils	11300	“
Surface Waters	1-10 µg/l	Fergusson, 1990
Oceans	20 µg/l	Boyle and Joansson, 1973
Marine Plants	2600	“
Marine Animals	1000	“
Human Hair	650	Mertz, 1986
Human Organs	20	“

In the natural environment As occurs in a variety of mineral forms, principally as discrete sulphides, arsenides, arsenates and oxides. A comprehensive list of As-bearing minerals (compiled by the British Natural History Museum, Department of Mineralogy) is provided in Appendix 1.

Arsenic possesses four valency states ranging from -3 to +5. The least common is the (-3) state, which forms the gaseous compound arsine (AsH₃), stable only at extremely low redox potentials (around -1V). Native arsenic occasionally precipitates from hydrothermal fluids under acutely alkaline-reducing conditions. The trivalent (+3) and pentavalent (+5) states dominate under most surface environment conditions.

Arsenic is strongly chalcophile, and sulphides such as realgar (As_4S_4) and orpiment (As_2S_3) are the favoured 'mono-metallic' primary mineral phases under most pH-Eh conditions. The most commonly occurring As mineral is the iron-arsenic sulphide arsenopyrite (FeAsS) which is frequently associated with ore deposits of Au, Cu, Sn, W, Ag, Zn and Pb. In many ore assemblages, mixed sulphides such as enargite (Cu_3AsS_4) and gersdorffite (NiAsS), and arsenides of Co and Fe are also common. The principal carrier of As in many sulphide ores is pyrite (FeS_2), in which up to 0.5% As may be present through lattice substitution for sulphur.

Several secondary As minerals are derived from the low temperature alteration of sulphides such as arsenopyrite and realgar. Hydrous arsenates and sulpharsenates, notably scorodite ($\text{FeAsO}_4 \cdot 2\text{H}_2\text{O}$) and beudantite ($\text{PbFe}(\text{AsO}_4)(\text{SO}_4)(\text{OH})_6$), are the most common secondary As minerals. Oxides such as arsenolite (As_2O_3) have also been noted as coatings on FeAsS surfaces in disseminated sulphide deposits, and on native As (e.g. Breward and Williams, 1994).

1.2.2 Hydrogeochemistry

The concentration of As in unpolluted fresh waters typically ranges from 1 to 10 $\mu\text{g/l}$ (Table 1), rising to 100 to 5000 $\mu\text{g/l}$ in areas of sulphide mineralisation and mining. The aqueous chemistry of As differs significantly from that of most true metals. Binary compounds either react with water, or are insoluble. At moderate or high redox potentials, As can be stabilised as a series of pentavalent (arsenate) oxyanions: H_3AsO_4 (pH < 3 Eh > 500 mV), H_2AsO_4^- (pH 3-7 Eh > 250 mV), HAsO_4^{2-} (pH 7-12, Eh > -300 mV) and AsO_4^{3-} (pH > 12 Eh > -600 mV). However, under most reducing (acid and mildly alkaline) conditions, the trivalent arsenite species (H_3AsO_3) predominates. At extremely low Eh values and under alkaline conditions, AsO_2^- forms a stable aqueous phase (Figure 1). Disequilibrium between inorganic As species in natural waters is common due to kinetic constraints on As(III) and As(V) transformations. Fergusson (1990) has reported the persistence of arsenite for several weeks in oxic marine and (near-neutral) lake waters, following transport from deeper anoxic waters by seasonal currents or thermal overturn.

Arsenic forms stable bonds with carbon to yield a range of alkyl/methyl species and associated salts. Their contribution to the total As budget of natural waters is, however, usually small (<10%, Andreae 1986). Methyl As species are mainly produced by microbial metabolism of inorganic species (S-adenosylmethionine constituting the most common As methylation agent), although abiotic methylation reactions are also known (Abernathy, 1993). In fresh water, the dominant phases are monomethyl and dimethyl compounds: $\text{CH}_3\text{H}_2\text{AsO}_3$ (monomethylarsonic acid) and $(\text{CH}_3)_2\text{HAsO}_2$ (dimethylarsinic acid).

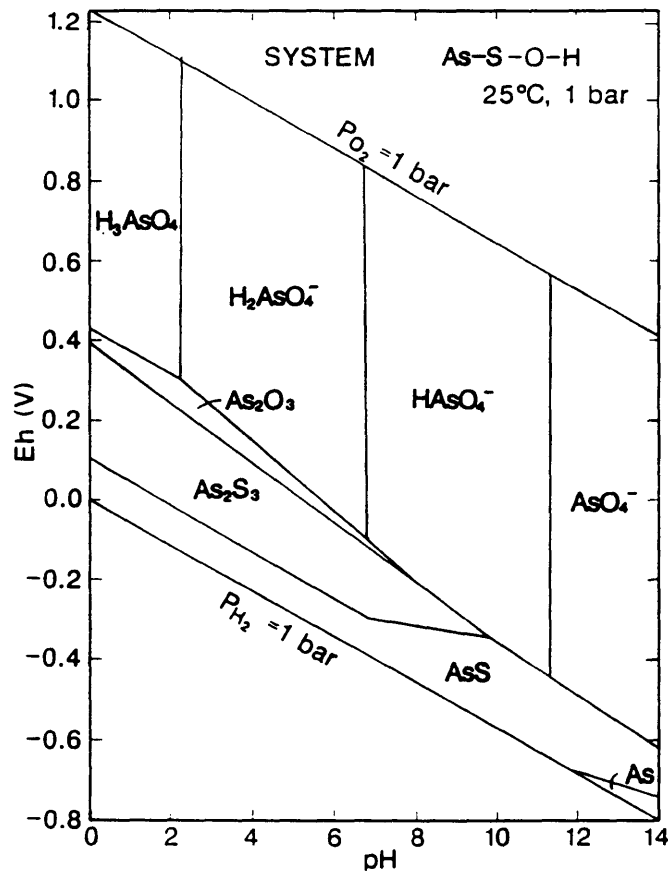


Figure 1. Eh-pH diagram for the system As-S-O-H (from Brookins, 1988).

The retention of As in solution is constrained by co-precipitation with elements such as Fe, Ba, Co, Ni, Pb and Zn, of which Fe and Ba are particularly important due to their low arsenate solubility products. Colloidal reactions may be involved in the precipitation of scorodite (signified by the common occurrence of green gel coatings on FeAsS-rich detritus). The sorption of As by hydrous oxides (or related gel complexes), clays and humic organics has been widely documented (e.g. Pierce and Moore 1982). The relative efficiency with which individual As species are sorbed to amorphous oxides is pH dependent, but generally decreases from arsenate through organoarsenic species to arsenite (Bowell 1994). Hydrous Fe oxide gels and colloids are particularly instrumental in scavenging As oxyanions, due to their strong positive charge characteristics across a wide pH range (Boyle and Jonasson 1973).

1.2.3 Soil chemistry

In soils, the normal concentration range for As is 100 to 40 000 $\mu\text{g}/\text{kg}$ (Ure and Berrow 1982), rising to $>500\ 000\ \mu\text{g}/\text{kg}$ over many sulphide ore deposits (e.g. Williams et al. 1994). Although geology exerts the primary control on As concentrations in soils, significant contributions can also come from atmospheric deposition of dust from industrial process such as coal burning and metal smelting and from As-based pesticides (Royal Society of Chemistry, 1982). The enhancement of soil As by phosphate fertilizers and sewage sludges has also been widely reported (e.g. Fergusson 1990). In free draining profiles, As resides predominantly as arsenate (AsO_4) and is extensively sorbed to clays and ferric oxides. Arsenates of Fe and Al, the dominant phases in acid soils, exhibit low solubility relative to $\text{Ca}_3(\text{AsO}_4)_2$, which dominates in many calcareous soils. The mobility of As in oxic soils is thus strongly influenced by Fe content and pH. In anaerobic soils, As may be mobilised and leached through bacterial or abiotic reduction of AsO_4 compounds to soluble arsenite salts.

Down-profile As distributions vary markedly in accordance with the local soil regime. Adriano (1986) suggested that As is enriched in the surficial levels (upper 20 cm) of unpolluted temperate soils. Similar profiles in freshwater sediments have been ascribed to sub-surface anoxia and the resultant leaching of reduced species (e.g. Farmer and Lovell 1986). However, Bowell (1993) has shown that enrichment of As in the O/A horizon of rain-forest soils in Ghana can be related to complexation with organic matter. Soil profiles with maximum As concentrations in the B horizon, or in the interfacial saprolite, have been reported from gold mining localities in Malaysia (Williams et al. 1994). In these instances, the As distribution correlates closely with the concentration of fine-grained ferric oxide.

1.2.4 Toxicology and human exposure

The main pathways through which As in the environment enters the human body are summarised in Figure 2. The accumulation of As in plants grown on As-polluted soils may be a potential health hazard to man through the food chain, although vegetation may impede exposure to As in soil as it does not move readily from the roots and stem to the leaves. Many plant species assimilate very little As, as they themselves are poisoned by it (Crounce, 1983). However, some species, for example *Pseudotsuga taxifolia* (Douglas Fir) have been shown to act as As accumulators in areas of high soil As content (Porter and Peterson 1975; Warren et al. 1968). Fish and shellfish typically contain high levels of As, usually in the form of organic-As compounds, which are apparently of very low toxicity to man (Crounce 1983).

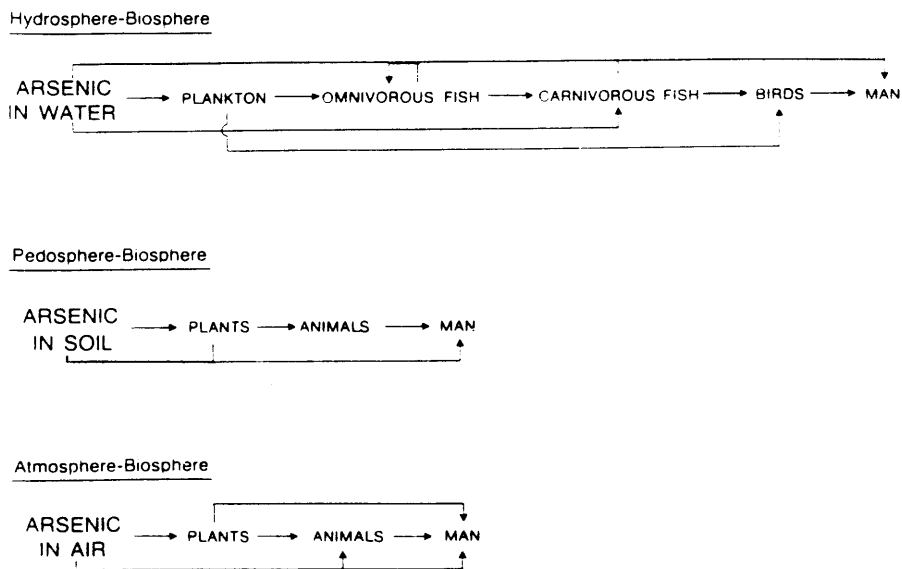


Figure 2. Sources and pathways of As to man via the food chain (modified from Boyle and Jonasson, 1973)

Arsenic is a normal component of the human diet. Concentrations of As in grain, meat and vegetables lie in the ranges 10-200 $\mu\text{g}/\text{kg}$ with substantially higher values (approximately 1000 $\mu\text{g}/\text{kg}$ present in most seafood; Fergusson 1990). The US-EPA has estimated an average As intake of 53 $\mu\text{g}/\text{day}$ for US citizens, of which up to 80% may be organoarsenic (derived from fish, shellfish and vegetables) and 20% is in inorganic form (derived from meat and grain; Abernathy 1993). In uncontaminated areas, the average ingestion of As via drinking water is around 5 $\mu\text{g}/\text{day}$ (Fergusson 1990).

Inorganic As is one of the oldest known poisons to man and is toxic to most animals. The main sources of chronic As poisoning documented in the past include exposure to dust from industrial processes; exposure to As-based pesticide sprays, contamination of food and water supplies and use of medicines or cosmetics enriched in As (Fergusson 1990). Soluble inorganic As species are readily absorbed in the gastrointestinal tract and are generally considered 100% bioavailable for purposes of risk assessment calculation (Chaney et al. 1993). In contrast, *in vivo*, *in vitro* and mineralogical assessments of particulate As in soil and mine waste (e.g. Chaney et al. 1993; Tsuji 1993; Davis and Ruby 1993) indicate relatively low bioavailabilities (<10%). For populations not subject to occupational exposure, dietary ingestion (including drinking water) is thus more significant than inhalation as a mechanism for As intake.

Chronic As poisoning particularly affects the skin, mucous membranes, nervous system, bone marrow, liver and heart. A detailed review of human effects of As ingestion has been provided by Abernathy (1993). Acute oral exposure typically induces gastro-intestinal irritation, loss of peripheral nerve response and, ultimately, cardiovascular failure. The estimated lethal dose in adults is 70-180 mg.

Examples of chronic As poisoning associated with regionally contaminated water have been documented from numerous countries including Taiwan (Tseng et al. 1968; Chen et al. 1988), India (Chakraborty and Saha 1987), Mexico (Espinoza, 1963; Cebrian et al. 1983) and Chile (Borgono et al. 1980). The characteristic effects of long-term consumption of water containing $>50\text{-}1000\ \mu\text{g/l}$ are hyperkeratosis, hyperpigmentation, malignant melanoma and peripheral arteriosclerosis (Blackfoot disease). The role of As exposure in the development of bladder, liver and kidney cancers (notably, unique to humans) has recently been highlighted through clinical (e.g. Sasieni and Cuzick 1993) and epidemiological (e.g. Chen 1992) studies. Arsenic occurs throughout the body, but tends to be concentrated in the hair and nails during chronic As exposure (hence the use of these media to determine human As exposure in epidemiological studies).

Arsenic toxicity is strongly dependent on chemical form. The arsene gas state exhibits the greatest toxicity, whereas the more commonly occurring forms decrease in toxicity by approximately an order of magnitude through each stage of the sequence $\text{As(III)} > \text{As(V)} > \text{methyl-As}$ (Abernathy 1993; Chen et al. 1994). In most fauna, As(III) toxicity results from reactions with thiol (HS^-) groups to form stable thio-As derivatives. Many key cellular proteins contain free thiol groups. Hence, reaction with As(III) can lead to a loss of protein function. Arsenate toxicity is manifested via reduction to As(III) , and through substitution for phosphate in normal cellular reactions.

Mammals possess variable abilities to detoxify inorganic As through a sequence of reduction of As(V) to As(III) , methylation and excretion via the kidneys. Reduction of As(V) to As(III) is necessary, as the enzymes responsible for methylation appear to require As(III) as a substrate on which to attach the methyl group. In humans, inorganic As is metabolized to form monomethylarsonic acid (MMA) and dimethylarsenic acid (DMA) whereas in most other mammals DMA is the main metabolite (Buchet and Lauwerys 1993; Vahter 1993). Neither MMA nor DMA binds strongly to biological molecules in mammals therefore methylation is an important detoxification mechanism. There is some evidence to suggest that the dose response curve for As is non-linear and that adverse health effects (such as occur in areas of high As exposure) become disproportionately pronounced once the methylation potential of the body has been saturated (US-EPA, 1993).

Current UK, US-EPA and EC standards for As in potable waters stand at $50\ \mu\text{g/l}$, although a future reduction of the US-EPA threshold is anticipated in response to evidence of chronic impacts at lower exposures (e.g. Chen et al 1992). An international interim guideline of $10\ \mu\text{g/l}$ has recently been adopted by the WHO (Van Leeuwen, 1993).

1.3 Ron Phibun District

1.3.1 History of the As-toxicity problem

Health problems attributable to As toxicity in Ron Phibun District, Nakhon si Thammarat Province, southern Thailand, were first recognised in 1987 when a resident was diagnosed as suffering from arsenical skin cancer following referral to the Institute of Dermatology in Bangkok. The condition was initially ascribed to the use of Chinese medicine, but subsequent investigations rapidly confirmed that As exposure was related to contaminated shallow groundwater in the Ron Phibun area.

Following widespread national media coverage and attendant public concern, detailed medical and epidemiological investigations were initiated (involving government and NGO personnel) to establish the size of the affected population, its geographic distribution and the precise sources of As contamination. In 1988, the population 'at risk' was estimated at 15,000, with over 1000 recorded cases of deleterious skin disorders directly attributable to chronic arsenism.

Since 1988, the DMR has been engaged in research to assess the sources of As contamination at Ron Phibun, and its distribution in surface waters and aquifers. The Thai government has recently given 5 million baht (£135 000) to DMR for remediation work to resolve the problem, but the optimum solution has yet to be identified.

1.3.2 Physiography

Ron Phibun District lies approximately 800 km south of Bangkok in Nakhon si Thammarat Province, southern Thailand (Figure 3). Ron Phibun is the main town within the district, which is split into 14 village areas (Figure 4). To the west, the Khao Luang mountain range forms a mountainous backbone to peninsular Thailand, extending north-south in a series of en echelon ridges and sub-ranges. Ron Phibun lies at the foot of the Ron Na-Suang Chan sub-range, a densely vegetated area of steep relief rising to 1000 m. To the east, a flat alluvial plain, characterised by low-lying marshy ground and heavily cultivated with rubber plantations and rice paddies, extends to the Gulf of Thailand coast (Figure 5).

Soils are poorly developed in the rocky terrain of the Ron Na-Suang Chan sub-range. Where present they consist of an organic rich (dark brown) 'A' horizon (5-20 cm deep) underlain by a yellow brown silty clay 'B' horizon containing rock fragments (20-50 cm deep). At the foot of the mountain range, soils comprise light brown-orange sandy alluvial outwash. To the east, on the cultivated alluvial plain, soils are clay-rich comprising a light brown-grey 'A' horizon (0-30 cm) and grey 'B' horizon (30-60 cm) containing orange oxidized fragments. Soils in this area are variably gleyed, due to saturation-induced anoxia.

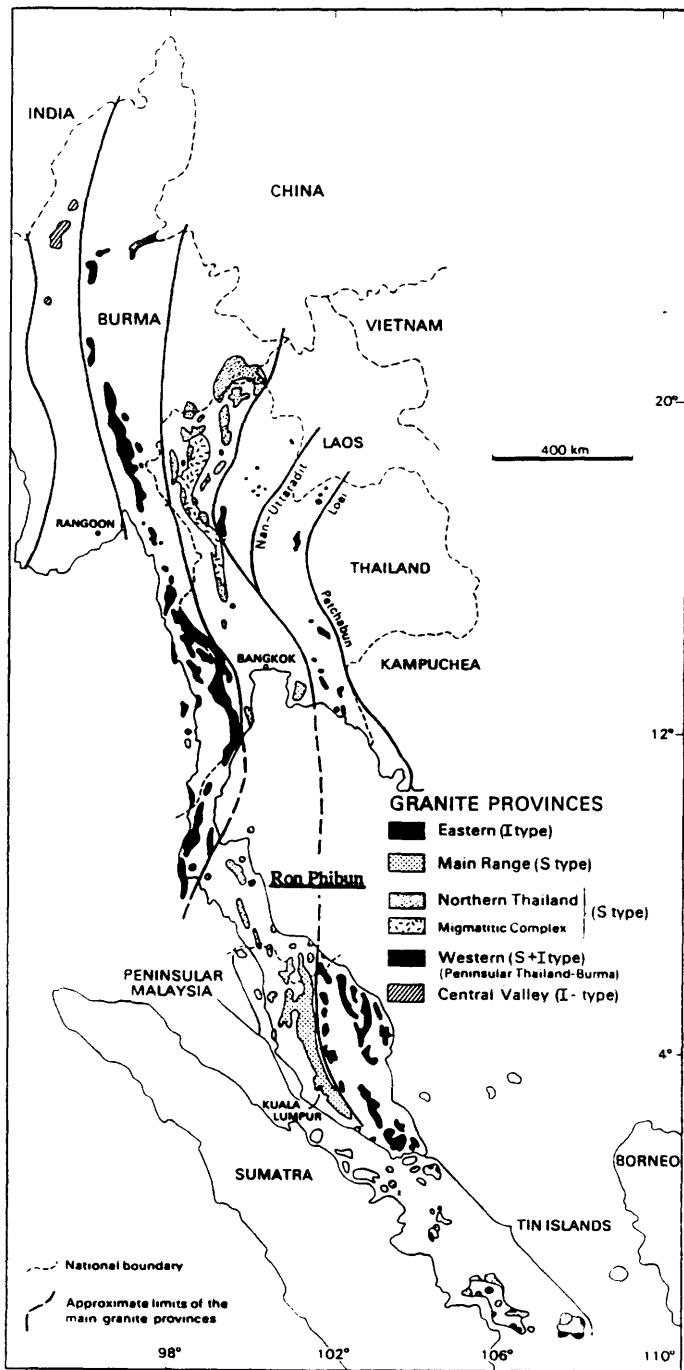


Figure 3. Map of the granite provinces of South-east Asia showing the location of Ron Phibun District (modified after Cobbing et al. 1992).

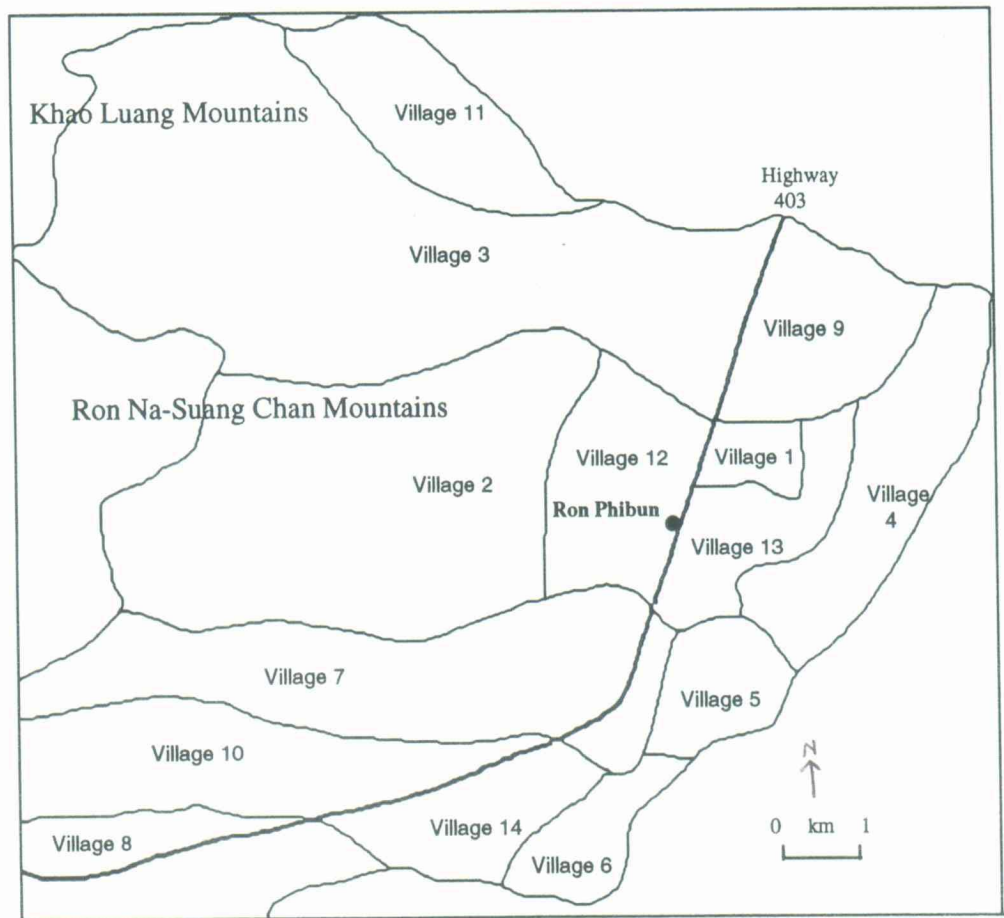


Figure 4. Location of the fourteen village areas in Ron Phibun District.

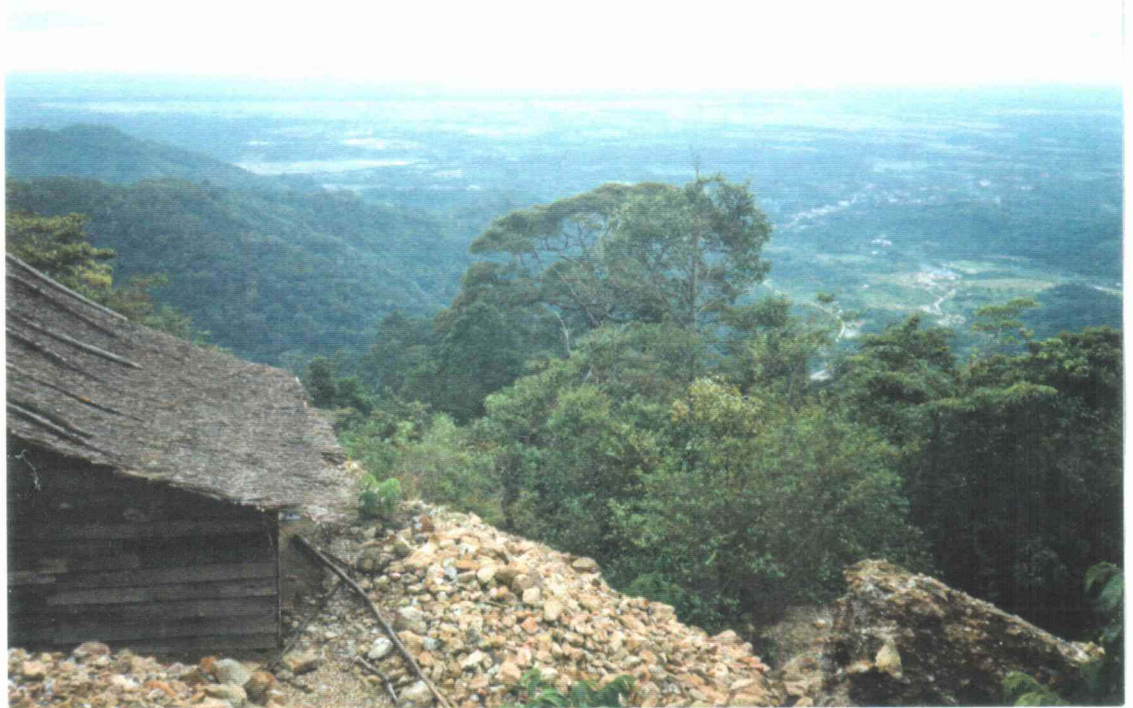


Figure 5. View from arsenopyrite waste pile 6 in the Ron Na-Suang Chan Mountains across Ron Phibun town and the alluvial plain.

1.3.3: Geology

The Thai peninsular forms part of the SE Asian 'tin belt', a zone of granite-related Sn mineralisation extending for approximately 4000 km from Burma to Indonesia, from which around 70% of the world's historical Sn production has been derived. Ron Phibun lies in the Main Range province of the belt (Figure 3), characterised by S-type biotite and biotite-muscovite granitoids of Triassic age, with abundant pegmatitic veining.

The local geology of the Ron Phibun area (Figure 6) can be resolved into four units:

(i) Cambro-Ordovician sedimentary rocks, comprising siltstones and interbedded shales with limestone lenses, quartzite and phyllite, which outcrop along the eastern border of the Ron Na-Suang Chan mountain range, striking approximately northwest-southeast.

(ii) Dark grey limestones and argillaceous limestones of Ordovician age, exposed to the east of the Cambro-Ordovician sequence and topographically expressed as a small hilly range to the north of Ron Phibun.

(iii) Triassic granitoid intrusions, which form the mountainous area to the west of Ron Phibun. The lithologies are medium-course grained biotite-muscovite granites with minor intrusions of tourmaline-muscovite granite, characteristic of the southern sector of the Khao Luang batholith. The granite is extensively faulted and pegmatite-veined in predominantly northeast-southwest and northwest-southeast directions.

(iii) Quaternary colluvial and alluvial deposits of gravel, sand, silt and clay mask much of the Palaeozoic sedimentary cover between the Ron Na-Suang Chan mountain range and the Gulf of Thailand coast. The colluvial deposits (derived from outwash from the Main Range granites) reach a maximum thickness of around 50 m in the vicinity of Ron Phibun.

1.3.4 Mineralisation and mining

Primary and placer Sn-W-(As) deposits have been worked in the Ron Phibun area for almost a century. Cassiterite (SnO_2) and wolframite $(\text{Fe},\text{Mn})\text{WO}_4$ mineralisation, with abundant arsenopyrite and pyrite, occurs widely in pegmatites and greissenised quartz-vein margins throughout the Khao Luang batholith. Ore-bearing veins, grading 5-10 % (SnO_2) with 1% arsenopyrite, typically extend for distances of 10-40 m, averaging 10-20 m deep and 3-35 cm wide. Vein orientations are characteristically E-W. Mining has conventionally been carried out via adits which follow the vein trend, and by shafts that intersect the veins. Prior to the collapse of the world tin price in the 1980s, over 20 active Sn concessions were held in the Ron Na-Suang Chan mountain range. Arsenic-rich waste piles derived from ore-dressing activities are scattered throughout the former Sn concession areas on the steep mountain slopes immediately north-east of Ron Phibun town.

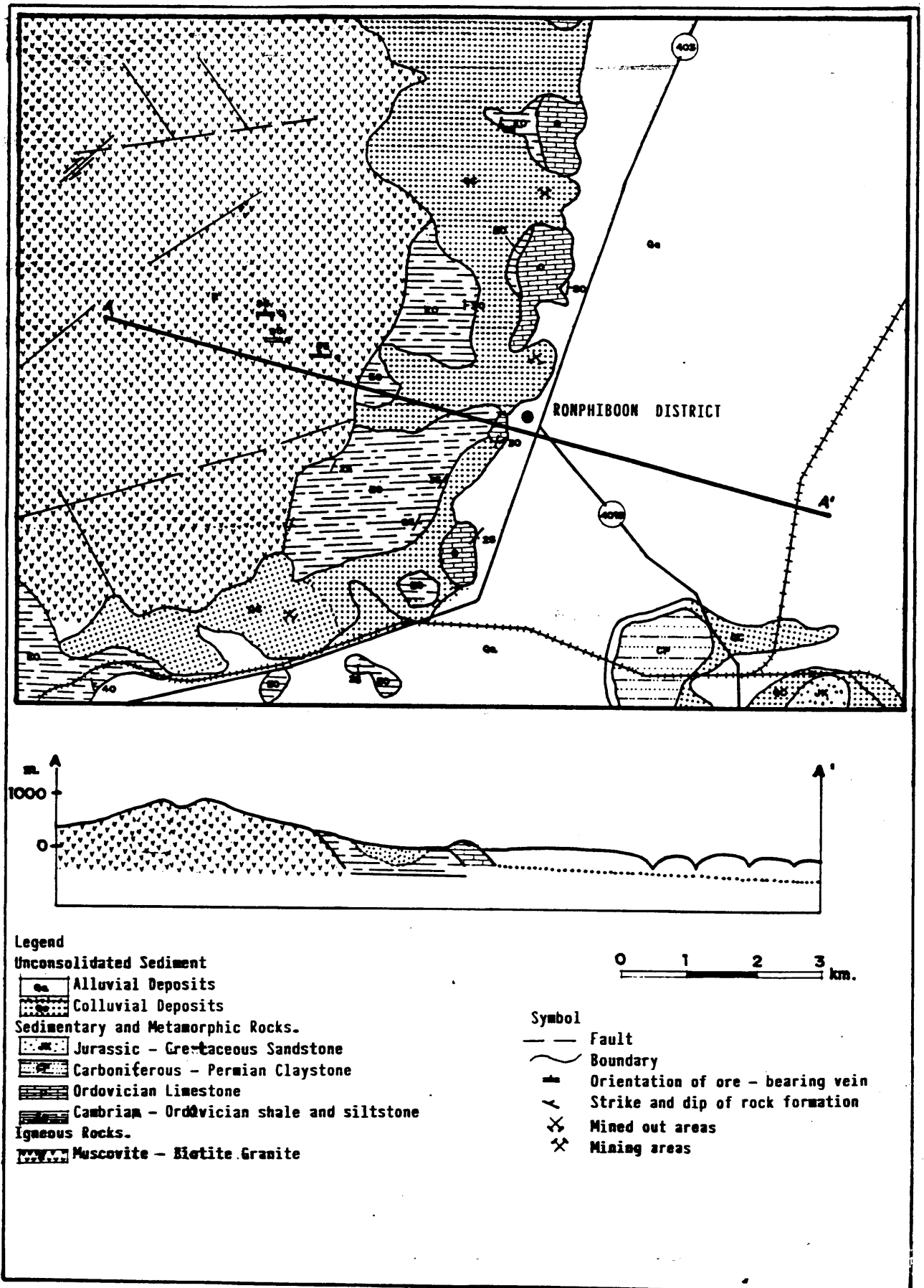


Figure 6. The geology of Ron Phibun District (from DMR).

Alluvial Sn deposits occur widely within the Quaternary cover at the foot of the Ron Na-Suang Chan mountain range. Two cassiterite-rich layers at depths of 10m and 25 m have been worked for several decades by dredging and open pit methods. While only two alluvial mines remain in operation, large dredged ponds derived from former extractive operations cover several square km to the north of Ron Phibun town. In addition to the formal extractive sector, small scale prospecting/panning for cassiterite by villagers of the Ron Phibun area is widespread.

Cassiterite produced from both the mechanised and the informal alluvial mining sectors has largely been processed at one of two ore-dressing plants. The first, located north-west of Ron Phibun town on the mid-slopes of the Ron Na-Suang Chan mountain range, ceased operation 3 years ago. The second, located in Ron Phibun town, is still operative. Separation of cassiterite is achieved by a combination of gravitation, flotation and electromagnetic methods. Flotation is specifically utilised to remove arsenopyrite from cassiterite-bearing heavy mineral concentrates. The method involves the addition of H_2SO_4 as a pH regulator, a potassium amyl xanthate collector (to increase the hydrophobic properties of FeAsS) and a pine oil frothing agent to collect the arsenopyrite residue. Once removed, the arsenopyrite is discarded.

1.3.5. Hydrogeology

Ron Phibun has a high average rainfall of c. 2100 mm per year. Surface drainage is orientated predominantly west-east, with headwaters in the Ron Na-Suang Chan mountain range feeding a series of systems which ultimately enter the Gulf of Thailand. The principal bedrock mining areas occupy the headwaters of the Hai Ron Na, which flows south-east from the granite massif through areas of alluvial mining to the north of Ron Phibun. Other stream systems draining areas of alluvial mining include Klong Sak, Klong Rak Mai and Klong Nam Khun (Figure 7). In its upper reaches the Hai Ron Na is steep, deeply incised and fast flowing but becomes wider (10 m) and more sluggish on the alluvial plain. To the east of the Ron Phibun town the majority of streams are slow flowing and have been canalised for irrigation.

There are two significant aquifers in the area. The first is a shallow aquifer with a depth of <10 m consisting of unconsolidated alluvial gravel, sand and clay, yielding 20-50 m³/hr. A second, carbonate aquifer is developed in solution cavities, bedding planes and fault zones within Ordovician limestones of the Thung Song Group, at depths of >15 m. This aquifer generally yields 10-20 m³/hr, with an easterly or south-easterly flowpath (Figure 8) and an average flow rate of 0.5-1.0 m/day.

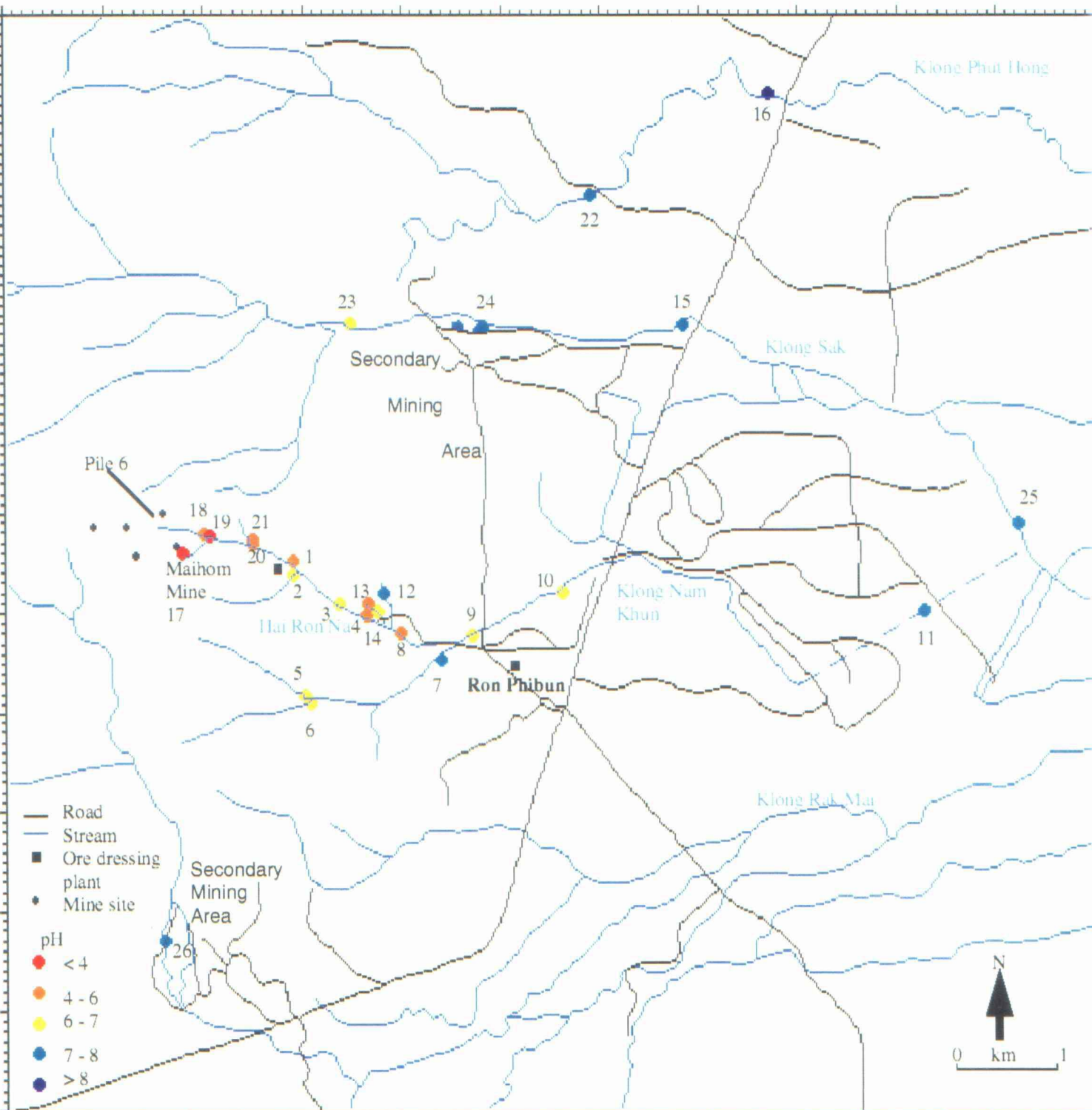


Figure 7. Surface water pH values recorded at sites RPW 1- 26 in Ron Phibun District, August 1994.

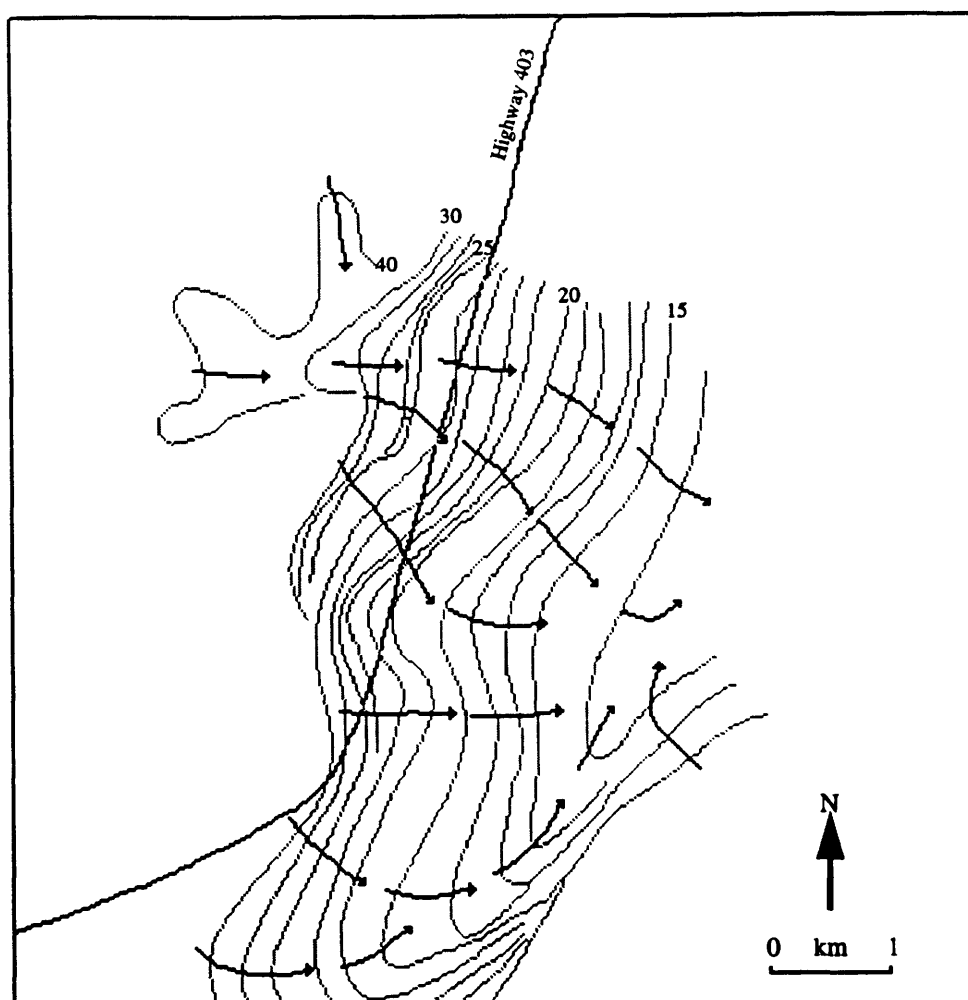


Figure 8. Groundwater flow paths and piezometric contours in Ron Phibun District (from DMR)

1.4 Previous investigations

1.4.1 Medical and epidemiological studies

Epidemiological research related to arsenism in the Ron Phibun area was initiated by the Ministry of Public Health in 1987-1988 (selected results of which are summarised in Table 2). Approximately 1000 people ranging in age from 4 months - 85 years were shown to be suffering from skin manifestations caused by As exposure, of which one has subsequently died and 20 have arsenical skin cancer. Investigations of the school-age population showed As concentrations in hair and fingernails to be elevated in up to 80% of pupils. A strong spatial correlation was confirmed between shallow well-water (< 15m) As concentrations and human body-burdens. While highest As values for hair and fingernail samples were recorded in areas with most acute shallow aquifer contamination (including Ron Phibun town) several subjects showed evidence of abnormal As assimilation in village areas with water concentrations of below 50 $\mu\text{g/l}$ (the US-EPA, EC and former WHO maximum permissible level), suggesting that alternative exposure pathways (notably the food chain and inhalation of dust) may also be significant.

Table 2. Arsenic concentration in randomly selected unaffected adolescents and shallow well waters in Ron Phibun District (Piamphongsant and Udomnitikul, 1989).

Sex	Age	Village No.	As Hair µg/kg	As Nails µg/kg	As Well Water µg/l
F	18	12	1400	4100	840
F	18	4	680	380	15
F	18	2	350	440	15
F	18	13	1100	880	40
M	18	2	460	1500	20
F	18	3	430	880	24
F	18	6	290	550	190
F	16	4	390	56000	150
F	18	2	990	1200	15
M	13	2	680	6100	88
M	15	1	1800	2100	49
M	13	7	530	910	90
M	13	7	1500	1900	105
M	20	3	30	740	32
M	15	3	610	6000	15
M	18	2	970	1600	20
M	15	8	2000	1000	15
F	13	4	1100	1100	20
F	15	2	3100	5500	790
F	15	1	2300	1100	40
M	13	1	1300	2000	50
F	18	1	980	2500	17
M	15	8	460	800	15

Table 3: Prevalence of clinical symptoms of arsenism in randomly selected members of the population in Ron Phibun District, 1994. (Dr Piamphongsant pers. commun.)

Village Number	Number of Samples	Number showing Clinical signs	Prevalence %
12	93	50	53.76
1	32	17	53.13
4	35	14	40.00
9	41	16	39.02
5	40	15	37.50
8	37	13	36.11
14	23	8	34.78
2	51	15	29.41
6	30	7	23.33
7	87	20	22.99
11	24	5	20.83
3	40	8	20.00
10	45	9	20.00
13	41	8	19.51
Total	619	197	33.11

A follow-up study of school pupils in 1992 showed no dramatic reduction of human arsenic assimilation. Of 2400 pupils sampled in Ron Phibun District, 89% had excess blood As concentrations and 22% showed skin manifestations directly attributable to As exposure. A parallel study, funded by the Japanese government, concluded that in the areas of most acute contamination (including Ron Phibun town) up to 93% of the population showed signs of melanosis and 76% had palmoplantar hyperkeratosis.

Data collated by the Institute of Public Health during 1994 have confirmed that the above-noted problems of arsenism in several village areas of the Ron Phibun District (Table 3) remain to be resolved.

1.4.2 Geological and geochemical studies

1.4.2.1 Contaminant sources:

Investigations of the distribution of As in soil, surface water, stream sediment and groundwater have been conducted by DMR since 1989. Three important contaminant sources have been identified and tentatively prioritised:-

(i) Primary mining sites in the Ron Na-Suang Chan mountains: Substantial waste rock and residual arsenopyrite piles have accumulated in the primary mining area on the eastern flank of the Ron Na-Suang Chan mountains (Figure 7). There are 5 locations in which high-grade As-Sn slags are present. DMR have estimated the cumulative amount of slag (with As concentrations in the range 1- 39%) to be 2000 m³. In addition to this high-grade waste, there are large piles (several thousand tons) of vein quartz and granite containing significant concentrations of arsenopyrite.

(ii) Ore dressing plants within, and to the west of Ron Phibun town;

(iii) Disseminated waste from small-scale panning and flotation activities undertaken by the informal mining sector. Arsenopyrite-rich waste has been discarded over open ground by both the ore dressing plant operators and small-scale prospectors, without due regard for potential long-term toxic effects. The environmental hazard is exacerbated by the use of H₂SO₄ during flotation, as the residue is inherently acid, and the As is thus more readily leached.

1.4.2.2 Surface waters:

Arsenic levels in four streams draining the mined area have been monitored by DMR since 1991. Results (Table 4) indicate an As range of 150 - 750 µg/l in waters draining from the Ron Na-Suang Chan mountains. A downstream increase (to within the range 100 - 1100 µg/l) occurs as drainage passes through Ron Phibun town, suggesting significant contamination from the ore dressing plant. To the east of Ron Phibun, concentrations

decline, and values at sites c. 30 km downstream of the town are routinely below US-EPA and WHO standards.

Table 4. Arsenic contamination in selected surface waters in Ron Phibun District (monitored by DMR between 1992 and 1994).

Stream Name	No. Sample	As concentration (mg/l)			Remarks
		Min.	Max.	Av.	
Huai Hua Muang	55	0.02	1.60	0.46	pass by primary mining areas and ore dressing plant, have W-E flow direction.
Huai Ron Na	26	0.01	0.27	0.15	source of water comes from mining areas and flow to the east.
Huai Nong Pak	25	0.05	1.10	0.26	source of water comes from mining areas and flow to the south.
Huai Suang Chan	5	0.12	1.0	0.75	source of water comes from mining areas and flow to the north.
Klong Num Khun	22	0.10	1.1	0.61	monitored from the town to the east about 5 km.
Klong Num Khun	36	0.01	0.15	0.06	monitored further to the east and the north about 12 km
Tributaries to Pak Phanong Bay	8	0.00	0.05	0.01	original source of water comes from above streams, monitoring distance is 30 km

1.4.2.3 Groundwaters:

Concentrations of As in shallow (<15 m) groundwaters are frequently higher than those in surface drainage, with a maximum recorded value of 9000 µg/l (Table 5). The deeper carbonate aquifer exhibits a lower level of contamination. Of 36 deep (>15 m) boreholes investigated by DMR, 34 yielded As values of <50 µg/l.

Table 5. Arsenic concentrations in selected shallow groundwaters from Ron Phibun District (monitored by DMR between 1991 and 1994).

Village Number	% Wells > 50 µg/l As	Range As µg/l	Mean As µg/l
12	48	80 - 9000	1620
2,13,1,3	70	60 - 1200	240

1.4.2.4 Sediments and soils:

Stream sediment and A horizon soil samples from Ron Phibun District (dry sieved to <177 µm) have been analysed for As using an alkali fusion-Gutzeit method at DMR, Bangkok. Stream sediment As distributions appear to correlate closely with those in surface waters, concentrations ranging from 10-1000 µg/g. The soil concentration range in the area is 50 - 5000 µg/g, the highest values occurring in village areas 12 and 2 (Figure 4).

1.4.3 Problem alleviation

Attempts to reduce human As exposure in Ron Phibun district have, to date, focused on reducing the local consumption of contaminated water through improved awareness, coupled with the provision of alternative supplies. In view of the acute problems associated with shallow groundwater consumption, 36 deep boreholes were sunk in the district by DMR during the period 1989-94, with water also imported via pipelines from boreholes in outlying areas. The latter solution has, however, proved costly and is only viable as a short term option. Additional supplies have been acquired by issuing large rainwater storage jars (capable of holding up to 1 year's domestic supply) to all households.

Despite a concerted effort to improve awareness of As toxicity hazards amongst the Ron Phibun population, the reduction of human As assimilation has been disappointingly small. Recent surveys have confirmed that many inhabitants continue to utilise shallow boreholes, as these tend to be most conveniently located (at virtually every dwelling) and yield water which is soft and palatable in comparison to that from the deeper carbonate aquifer. Rain-water storage jars have proved of limited value due to problems of algal growth and general maintenance.

In 1994, research towards the isolation and neutralisation of As contaminant sources at Ron Phibun was initiated in an attempt to mitigate the long-term environmental hazard. A proposal to seal all high-grade arsenopyrite waste currently situated within the Ron Na-Suang Chan mountains in an impermeable landfill is under consideration. This will be a major operation, requiring costly access-road construction in the Ron Na-Suang Chan

range. The precise importance of the waste piles as a regional contaminant source has not yet been established. Further research into the sources of As, and remediation options available, is thus urgently required.

2. CURRENT INVESTIGATION

2.1 Waste characterisation

Selected samples of tailings and flotation waste were collected from the vicinity of the former Maihom adit working (coded RPT1) and one additional site (coded RPT2, DMR waste pile 6) on the eastern margin of the Ron Na-Suang Chan massif, 4 km west of Ron Phibun (Figure 7 for locations). At each site, a single tailings sample (RPT1 & 2) and a high-grade 'arsenopyrite' waste sample (RPT1A & 2A) were selected for mineralogical characterisation.

Tailings from the two sites were visually similar, both being predominantly composed of quartzo-feldspathic detritus with abundant tourmaline. The flotation waste samples were probably derived from analogous primary materials, but differed significantly in preservation. Sample RPT1A consisted of pale green clay with sporadic occurrences of coarse (>2 mm) arsenopyrite, and appeared typical of much of the highly degraded superficial material covering the 'high-grade' waste. Sample RPT2A consisted of partially lithified arsenopyrite, on which a yellow-green framboidal coating (up to 2 mm thick) was evident.

2.1.1. Tailings characteristics

X-ray fluorescence analysis of a sub-sample of tailings RPT2 confirmed a total As concentration of around 7%. The distribution of As between >4 mm, <4 mm, <1 mm, <500 μm , <250 μm , <125 μm , <63 μm and <20 μm size fractions of the waste assemblage was assessed by wet screening of c. 0.75 kg material through a conventional sieve set using de-ionised water. All size fractions in the 500-20 μm range were subsequently super-panned to differentiate heavy mineral (HMC) and light 'tail' components. Water-soluble phases were recovered by evaporating the wash-water (around 13 litres) to dryness.

Data showing the relative contribution of the respective size fractions to the total sample mass and As load are provided in Table 6, from which the following features are evident :-

1: The tailings particle size distribution shows a distinct bimodal trend, dominated by coarse (>1 mm) sand/gravel fractions (c. 390 g or 55% total mass)), and an ultrafine (<20 μm) clay fraction (97 g or 13% total mass).

2: Weight-percentage data for the heavy mineral and tail components in each of the sub-500 μm size fractions (Table 6) indicate that the HMC is only a small component of the solid assemblage throughout the analysed size range (max. 6.3% total mass). In the >0.63 μm fractions, the dominant phases constituting the light 'tail' component are quartz and feldspar sand/silt grains. In the <63 μm classes, the tail is dominated by clays.

Table 6. Grain size and gravimetric partitioning of As in Ron Phibun tailings sample RPT2.

Fraction	Tot. wt. g	Tail wt. g	% total	HMC wt. g	% total	Tail As g	As conc. %	HMC As g	As conc. %
>4mm	216.6								
1-4mm	174.2								
>0.5mm	61.5								
>250 μm	52.8	51.7	97.8	1.12	2.2	6.2	11.9	0.12	10.7
>125 μm	37.8	36.6	96.9	1.17	3.1	5.3	14.4	0.10	8.5
>63 μm	21.65	20.3	94.1	1.26	5.9	4.1	18.9	0.10	7.9
>20 μm	13.3	12.5	93.7	0.83	6.3	3.6	28.7	0.07	8.4
<20 μm	97.54	97.54	100	-	0	28.0	28.8	-	-
Evap.	31.86	31.83	100	-	-	1.2	3.7	-	-

3: The proportion of total As within the heavy mineral component is small. In the four size fractions for which comparative data are available, absolute concentrations of As in the HMC are lower than in the corresponding 'tail' (by up to a factor of c. 3.5). This situation contrasts with tailings wastes previously studied from southern Africa and Asia, in which the heavy mineral fraction, although volumetrically small, routinely yields As concentrations at least an order of magnitude greater than those in the lighter 'tail' (e.g. Williams and Smith, 1994). The distribution observed at Ron Phibun indicates that the tailings are intensely altered and degraded. Arsenic within the matrix is no longer held in primary phases such as FeAsS, but is predominantly partitioned into secondary oxidation products.

4: The As concentration within the 'tail' component is inversely correlated with particle size, rising from 11.9% in the 250-500 μm fraction to 28.8% in the <20 μm fraction. This trend is common in weathered matrices holding an abundance of adsorbed arsenates due to disproportionate enrichment in fractions with the largest specific adsorption surfaces. However, the very high concentrations recorded in the <20 μm range in RPT2 are principally attributable to the precipitation of discrete ultrafine secondary As minerals,

notably scorodite. This interpretation has been confirmed by X-ray diffraction analysis of the <20 µm fraction (Figure 9) which shows the assemblage to consist almost entirely of scorodite (FeAsO₄·H₂O), with minor kaolinite and muscovite peaks.

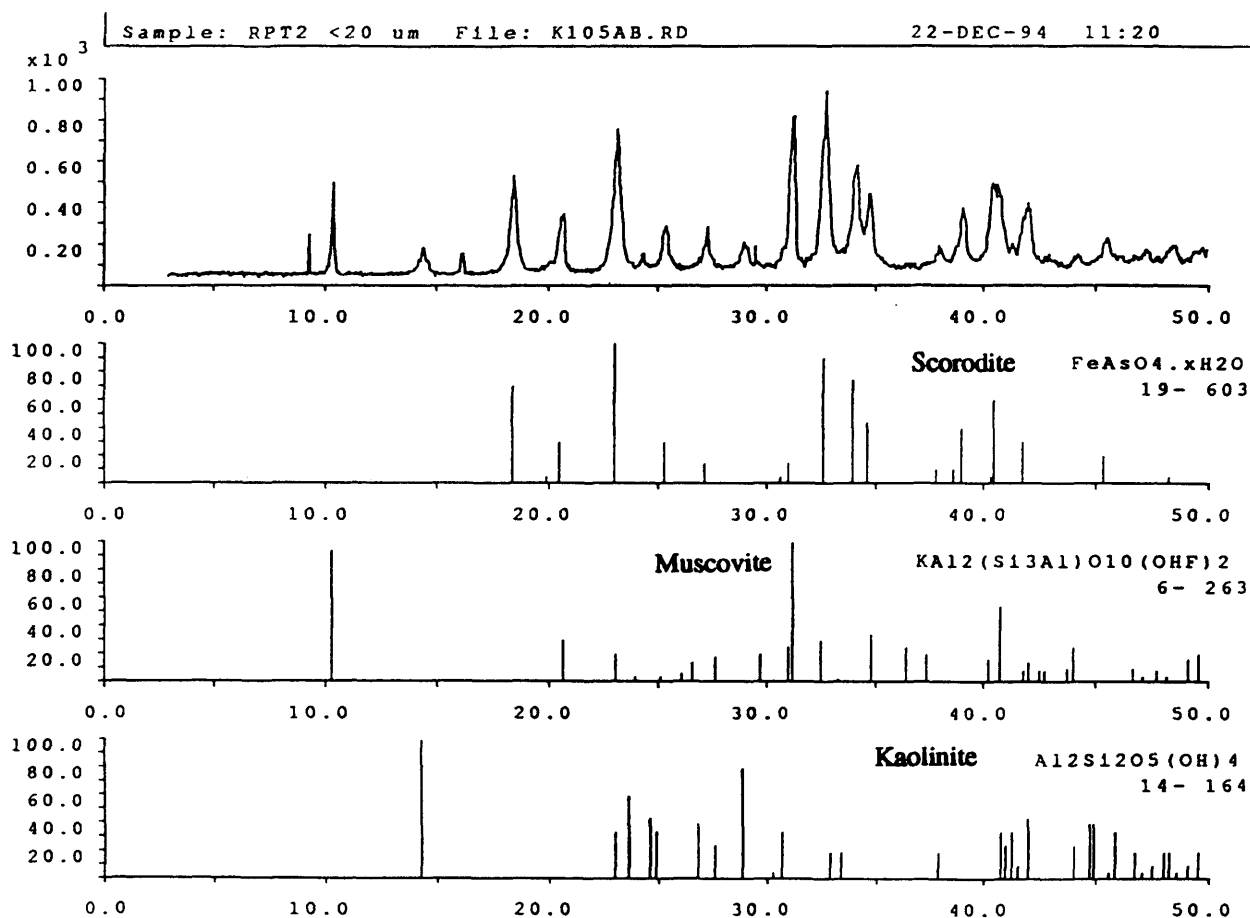


Figure 9. XRD trace of the < 20 µm fraction of tailings sample RPT2.

5: The <20 µm fraction is particularly important with respect to the overall As mass-balance. The fraction constitutes 13% of the tailings mass yet, with an As concentration of 28.8%, accounts for 50% of the total As budget.

6: Water-soluble mineral phases account for approximately 5% of the total tailings mass, but the As concentration of this fraction is low (<4%) relative to the finer particulate components of the light 'tail'.

Qualitative data illustrating the size and gravimetric distribution of Sb, Sn, Cd, Ag, Rb, Bi, Pb, W and Zn in the light 'tail' fraction of sample RPT2 are given in Table 7. The distribution of Cd, Pb and Zn shows a striking contrast to that of As, being disproportionately enriched in the soluble fraction (recovered following evaporation of the washwater). Ratios of XRF-peak heights for the <20 µm vs. evaporate fractions are 0.11 for Cd, 0.41 for Pb and 0.14 for Zn (the value for As = 7.1). This discrepancy reflects the presence of a secondary heavy metal assemblage in the waste which includes soluble sulphate (and possibly carbonate) crusts, formed on particle surfaces by evaporative saturation of interstitial water, while As resides in less soluble ferric arsenate (scorodite) phases. A water-soluble U and Cu component was also noted from the XRF spectra for the RPT2 evaporation residue.

Table 7: Grain size and gravimetric partitioning of selected trace elements in Ron Phibun tailings sample RPT2. Values indicate XRF peak-heights and provide an indication of relative concentration.

Fraction	Sb	Sn	Cd	Ag	Bi	Pb	W	Zn	Others
>4mm	-	-	-	-	-	-	-	-	-
1-4mm	-	-	-	-	-	-	-	-	-
>0.5mm	-	-	-	-	-	-	-	-	-
>250µm	12	40	16	2	42	21	8	60	-
>125 µm	20	47	15	10	54	25	8	73	-
>63µm	17	42	24	8	64	30	13	85	-
>20µm	15	52	20	9	60	42	17	95	Zr
<20µm	15	20	20	17	80	38	18		Zr
Evap.	ND	ND	170	ND	8	92	2	700	U, Cu

2.1.2. High-grade waste characteristics:

The total As concentrations in 'high-grade' flotation waste samples RPT1A and RPT2A were established by XRF analysis to be c. 30% in both instances. Such values substantiate data provided by DMR indicating that high-grade waste piles on the Ron Suang Chan mountain flank constitute a major potential contaminant source for As.

Subsequent analysis of sample RPT1A involved wet sieving to separate the >500 µm, 500-20 µm and <20 µm fractions. The contributions of the respective size classes to the total sample mass were variable, with the ultrafine fraction clearly dominant (>500 µm - 4.8%, 500-20 µm - 8.8%, <20 µm - 86.4%).

X-ray fluorescence analysis of the <20 µm component of RPT1A confirmed that this fraction is highly As-rich (>20%), and must therefore be the principal contributor to the As mass balance in the high-grade waste. The dominant mineral phase is the secondary

arsenate scorodite, as confirmed by the XRD trace shown in Figure 10. The proportion of total As held in primary sulphides is small.

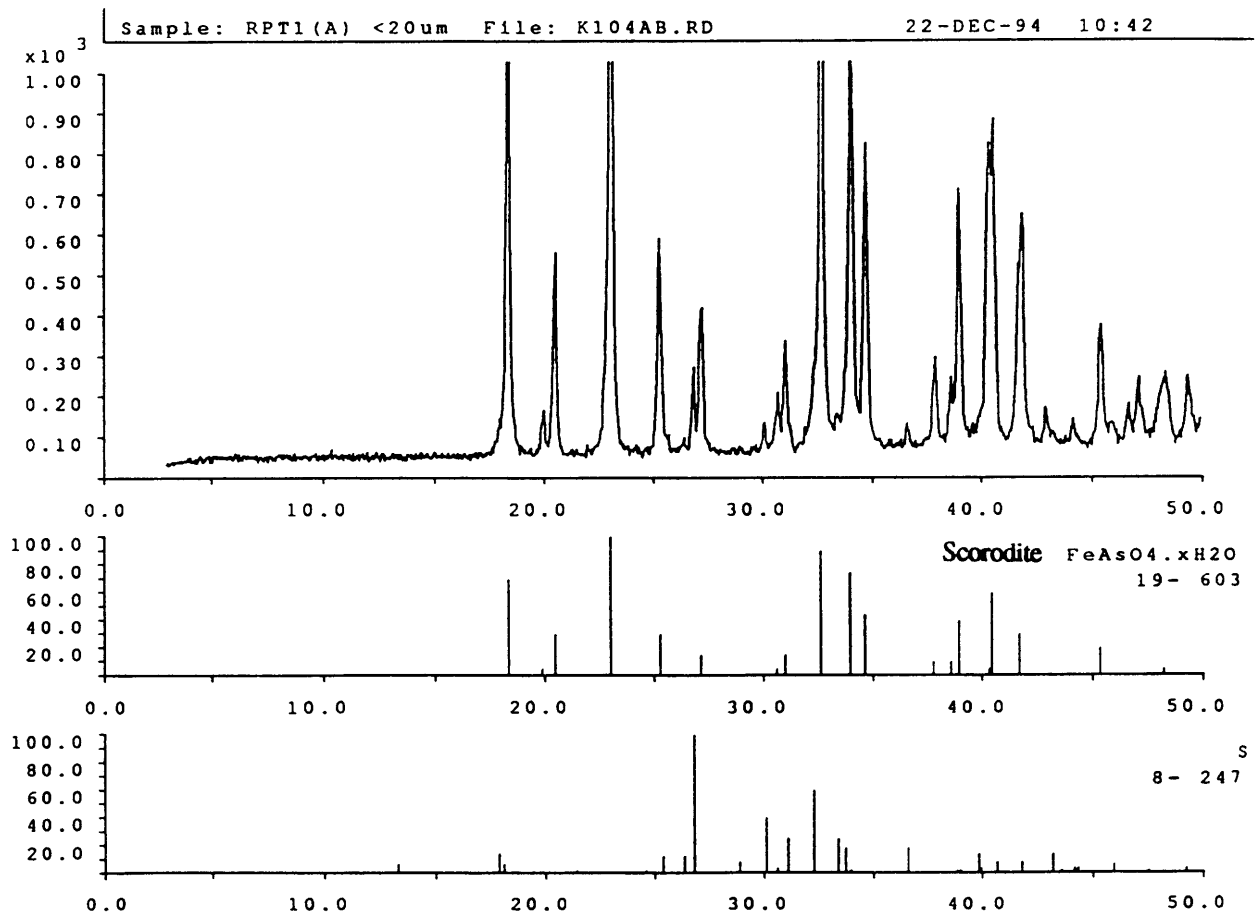


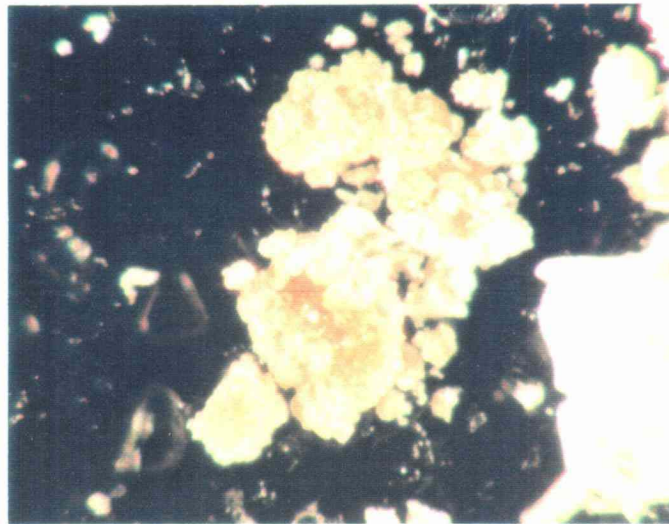
Figure 10. XRD trace of the < 20 μm fraction of tailings sample RPT1A.

A sub-sample of the <500 μm component was super-panned to facilitate mineralogical examination of the HMC assemblage in the waste. The weight of HMC obtained was <2 g (constituting only 4% of the total sample mass). Magnetic separation and analysis confirmed that As within this fraction occurs almost exclusively as arsenopyrite (which dominated the weak/non-magnetic fraction along with minor cassiterite). A moderately magnetic fraction was characterised by composite grains, biotite and amphibole, while strongly magnetic extracts contained white rounded pellets of clay, magnetite and garnet.

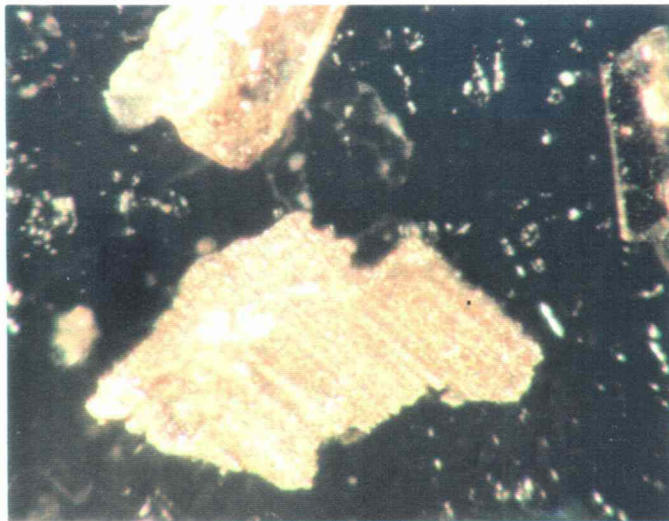
The mineralogical data obtained for RPT1A suggest that reference to the flotation waste accumulations as 'arsenopyrite piles' may be inaccurate. The extent of weathering of much of this material is such that the As balance is actually dominated by ultrafine secondary arsenates.

2.1.3. General mineralogical observations

Selected mineral grains from the heavy mineral fractions of samples RPT2 and RPT1A, plus a sample of the green crystalline coating on the surface of RPT2A (Figure 11) were mounted on a glass slide and characterised by a combination of binocular microscope and electron microprobe methods. A photograph and sketch-key of the analysed grains is provided in Figure 12. Specific mineral phases identified by microprobe analysis are listed in Table 8. Notable trends include the relatively complex nature of the sulphide assemblage which carries As (arsenopyrite (Figures 11 and 12), pyrite, chalcopyrite), and the high concentration of W in scheelite (identified by short-wave UV-lamp scanning).



(a)



(b)

Figure 11. Magnified photograph of (a) scorodite and sulphur grains and (b) arsenopyrite (bottom grain in picture) from tailings sample RPT1A.



Figure 12. Photograph and sketch of selected grains and coatings from tailings sample RPT1A.

Table 8. List of mineral phases identified by electron microprobe analysis from tailings sample RPT1A.

MINERAL NAME	GRAIN NUMBER
TOURMALINE	RPT1(A)/1, 10, 21, 23, 24,
ARSENOPYRITE	RPT1(A)/2, 5, 6, 7, 14, 15, 17, 19, 20,
CASSITERITE	RPT1(A)/3, 4, 6, 13
BIOTITE	RPT1(A)/8, 22, 28
HUBNERITE	RPT1(A)/25
WOLFRAMITE	RPT1(A)/21, 27, 34
SCORODITE	RPT1(A)/30, 31, 33, 35,
SCHEELITE	RPT1(A)/40, 41
QUARTZ	RPT1(A)/13
SULPHUR	RPT1(A)/6, 36, 38
SPHALERITE	RPT1(A)/39
PYRITE	RPT1(A)/9, 18, 29
IRON OXIDE	RPT1(A)/11
MUSCOVITE	RPT1(A)/27

2.2 Hydrogeochemistry

2.2.1. Methodology.

Surface water samples were collected from 24 locations along the water courses Hai Ron Na, Klong Sak, Klong Rak Mai, Klong Nam Khun and Klong Phut Hong up to a distance of 7 km downstream of the mined area. In addition a sample from the Maihom mine shaft and a sample of tailings pond water in the alluvial mining area to the north of Ron Phibun were collected (Figure 7). Measurements of pH, Eh, temperature and conductivity were collected in the field using a range of Orion Instruments meters and temperature-compensated electrodes. Meters were calibrated every 2-3 measurements, using commercial buffer solutions (pH 4,7 and 9), a KCl conductivity standard (12.8 mS at 20 °C) and a Zobell Eh standard (230 mV).

The suite of samples collected at each site for geochemical analysis included: (i) 30 ml unfiltered HNO₃-acidified water, (ii) 30 ml filtered (0.45 µm Millipore™) unacidified water, (iii) 30 ml filtered (0.45 µm Millipore™) HNO₃-acidified water, (iv) 30 ml filtered (0.45 µm Millipore™) HCl-acidified water. Additional samples, collected at selected localities only, included: (v) 30 ml filtered (0.20 µm Millipore™) HNO₃-acidified water, (vi) 5 ml filtered (0.45 µm Millipore™) filtered water with 0.5 ml dipiridyl reagent. Unless otherwise indicated, all data presented in this report relate to 0.45 µm filtered HNO₃ or HCl-acidified waters.

Filtered waters were collected by drawing 30 ml of water into a plastic syringe (pre-rinsed in the stream water) and passing it through a sealed filtration cartridge (loaded with a filter of appropriate pore-size) into a sterile Sterilin™ storage tube. Samples were acidified within a few hours of collection by addition of 0.3 ml of concentrated ARISTAR grade acid (HNO₃ or HCl). Addition of 1% vol/vol acid reduces the pH of samples to approximately 1.0, thus preventing adsorption of dissolved metals to the interior walls of the storage tube and minimising post-sampling microbial activity.

Water samples from 23 shallow wells and 13 deep boreholes were collected using the procedures outlined above. Deep boreholes were pumped for 10 minutes prior to sampling to ensure that samples of aquifer water had not been subject to oxidation in the well piping.

Determinations for Sr, Cd, Ba, Si, Mn, Fe, P, S, B, Mg, Na, Al, Be, Ca, Zn, Cu, Li, Zr, Co, Ni, Y and K were made by ICP-AES. Total As analyses were carried out by a combination of ICP-AES and hydride-generation AAS methods, the latter utilising a flow-injection (FIA) introduction system. The FIA system facilitates the simultaneous reduction of As to arsene and injection into the chamber by merging a flow of 0.2% NaBH₄ with the sample carrier. The sample is carried via a 200 µl loop and mixed with the reductant before

entering a gas liquid separator. An argon stream then carries the arsene produced into a heated quartz tube atom cell where it decomposes, allowing the As concentration to be measured by AAS (Nakashima 1979).

Analyses of As (III) were made by hydride generation FIA following the suppression of arsenate by the addition 0.1 ml of 200 mg/l Zr (as chloride) to 5 ml of sample.

Ferrous iron was determined by colorimetric analysis of dipiridyl-spiked waters (10% vol/vol).

Analyses of NO₃, Cl⁻ and SO₄ were carried out by ion chromatography. Bicarbonate determinations were made by HCl titration. Practical detection limits for all determinants are listed in Table 9. Results falling below the limit of detection were set to 0.5 DL for purposes of statistical analysis. Pearson correlation coefficients were calculated following log-transformation of the data to reduce the influence of outlying values on results.

Table 9. Practical detection limits (LoD) for all elements and ions determined in water samples.

Element/ Ion	LoD mg/l	Element/ Ion	LoD mg/l	Element/ Ion	LoD mg/l
Sr	0.001	Cd	0.007	Ba	0.002
Si	0.011	Mn	0.002	Fe	0.007
P	0.028	B	0.017	Mg	0.026
V	0.006	Na	0.022	Mo	0.011
Al	0.014	Be	0.0002	Ca	0.010
Zn	0.005	Cu	0.003	Pb	0.044
Li	0.001	Zr	0.004	Co	0.022
Ni	0.019	Y	0.002	La	0.005
K	0.035	Cr	0.013	As	0.0025
As (III)	0.005	Fe (II)	0.050	HCO ₃	20.00
Cl	0.050	SO ₄	0.100	NO ₃	0.100

A sub-suite of 29 surface water, shallow groundwater and deep aquifer waters was filtered through <0.2 µm Millipore membranes (and subsequently acidified) to assess the possible influence of ultrafine colloidal particulates on the <0.45 µm water analytical results. The dissolved cation values for this suite were found to fall routinely within 5% of those for the corresponding <0.45 µm (HNO₃ acidified) samples. Accordingly, it is concluded that the concentrations of major and trace elements reported in <0.45 µm filtered waters from Ron Phibun (Tables 10- 12) reflect genuine solutes, with only a minimal influence exerted by colloids or other particulates (such as bacteria) in the 0.2 - 0.45 µm range.

2.2.2. Surface waters

2.2.2.1 pH, Eh and conductivity:

Surface water pH values were recorded in the range 2.99 - 8.19 (Table 10 and Figure 7), reflecting three distinctive (granitic, alluvial and carbonate) lithological signatures, variably modified by mining and mineral processing activity. The inherently acid waters (pH <6) over the granite massif of the Ron Na-Suang Chan range are significantly depressed (to <4) in the vicinity of former bedrock Sn-W mining activities on the eastern flank of the range, notably in the adit of the former Maihom Sn-W mine (RPW 17) and its outflow drainage, which feeds the headwaters of the Hai Ron Na system (RPW 19). Relatively acid waters persist in the Hai Ron Na for a distance of approximately 1 km downstream of the primary mining area (with pH values of 4.51, 4.50 and 4.39 at RPW 20, 21 and 1 respectively), after which significant buffering occurs in response to mixing of the mine drainage with a north-east flowing tributary, draining an apparently unmined catchment (pH 6.3, RPW 2). Spring water emerging from an alluvial/sedimentary sequence in village 2 (Figure 4) has a pH of 5.5, suggesting that aquifer recharge water derived from the granite may exert a wider impact on surface water quality (RPW 13).

In the mid- and lower-reaches of the Hai Ron Na, pH values lie predominantly in the range 6-8, with significant buffering provided by south- and east-northeast-flowing tributaries (e.g. RPW 12 - pH 7.04) draining unmined deep alluvium or shale/siltstone lithologies. A localised depression of pH values (pH <6) is, however, evident in the vicinity of village 2 (Figure 4), possibly due to panning activities by local villagers.

The pH characteristics of catchment areas extensively affected by alluvial Sn mining are exemplified along an unnamed southern tributary system of the Hai Ron Na, and in the upper reaches of Khlong Sak. The pH values in the upper sectors of these systems portray a weakly acidic regime (pH 6.2, 6.4 and 6.84 at RPW 5, 6 and 23 respectively). The waters of both of these catchments show increasing pH values in their lower reaches (RPW 7 and 15 respectively) due to buffering over limestone lithologies.

Waters from a tailings pond in the secondary mining area to the north of Ron Phibun town and from the Klong Phut Hong catchment, outwith the mined area, were found to be neutral or alkaline (7.45, 7.01 and 8.19 for RPW 24, 22 and 16 respectively), consistent with the calcareous nature of the underlying bedrock.

Corrected Eh data were recorded in the range 265 - 630 mV (Table 10). The highest Eh value (630 mV) was recorded in the acid waters of the Maihom adit (RPW 17), with a relatively high value of 490 mV characterising the headwater of the Hai Ron Na immediately

Table 10. Physio-chemical properties of surface water samples RPW1-RPW26, Ron Phibun District.

Determined	RPW1	RPW2	RPW3	RPW4	RPW5	RPW6	RPW7	RPW8	RPW9	RPW10	RPW11	RPW12	RPW13	RPW14	RPW15	RPW16	RPW17	RPW18	RPW19	RPW20	RPW21	RPW22	RPW23	RPW24	RPW25	RPW26	
Si (mg/l)	.004	.034	.009	.011	.115	.049	.044	.040	.072	.073	.071	.117	.007	.012	.052	.011	.019	.003	.005	.006	.004	.008	.005	.012	.005	.048	.009
Ca (mg/l)	29.3	3.5	21.4	13.4	3.5	3.5	3.5	3.5	3.5	3.5	3.5	3.5	15.3	8.7	3.5	3.5	24.7	24.2	102.3	37.3	25.4	3.5	3.5	3.5	3.5	3.5	3.5
Mg (mg/l)	.007	.006	.005	.014	.013	.013	.021	.038	.026	.036	.031	.021	.003	.012	.090	.003	.016	.009	.009	.008	.008	.008	.006	.004	.003	.012	.012
Na (mg/l)	.001	.001	.001	.001	.001	.001	.001	.001	.001	.001	.001	.001	.001	.001	.001	.001	.001	.001	.001	.001	.001	.001	.001	.001	.001	.001	.001
Fe (mg/l)	.222	.004	.118	18.9	.017	.057	.071	.517	.176	.113	.046	.084	.073	.044	.043	.043	.110	.107	.249	.208	.304	.087	.037	.032	.012	.008	.116
P (mg/l)	.040	.004	.008	.164	.073	.044	.159	.733	.307	.233	.087	.302	.004	.008	.021	.144	4.188	.418	.045	.027	.156	.027	.042	.037	.042	.008	.112
K (mg/l)	.014	.028	.014	.014	.018	.014	.044	.033	.033	.039	.030	.045	.004	.014	.014	.014	.014	.014	.014	.014	.014	.014	.014	.014	.014	.014	.014
Cl (mg/l)	1.985	.689	.489	.673	4.644	3.456	3.053	1.545	2.613	2.583	2.514	3.495	.529	.607	1.427	3.866	1.367	.403	.353	.470	.604	.493	.394	.394	1.440	.460	
NO ₃ (mg/l)	.050	.050	.050	.050	.050	.050	.050	.050	.050	.050	.050	.050	.050	.050	.050	.050	.050	.050	.050	.050	.050	.050	.050	.050	.050	.050	.050
NO ₂ (mg/l)	.003	.003	.003	.003	.003	.003	.003	.003	.003	.003	.003	.003	.003	.003	.003	.003	.003	.003	.003	.003	.003	.003	.003	.003	.003	.003	.003
Ammonia (mg/l)	201	451	130	171	35.8	165	168	553	439	583	541	406	351	82.8	4.8	66.8	66.3	131	98.4	137	208	61.1	50	50	50	50	118
Ammonium (mg/l)	10.4	19.4	9.6	7.4	25.6	18.8	24.9	28.4	20.8	17.4	20.8	17.4	20.8	17.4	20.8	17.4	20.8	17.4	20.8	17.4	20.8	17.4	20.8	17.4	20.8	17.4	20.8
pH	4.39	6.28	6.18	5.19	6.26	6.48	7.49	5.01	6.03	6.39	7.00	7.04	5.59	6.20	7.90	8.19	2.99	4.88	3.48	4.51	4.50	7.01	6.84	7.45	7.50	7.10	
EC (µS/cm)	218	511	246	221	378	378	378	378	378	378	378	378	378	378	378	378	378	378	378	378	378	378	378	378	378	378	378
Cond (µS)	718	1119	546	523	818	718	718	718	718	718	718	718	718	718	718	718	718	718	718	718	718	718	718	718	718	718	718
DO (mg/l)	405.1	437.5	438.1	436.4	424.2	407.6	403.5	374.6	364.5	341.6	400.3	293.6	344.000	362.7	630.0	408.9	490.0	467.8	468.0	396.9	391.1	346.2	346.2	346.2	346.2	346.2	346.2

Cond = conductivity Eh = corrected Eh Values below detection limit set to 0.5 LoD = no data elements recorded entirely below the LoD are not included

Table 11. Physio-chemical properties of shallow groundwater samples RPSW1-RPSW23, Ron Phibun District.

Determined	RPSW1	RPSW2	RPSW3	RPSW4	RPSW5	RPSW6	RPSW7	RPSW8	RPSW9	RPSW10	RPSW11	RPSW12	RPSW13	RPSW14	RPSW15	RPSW16	RPSW17	RPSW18	RPSW19	RPSW20	RPSW21	RPSW22	RPSW23	
Si (mg/l)	.011	.007	.113	.125	.033	.200	.194	.114	.133	.129	.198	.138	.111	.315	.039	.013	.049	.232	.044	.028	.050	.079	.058	
Ca (mg/l)	3.5	18.9	3.5	3.5	3.5	3.5	3.5	3.5	3.5	3.5	3.5	3.5	3.5	3.5	3.5	3.5	3.5	3.5	3.5	3.5	3.5	3.5	3.5	
Mg (mg/l)	.008	.012	.057	.027	.063	.081	.028	.034	.015	.052	.075	.048	.113	.055	.009	.028	.039	.092	.028	.031	.070	.062	.019	
Na (mg/l)	3.1	1.5	9.9	13.8	10.3	15.4	10.3	16.3	9.1	8.2	14.3	21.8	7.2	15.5	12.2	16.0	0.8	12.9	17.0	6.8	5.6	6.6	7.8	
Fe (mg/l)	.001	.001	.001	.001	.001	.001	.001	.001	.001	.001	.001	.001	.001	.001	.001	.001	.001	.001	.001	.001	.001	.001		
P (mg/l)	.038	.048	.022	.044	.027	.044	.027	.044	.027	.044	.027	.044	.027	.044	.027	.044	.027	.044	.027	.044	.027	.044	.027	
K (mg/l)	.038	.048	.022	.044	.027	.044	.027	.044	.027	.044	.027	.044	.027	.044	.027	.044	.027	.044	.027	.044	.027	.044	.027	
B (mg/l)	.017	.008	.022	.023	.022	.022	.022	.022	.022	.022	.022	.022	.022	.022	.022	.022	.022	.022	.022	.022	.022	.022	.022	
Mg (mg/l)	.059	.422	3.132	3.229	.887	7.048	5.245	3.681	3.645	5.008	6.399	2.936	1.807	7.569	1.691	3.233	1.499	2.371	1.235	.632	1.696	2.430	1.822	
NO ₃ (mg/l)	4.9	5.4	5.4	4.9	4.8	63.9	29.2	14.9	22.4	27.9	39.2	26.6	8.8	30.3	7.9	8.8	11.0	245.2	19.3	17.8	4.8	19.3	7.4	
NO ₂ (mg/l)	.003	.003	.003	.003	.003	.003	.003	.003	.003	.003	.003	.003	.003	.003	.003	.003	.003	.003	.003	.003	.003	.003	.003	
Ammonia (mg/l)	208	345	545	106	345	106	106	106	106	106	106	106	106	106	106	106	106	106	106	106	106	106	106	
Ammonium (mg/l)	3.9	2.9	50.5	62.8	11.2	91.8	105.4	56.9	72.4	64.7	60.9	42.8	46.8	110.1	8.3	5.9	33.9	71.8	23.4	16.8	32.7	22.6	29.9	
Zn (mg/l)	140.2	260.8	218.9	13.4	11.8	25.1	7.1	13.9	9.2	14.9	73.7	49.8	7.3	13.3	20.8	17.9	1173.7	17.1	16.9	22.1	32.7	22.6	22.6	9.1
Li (mg/l)	.002	.003	.002	.002	.005	.003	.003	.003	.003	.003	.003	.003	.003	.003	.003	.003	.003	.003	.003	.003	.003	.003	.003	.003
HCO ₃ (mg/l)	1.0	1.0	1.0	1.0	1.0	1.0	1.0	1.0	1.0	1.0	1.0	1.0	1.0	1.0	1.0	1.0	1.0	1.0	1.0	1.0	1.0	1.0	1.0	
Cl (mg/l)	1.0	1.0	1.0	1.0	1.0	1.0	1.0	1.0	1.0	1.0	1.0	1.0	1.0	1.0	1.0	1.0	1.0	1.0	1.0	1.0	1.0	1.0	1.0	
SO ₄ (mg/l)	1.0	1.0	1.0	1.0	1.0	1.0	1.0	1.0	1.0	1.0	1.0	1.0	1.0	1.0	1.0	1.0	1.0	1.0	1.0	1.0	1.0	1.0	1.0	
NO ₃ (mg/l)	.050	.490	.120	.030	.050	.050	.050	.050	.050	.050	.050	.050	.050	.050	.050	.050	.050	.050	.050	.050	.050	.050	.050	.050
NO ₂ (mg/l)	.003	.003	.003	.003	.003	.003	.003	.003	.003	.003	.003	.003	.003	.003	.003	.003	.003	.003	.003	.003	.003	.003	.003	.003
Ammonia (mg/l)	440	192	34.1	84	4.15	5114	880	42.3	39.6	1536	473	1071	12	2.75	1542	1.25	43.3	3.15	1.4	1.25	41.4	7.2	1.8	
Ammonium (mg/l)	22.8	11.8	6.41	7.13	125.0	47.1	125.0	47.1	125.0	47.1	125.0	47.1	125.0	47.1	125.0	47.1	125.0	47.1	125.0	47.1	125.0	47.1	125.0	
pH	6.41	6.37	6.41	6.41	6.41	6.41	6.41	6.41	6.41	6.41	6.41	6.41	6.41	6.41	6.41	6.41	6.41	6.41	6.41	6.41	6.41	6.41	6.41	
EC (µS/cm)	279	574	328	384	316	853	761	444	540	603	641	432	378	782	119	106	278	1780	278	272	272	272	272	
Cond (µS)	718	1119	546	523	818	718	718	718	718	718	718	718	718	718	718	718	718	718	718	718	718	718	718	
DO (mg/l)	399.6	437.3	438.4	436.5	420.9	420.9	420.9	420.9	420.9	420.9	420.9	420.9	420.9	420.9	420.9	420.9	420.9	420.9	420.9	420.9	420.9	420.9	420.9	

Table 12. Physio-chemical properties of deep groundwater samples RPDW1-RPDW13, Ron Phibun District.

Determinand	RPDW1	RPDW2	RPDW3	RPDW4	RPDW5	RPDW6	RPDW7	RPDW8	RPDW9	RPDW10	RPDW11	RPDW12	RPDW13
Sr (mg/l)	.214	.365	.263	.197	.163	.169	.217	.199	.329	.639	.111	.321	.358
Ba (mg/l)	.012	.047	.004	.033	.043	.033	.216	.295	.090	.036	.117	.111	.041
Si (mg/l)	.27	.29	.24	.20	.15	.13	.34	.36	.13	.13	.15	.16	.14
Mn (mg/l)	.032	.227	.320	.294	.096	.011	2.304	.635	.067	.100	.015	.511	.067
Fe (mg/l)	.078	2.428	.063	.028	2.280	.123	14.116	22.607	.778	1.824	.015	.343	.319
P (mg/l)	.145	.374	.243	.106	.154	.139	.906	.518	.111	.376	.048	.233	.062
B (mg/l)	.040	.024	.023	.026	.030	.025	.029	.008	.048	.059	.048	.037	.211
Mg (mg/l)	6.2	9.6	10.2	6.3	6.6	4.7	6.3	5.2	14.1	49.7	2.6	16.0	15.7
Na (mg/l)	9.4	16.2	14.3	9.7	6.6	10.7	16.4	101.4	75.6	209.7	25.6	14.6	15.0
Ca (mg/l)	85.7	90.5	92.4	97.1	103.5	94.1	82.4	60.1	69.1	73.1	35.5	100.7	90.4
Zn (µg/l)	3625	1055	434	1351	76	4175	6857	3941	766	612	12.	998	108
K (mg/l)	1.3	2.6	2.9	2.4	2.0	1.7	6.3	2.2	1.5	6.0	4.7	1.3	.618
HCO ₃ (mg/l)	332	351	320	356	372	354	307	264	457	653	78	404	394
Cl (mg/l)	3.9	15.7	36.9	6.0	5.6	4.7	3.8	132.0	7.9	28.9	42.3	20.7	5.8
SO ₄ (mg/l)	.720	1.360	2.170	2.660	.710	1.500	.240	.590	18.60	277.0	16.0	4.840	4.910
NO ₃ (mg/l)	.050	.050	.050	.050	.050	.120	.050	.050	.050	.050	28.20	.050	.050
Fed(X)(mg/l)	.070	1.860	.003	.003	2.260	.110	14.2	16.2	.740	.003	1.740	.330	.280
As (µg/l)	1032	13	9.1	3.1	1.25	3.06	133	3.25	2.8	3.35	23.8	8.7	1.25
As(III)(µg/l)	47	•	•	•	•	•	53.6	•	•	•	•	•	•
pH	6.52	6.81	7.09	7.27	7.11	7.01	6.60	6.44	6.96	6.92	6.87	6.67	6.95
Temp (°C)	27.7	30.3	28.9	28.2	28.2	27.3	26.9	27.7	26.8	26.6	26.8	26.6	27.1
Cond (µS)	550	650	675	621	626	600	645	990	801	1657	444	727	669
Eh (mV)	409.3	263.7	343.1	355.8	269.1	398.7	235.1	238.3	317.2	323.4	342.2	362.4	331.9

Cond = conductivity Eh = corrected Eh Values below detection limit set to 0.5 LoD . = no data elements recorded entirely below the LoD are not included

downstream of the primary mining area (RPW 19). Lowest Eh values occur in spring water rising in a marshy area in village 2 (RPW 14). The high organic content of the marsh substrate may account for the relatively reducing conditions at this site.

A relatively high conductivity value (460 μS) was recorded in the Maihom adit (RPW 17, Table 10). The upland area and streams draining the alluvial mining areas to the north and south of Ron Phibun are characterised by low conductivities ($< 100 \mu\text{S}$ at RPW 18, 21, 20, 26, 1, 3, 23, 24, 22, 16). The spring water rising in village 2 also shows a low conductivity (70 and 75 μS at RPW 13 and 14 respectively). An increase of values to within the range 200-328 μS at RPW 5, 6, 7, 9, 12, 10 and 15, is considered to reflect a systematic increase of total dissolved solids (mainly HCO_3^-) over calcareous bedrock (Figure 13). Towards the eastern margin of the sampling area, relatively high conductivities may be compounded by agricultural activities (e.g. RPW 11).

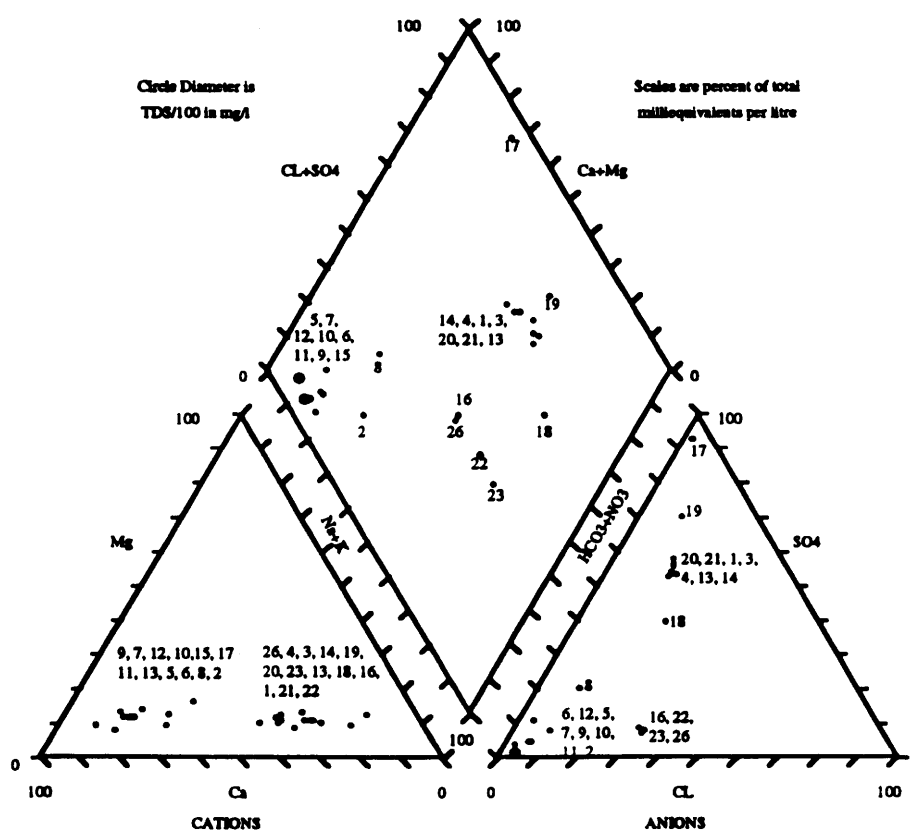


Figure 13. 'Piper diagram' showing major cation, anion and TDS characteristics of Ron Phibun surface waters.

2.2.2.2 *Total arsenic:*

Total As concentrations in surface waters were recorded in the range 4.8- 583 µg/l (Figure 14 and Table 10). With the exception of site RPW 15 all values exceed the WHO interim potable water standard of 10 µg/l. Only one additional site (RPW 5) yields a value compliant with the established EC/US-EPA threshold of 50 µg/l.

The lack of an identifiable pH control on the surface water As distribution ($R = -0.138$: pH vs. As, Table 13) is a striking feature of the data. A relatively low As value of 66 µg/l was recorded in the strongly acid Maihom adit (RPW 17, pH 2.99) while the mine-impacted headwaters of the Hai Ron Na system yielded values in the range 67 - 208 µg/l. Such a trend implies that the mobilisation of As may not be directly related to sulphide oxidation or the attendant generation of acid mine-waters. Furthermore, the Maihom adit and associated waste piles may not constitute the principal source of As inducing local/regional scale surface-water contamination. This supposition is supported by data showing that As concentrations recorded in the upper Hai Ron Na (max 208 µg/l at RPW 1) are substantially lower than recorded in an (apparently) unmined, lithologically analogous catchment, drained by a north-east flowing channel which enters the Hai Ron Na system near sample site 2 (451 µg/l).

The highest As concentrations recorded in surface waters occur downstream of village 2 (RPW 8, 555 µg/l), and downstream of Ron Phibun town (site 10, 583 µg/l) for a distance of at least 4 km (541 µg/l at RPW 11).

2.2.2.3 *Analytical arsenic speciation:*

Analytical data for specific As species, obtained exclusively for surface water samples holding >100 µg/l total As (RPW 1, 2, 3, 4, 6, 7, 8, 9, 10, 11, 12, 13, 18, 20 and 21) are shown in Table 10. Highest absolute concentrations of As(III) occur in waters with highest total As content (28.4 µg/l, 25.6 µg/l and 24.9 µg/l at RPW 11, 8 and 10 respectively). However, As(V) species remain dominant (>92% total As) throughout. This partitioning depicts a highly equilibrated system, as subsequently confirmed by geochemical modelling (section 2.3.2).

2.2.2.4 *Major anions*

The major anion concentrations in surface waters of the Ron Phibun area are shown in Table 10. The dominant anions, HCO₃, SO₄ and Cl, occur in the ranges 10 - 178, 0.87 - 178 and 2.87 - 4.28 mg/l respectively. The Maihom adit water (RPW 17) displays a typical mine-water anion signature, with pronounced SO₄ dominance (146 mg/l, >90% total anion concentration). Sites immediately downstream of the bedrock Sn-W mining area, in the upper Hai Ron Na catchment, are also characteristically SO₄-dominated (RPW 19, 20, 21,

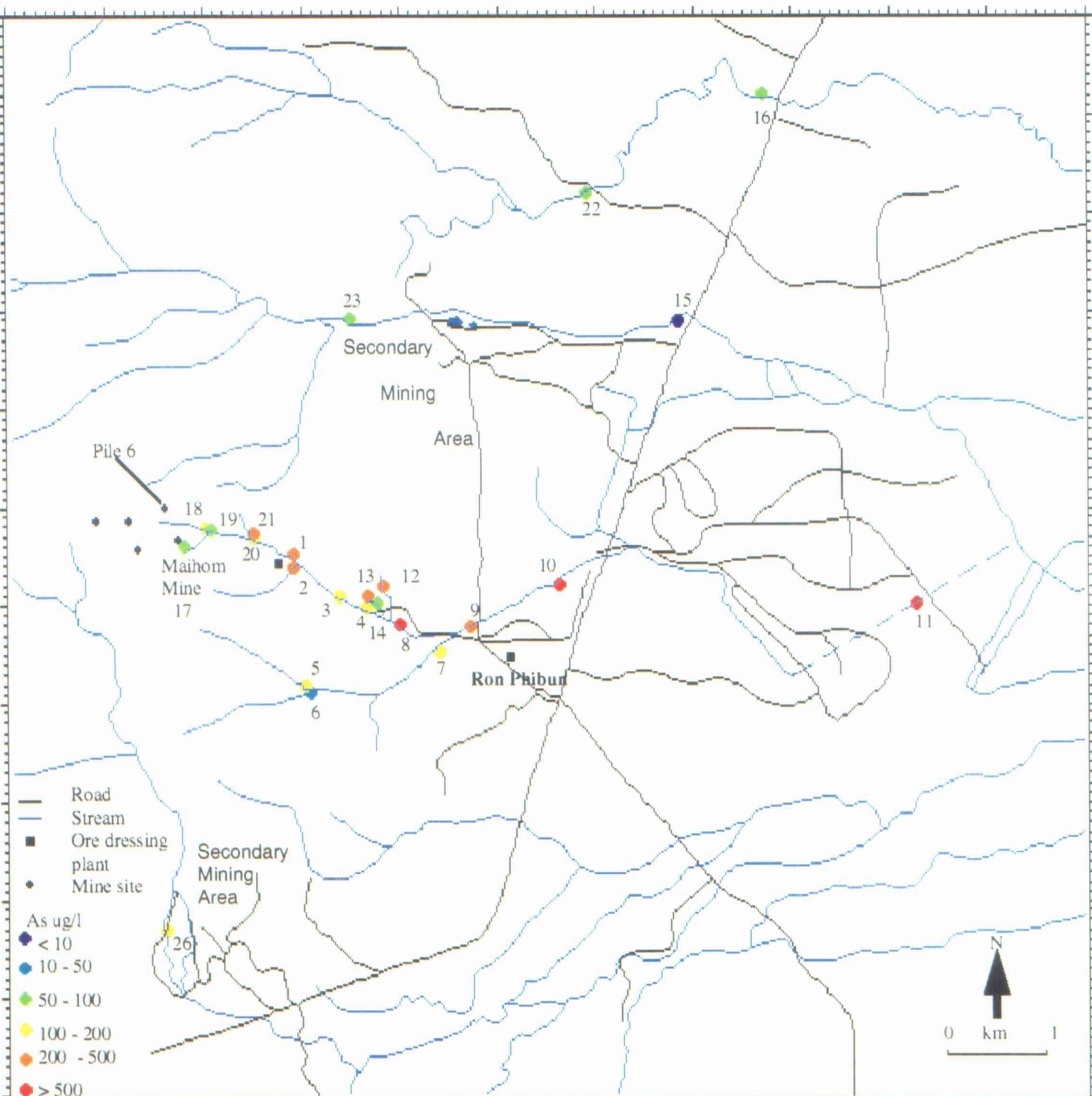


Figure 14. Arsenic concentrations in surface waters recorded at sites RPW1-26 in Ron Phibun District, August 1994.

Table 13. Pearson correlation matrix of determinands in surface waters, Ron Phibun District.

	Sr	Cd	Ba	Si	Mn	Fe	P	B	Mg	Na	Al	Be	Ca	Zn	Cu	Li	Y	K	HCO3	Cl	SO4	NO3	As	pH	Temp	Cond	EH
Sr	1.000																										
Cd	-.554	1.000																									
Ba	.687	-.255	1.000																								
Si	.760	-.139	.272	1.000																							
Mn	-.422	.621	-.003	.261	1.000																						
Fe	.179	.027	.273	.229	.520	1.000																					
P	.619	.486	.977	1.000	.456	.339	1.000																				
B	.159	.159	.460	.655	.621	.421	.334	1.000																			
Mg	.486	.159	.334	.695	.022	.466	.456	.339	1.000																		
Na	.835	.482	.621	.826	.421	.134	.640	.463	.440	1.000																	
Al	.576	.482	.621	.867	.377	.043	.466	.249	.870	.472	1.000																
Be	.835	.950	.164	.125	.607	.080	.219	.153	.501	.926	.926	1.000															
Ca	.981	.413	.718	.285	.685	.049	.107	.159	.433	.803	.438	.387	1.000														
Zn	.626	.958	.190	.266	.669	.043	.225	.106	.559	.571	.918	.862	.491	1.000													
Cu	.554	.936	.257	.194	.552	.080	.175	.167	.464	.509	.908	.862	.431	.860	1.000												
Li	.231	.569	.149	.595	.309	.141	.044	.309	.333	.320	.414	.551	.348	.419	.485	1.000											
Y	-.432	.432	.249	.165	.541	.515	.365	.484	.014	.792	.413	.520	.078	.455	.932	.349	1.000										
K	.951	.588	.664	.658	.507	.044	.513	.423	.941	.264	.258	.594	.910	.682	.506	.143	.425	1.000									
HCO3	.301	.209	.135	.217	.002	.022	.294	.152	.336	.264	.258	.236	.233	.292	.319	.052	.206	.192	1.000								
Cl	.255	.851	.129	.035	.561	.054	.031	.365	.188	.329	.831	.888	.104	.880	.728	.538	.703	.523	.319	1.000							
SO4	.367	.461	.104	.235	.190	.225	.247	.151	.355	.388	.435	.315	.330	.393	.624	.135	.531	.179	.227	.127	1.000						
NO3	.170	.073	-.026	.173	.072	.030	.046	.047	.111	.100	.826	.932	.261	.859	.846	.603	.870	.456	.160	.551	.048	1.000					
As	.145	.281	.005	.002	.222	.329	.034	.263	.119	.208	.322	.194	.093	.150	.447	.184	.559	.124	.084	.321	.815	.138	1.000				
pH	.777	.897	.115	.779	.072	.260	.571	.727	.801	.653	.028	.028	.851	.088	.074	.637	.083	.278	.690	.091	.262	.053	.141	1.000			
Temp	.030	.484	.109	.360	.185	.058	.237	.327	.091	.090	.387	.466	.057	.389	.586	.442	.616	.350	.027	.003	.568	.037	.594	.462	1.000		
Cond																											1.000
EH																											1.000

cond = conductivity R 95% = 0.344 (Koch and Link, 1970) elements recorded entirely below LoD are not included

20,13, 14, 1, 4, 3) (Table 10 and Figure 13). The majority of sites outwith the upper Hai Ron Na catchment are HCO₃-dominated, although Cl is a significant component of the anion budget at sites RPW 26, 16, 23 and 22 (Figure 13 and Table 10).

2.2.2.5 Major cations:

The dominant major cation, Ca, occurs within the concentration range 1.2 - 50 mg/l in Ron Phibun surface waters (Table 10). Dominance of Ca is evident both in the lowland drainage to the east of Ron Phibun town and in the granitic headwater reaches of the Hai Ron Na system (c. 75% total major cations). The strong statistical correlation between Ca and HCO₃ (R = 0.910, Table 13) indicates that CO₃/(H)CO₃ species typically prevail, although sulphate and silicate phases may occur in the more acid reaches of the Hai Ron Na (see section 2.3.2). Absolute concentrations of Ca are systematically highest in the east of the study area, reflecting the influence of carbonate terrain and calcareous overburden.

Sodium (concentration range 3.7 - 8.7 mg/l) is a significant component of the major cation budget of surface waters (>10%) throughout the study area, notably in the lowland regions to the east of Ron Phibun town. A strong statistical correlation between Na and Cl appears to confirm the presence of dissolved Na as NaCl (Table 13). Magnesium is a relatively insignificant component of the cation budget, ratios of Na/Mg typically exceeding 2.0. With the exception of the strongly acid adit water RPW 17, concentrations of K do not exceed 2 mg/l.

2.2.2.6 Minor and Trace Elements:

The minor and trace cations Al, Mn, Cd, Zn and Y show closely covariant surface water distributions, reflected by strong statistical correlations (Table 13). Copper also follows the distribution of this suite, although its statistical association is less apparent. These trace elements (except Fe) are negatively correlated with pH and positively correlated with SO₄ (Table 13), suggesting their direct liberation from sulphides by oxidation and attendant mobilisation in acid mine-waters.

Markedly enhanced concentrations of Al (10.5 mg/l), Fe (4.2 mg/l), Mn (1.4 mg/l), Cd (247 µg/l), Zn (4.2 mg/l) and Y (117.6 µg/l) occur in the Maihom adit water (site RPW 17), and are subsequently maintained throughout the upper reaches of the Hai Ron Na (sites 1, 18, 19, 20, 21 and 22). Values for Fe, Mn, Al and Cd at site RPW 17 exceed WHO thresholds for potable waters (300 µg/l Fe; 100 µg/l Mn; 200 µg/l Al and 5 µg/l Cd) by up to a factor of 52. It is also notable that Al, while not conventionally considered a 'major cation', accounts for approximately 30% of the total cation budget at this site. The influence of recharge water from the granitic margins of the Ron Na-Suang Chan range is indicated by enhancement of Al (398 µg/l) and Zn (201 µg/l) at site RPW13.

With the exception of sample RPW 24, in which is Al (2076 µg/l) is significantly enriched, surface waters to the north and south of Ron Phibun, and the Hai Ron Na downstream of village 2 (site RPW 8) display relatively low concentrations of all analysed minor and trace cations.

The speciation of Fe was determined at sites RPW 1, 2, 3, 14, 16, 17, 18, 20 and 22. None of the surface waters are dominated by Fe(II) species, with only three sites yielding values for ferrous Fe above the detection limit. The acid Maihom adit water (RPW 17) shows the highest absolute Fe(II) concentration (4.13 mg/l), while sites 16 and 22 in the Klong Phut Hong catchment to the north of the mined area yield values of 0.27 mg/l and 0.18 mg/l respectively. The stabilisation of predominantly ferric Fe phases in the surface waters of the Ron Phibun area suggests a high degree of equilibration with the pH/Eh regime, and accounts for the low total dissolved Fe loading reported in most samples.

2.2.3: Groundwaters:

2.2.3.1: pH, Eh and conductivity:

Shallow groundwater pH values were recorded in the range 5.9 - 7.4 (Table 11 and Figure 15). The lowest value of 5.9 was recorded at site RPSW 15, in a small village adjacent to the (now derelict) western ore dressing plant. Weakly acid or neutral pH values (6.0 - 7.0) were recorded over much of the alluvial lowland extending eastward from Ron Phibun town (sites 2,4,1,6 and 11) for a distance of at least 5.5 km (sites RPSW 18 and 19). Neutral or alkaline conditions were recorded in several wells in Ron Phibun town (RPSW 8, 9, 10 and 12), and 1 km north of Ron Phibun in the principal alluvial Sn mining area (RPSW 13 and 14).

Data for pH in deep aquifer waters yield a similar pattern to that in the shallow groundwaters, values lying in a narrow circum-neutral range 6.44 - 7.27 (Table 12).

The shallow groundwater redox regime is characteristically mildly or moderately oxidizing (294 - 438 mV). In the deeper aquifer, a wider Eh range encompasses distinctly reducing conditions (235, 238, 263 and 269 mV at sites RPDW 7, 8, 2 and 5 respectively), and moderately oxic waters (409 mV at site RPDW 1, Table 12). There is no evident stratification of the deep aquifer (Figure 16), with reducing conditions recorded sporadically at depths ranging from <20 - >35 m.

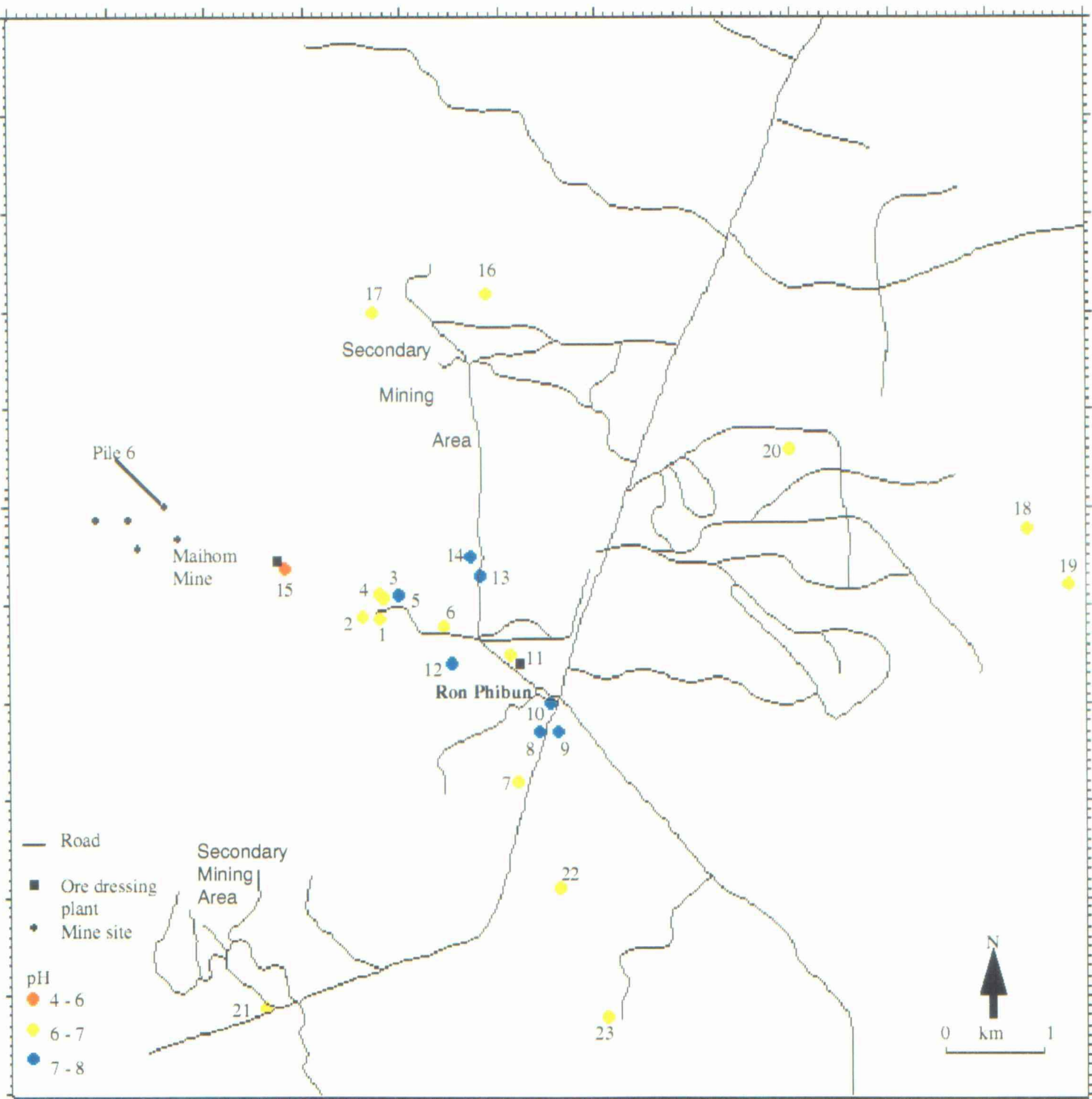


Figure 15. Shallow groundwater pH values recorded at sites RPSW1-23 in Ron Phibun District, August 1994.

A direct relationship is apparent between depth and conductivity in the deep aquifer (Figure 16), reflecting more equilibrated conditions (due to increased retention time at greatest depths).

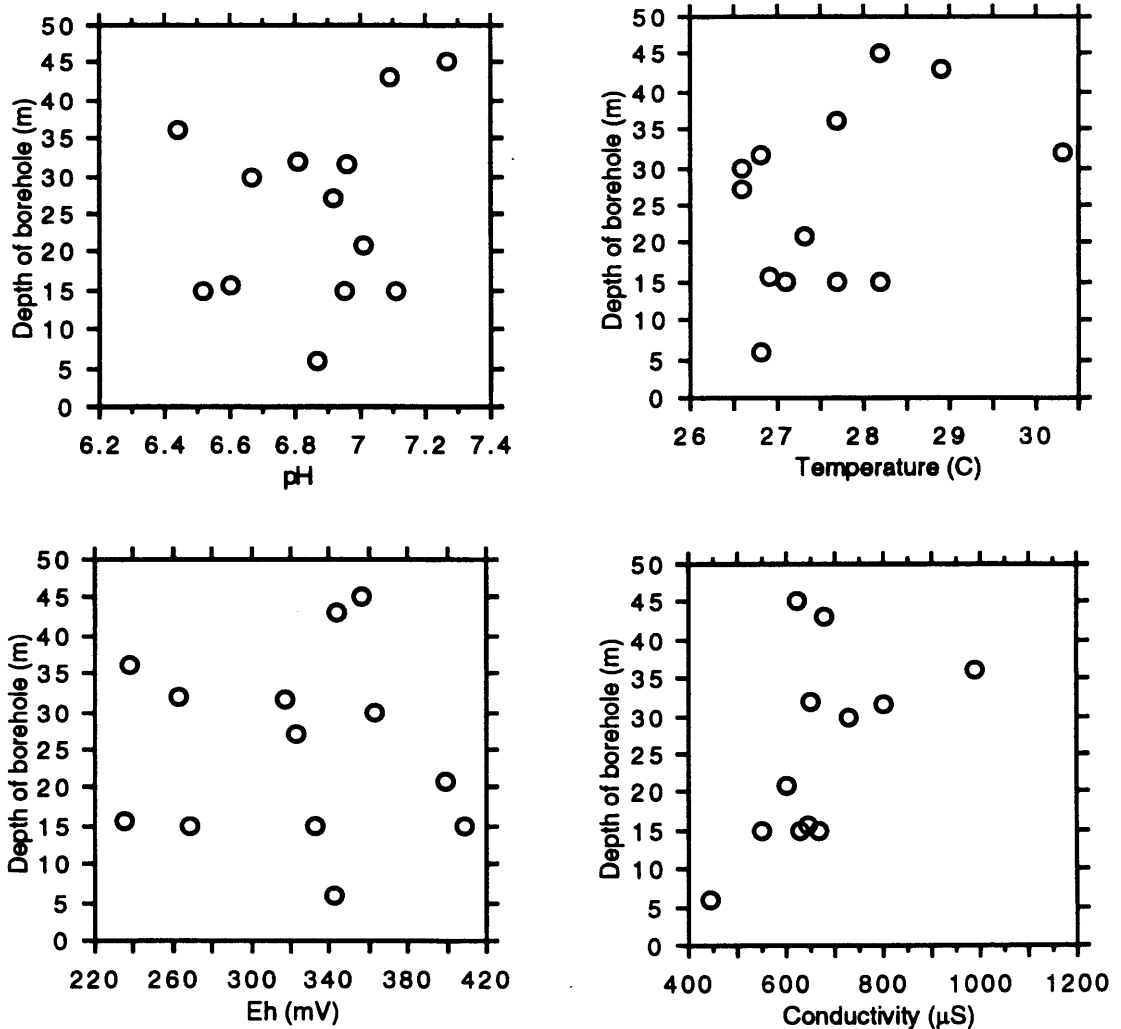


Figure 16. Co-variation of pH, Eh, temperature and conductivity with borehole depth in the carbonate aquifer at deep groundwater sites RPDW 1-13, Ron Phibun District.

2.2.3.2 Total arsenic:

Total arsenic values in the range 1.25 - 5114 $\mu\text{g/l}$ were recorded in shallow groundwaters (Table 11 and Figure 17). Nine of the 23 shallow wells sampled contained As levels above the EC/US-EPA potable water standard of 50 $\mu\text{g/l}$, while 16 yielded concentrations in excess of the 10 $\mu\text{g/l}$ WHO guideline. The spatial distribution of As in the shallow groundwater forms no clear pattern, adjacent wells frequently showing contrasting

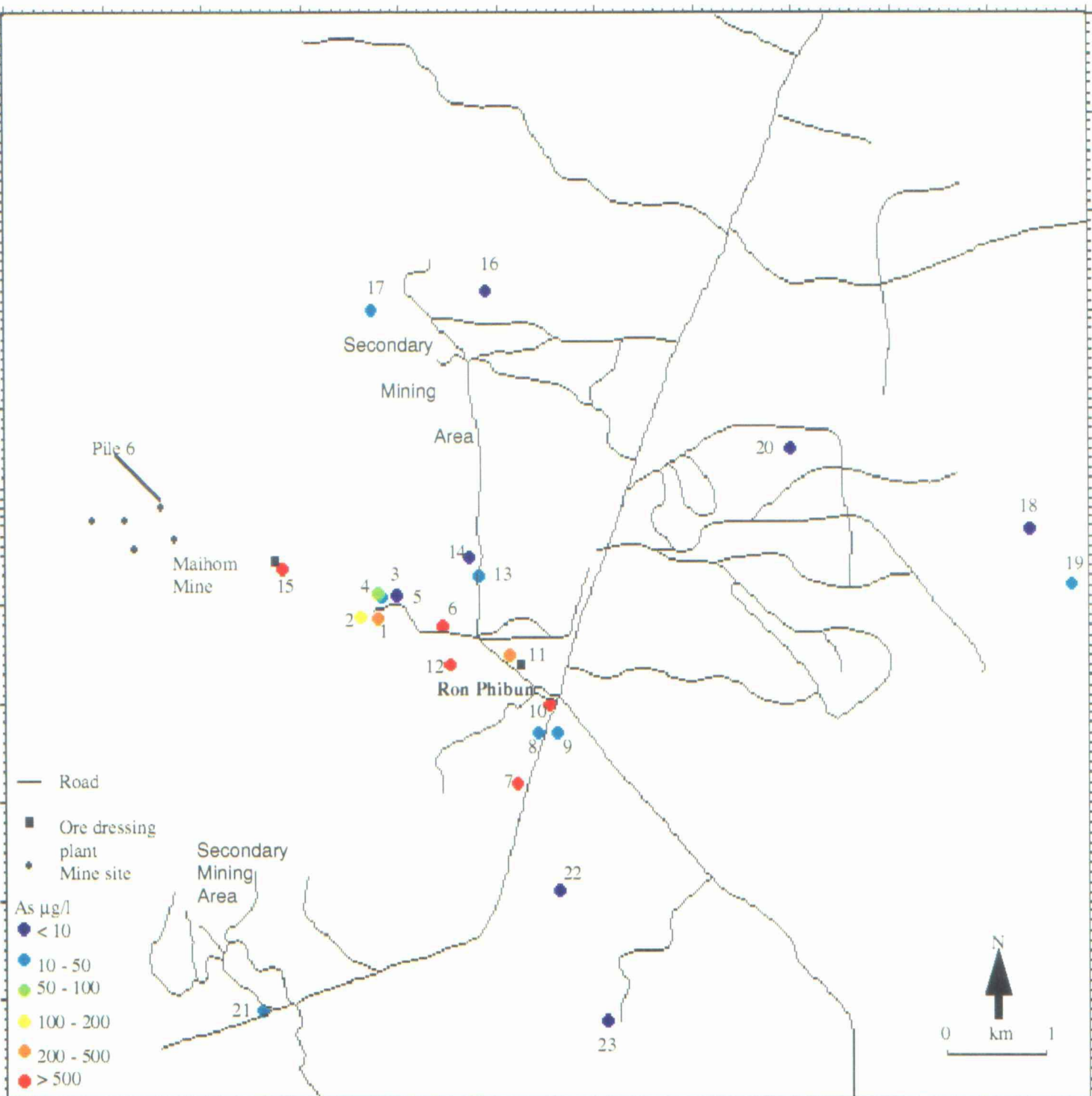


Figure 17. Arsenic concentrations in shallow groundwaters recorded at sites RPSW1-13 in Ron Phibun District, August 1994.

conditions of gross As contamination and relatively high water quality (for example RPSW 8 and 10). However, there is a clear tendency for acute As enrichment ($>1000 \mu\text{g/l}$, maximum $5114 \mu\text{g/l}$) within Ron Phibun town (Figure 17) and in village 2 (Figure 4) as previously reported by DMR. The localised contamination in Ron Phibun town and at RPSW 15 (village 2) can possibly be ascribed to As-rich waste deposition in the vicinity of the ore-dressing plants. In addition, the acid conditions prevalent at RPSW 15 probably result in an increased level of As in solution. The high As level recorded at site RPSW 7 (south of Ron Phibun) may be influenced by recharge from mine-impacted localities of the Ron Na-Suang Chan range, given the predominantly south-easterly direction of the groundwater flow-path in this area (Figure 8).

Arsenic concentrations in well samples from the principal alluvial mining areas to the north and south of Ron Phibun (RPSW 13, 14, 16, 17 and 21) are typically low or moderate ($<50 \mu\text{g/l}$), indicating that contamination from dredging activities is minimal and/ or localised. Arsenic concentrations in shallow groundwater in the agricultural area to the east of Ron Phibun are typically close to, or below, the WHO potable water threshold.

The deep carbonate aquifer waters of the Ron Phibun area show a predominantly lower level of As contamination than water from the overlying alluvial aquifer. Only two of the deep boreholes sampled (sites RPDW 1 and 7) were found to contain significantly enhanced As concentrations ($1032 \mu\text{g/l}$ and $113 \mu\text{g/l}$ respectively), all remaining values falling within the range $1\text{-}23 \mu\text{g/l}$ (Figure 18).

Although As concentrations in the shallow groundwater system vary independently of pH, As correlates significantly with Eh ($R = 0.461$) (Table 11 and Table 14). Data for the deeper carbonate aquifer show a clear inverse relationship between As and pH (Table 12 and Table 15). This is to be expected as As is more readily scavenged from solution by ferric or carbonate flocs or colloidal gels at higher pH. The control of Eh is, however, limited. The two deep boreholes which yield anomalous As levels, RPDW 1 ($1032 \mu\text{g/l}$) and RPDW 7 ($133 \mu\text{g/l}$), exhibit the highest and the lowest Eh values recorded in the entire deep groundwater suite (409 mV and 235 mV respectively).

2.2.3.3 Analytical arsenic speciation:

Arsenic speciation data for shallow and deep groundwaters holding $>100 \mu\text{g/l}$ As (RPSW 1, 2, 6, 7, 9, 10, 11, 12 and 15; RPDW 1 and 7) are provided in Tables 11 and 12. The highest absolute As(III) concentrations in shallow groundwaters occur in wells with the highest total As concentration (RPSW 6, 10 and 15). However, arsenate is the dominant species in all cases. (As(III) component = $2.4 - 6.1 \%$ total As). In contrast, the reducing

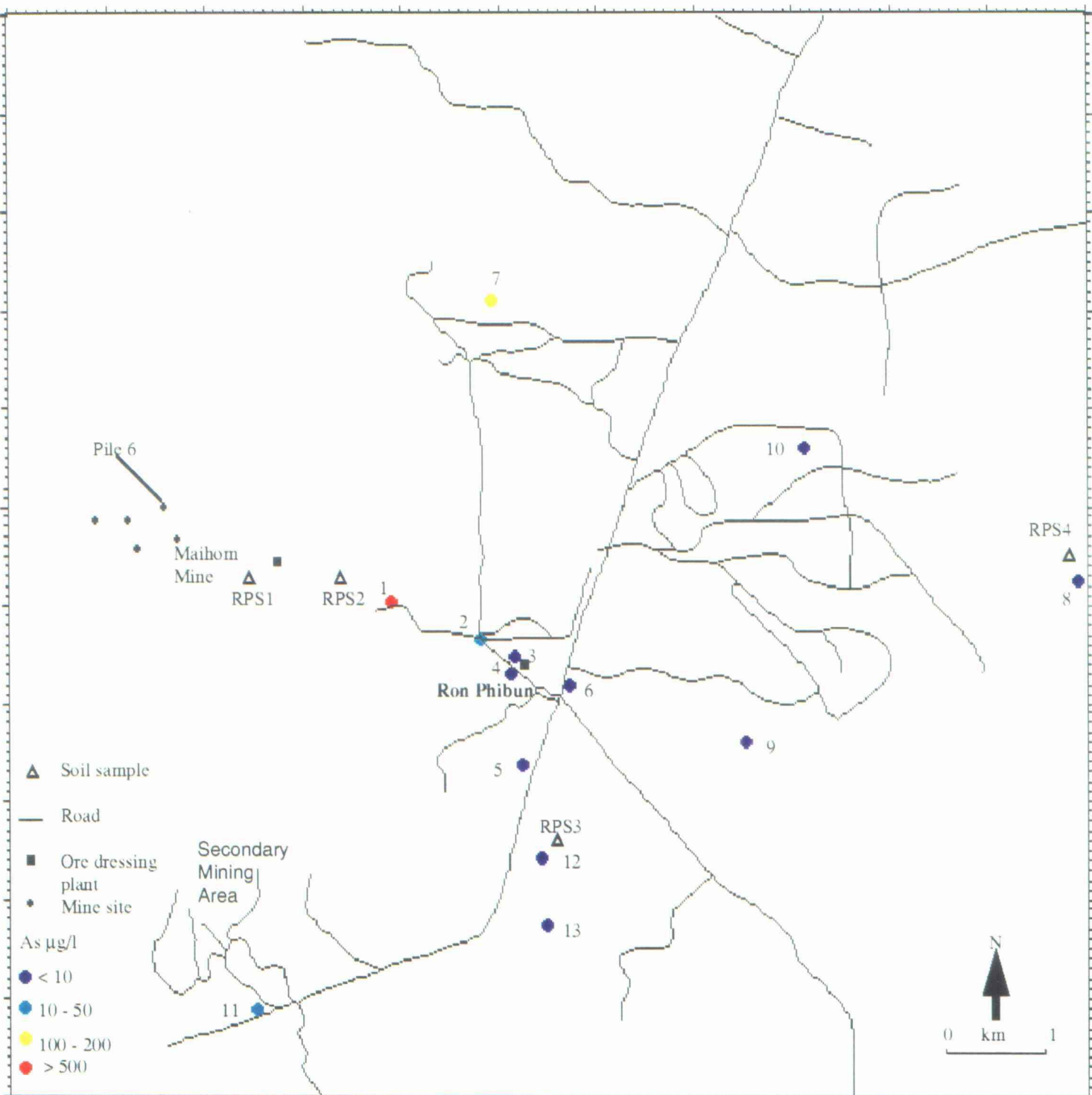


Figure 18. Arsenic concentrations in deep groundwaters recorded at sites RPDW1-13 in Ron Phibun District, August 1994 and the location of soil samples RPS1-4.

Table 14. Pearson correlation matrix of determinands in shallow groundwaters, Ron Phibun District.

	Si	Cd	Ba	Si	Mn	Fe	P	B	Mg	Na	Al	Be	Ca	Zn	Cu	Li	Ni	K	HCO3	Cl	SO4	NO3	As	pH	Temp	Cond	Eh			
Si	1.000																													
Cd	-.494	1.000																												
Ba	-.388	-.315	1.000																											
Si	-.292	-.057	-.091	1.000																										
Mn	-.059	-.015	-.112	-.000	1.000																									
Fe	-.333	-.104	-.229	-.314	-.000	1.000																								
P	-.323	-.104	-.229	-.314	-.000	-.277	1.000																							
B	-.623	-.324	-.349	-.415	-.171	-.277	-.000	1.000																						
Mg	-.930	-.400	-.426	-.443	-.200	-.601	-.176	-.601	1.000																					
Na	-.641	-.211	-.398	-.365	-.200	-.447	-.738	-.740	-.440	1.000																				
Al	-.653	-.542	-.280	-.082	-.082	-.338	-.518	-.492	-.562	-.000	1.000																			
Be	-.367	-.073	-.166	-.053	-.073	-.052	-.148	-.000	-.000	-.000	-.000	1.000																		
Ca	-.484	-.100	-.315	-.057	-.015	-.094	-.324	-.500	-.378	-.211	-.132	-.329	1.000																	
Zn	-.176	-.145	-.097	-.650	-.219	-.097	-.108	-.087	-.283	-.071	-.132	-.329	-.145	1.000																
Cu	-.218	-.045	-.242	-.260	-.475	-.305	-.223	-.045	-.152	-.000	-.145	-.000	-.145	-.223	1.000															
Li	-.353	-.178	-.311	-.157	-.150	-.080	-.669	-.611	-.405	-.702	-.357	-.747	-.964	-.753	-.400	1.000														
Ni	-.666	-.286	-.443	-.283	-.169	-.172	-.672	-.373	-.330	-.968	-.505	-.513	-.613	-.328	-.266	-.008	1.000													
K	-.199	-.107	-.016	-.033	-.049	-.062	-.359	-.489	-.378	-.381	-.159	-.185	-.043	-.262	-.040	-.041	-.210	1.000												
HCO3	-.090	-.040	-.183	-.238	-.100	-.229	-.314	-.051	-.009	-.273	-.293	-.185	-.043	-.226	-.119	-.124	-.000	-.449	1.000											
SO4	-.702	-.364	-.559	-.077	-.142	-.423	-.336	-.463	-.650	-.376	-.201	-.259	-.679	-.403	-.364	-.227	-.020	-.432	-.569	1.000										
NO3	-.108	-.008	-.042	-.347	-.278	-.401	-.148	-.415	-.111	-.164	-.105	-.109	-.021	-.249	-.248	-.402	-.000	-.432	-.569	-.435	1.000									
As	-.924	-.385	-.535	-.280	-.037	-.330	-.709	-.574	-.817	-.843	-.675	-.609	-.929	-.526	-.908	-.850	-.287	-.908	-.850	-.287	-.908	1.000								
pH	-.091	-.290	-.289	-.353	-.256	-.163	-.024	-.315	-.263	-.172	-.153	-.020	-.106	-.299	-.290	-.013	-.080	-.146	-.166	-.240	-.128	-.240	1.000							
Temp																														
Cond																														
Eh																														

Cond = conductivity R 95% = 0.360 (Koch and Link 1970) elements recorded entirely below LoD are not included

Table 15. Pearson correlation matrix of determinands in deep groundwaters, Ron Phibun District.

	Si	Ba	Si	Mn	Fe	P	B	Mg	Na	Be	Ca	Zn	Li	Y	K	HCO3	Cl	SO4	NO3	As	pH	Temp	Cond	Eh					
Si	1.000																												
Ba	-.148	1.000																											
Si	-.143	-.141	1.000																										
Mn	-.216	-.308	-.637	1.000																									
Fe	-.324	-.252	-.410	-.753	1.000																								
P	-.327	-.201	-.367	-.361	-.000	1.000																							
B	-.555	-.179	-.333	-.189	-.249	-.322	1.000																						
Mg	-.491	-.366	-.067	-.085	-.405	-.278	-.114	1.000																					
Na	-.096	-.371	-.253	-.277	-.258	-.241	-.477	-.238	1.000																				
Be	-.331	-.426	-.016	-.285	-.114	-.091	-.073	-.140	-.308	1.000																			
Ca	-.187	-.075	-.538	-.418	-.395	-.660	-.493	-.073	-.057	-.269	1.000																		
Zn	-.788	-.411	-.215	-.115	-.029	-.023	-.309	-.772	-.470	-.169	-.078	1.000																	
Li	-.145	-.464	-.493	-.308	-.506	-.357	-.590	-.211	-.446	-.083	-.296	-.283	1.000																
Y	-.068	-.175	-.232	-.279	-.189	-.477	-.331	-.065	-.338	-.006	-.743	-.464	-.074	1.000															
K	-.068	-.175	-.232	-.279	-.189	-.477	-.331	-.065	-.338	-.006	-.743	-.464	-.074	-.008	1.000														
HCO3	-.061	-.211	-.192	-.244	-.365	-.356	-.106	-.786	-.162	-.006	-.558	-.200	-.108	-.633	-.301	1.000													
Cl	-.061	-.071	-.681	-.357	-.255	-.310	-.439	-.617	-.625	-.231	-.344	-.423	-.640	-.323	-.095	-.263	1.000												
SO4	-.570	-.208	-.234	-.494	-.480	-.509	-.132	-.534	-.022	-.095	-.132	-.289	-.289	-.255	-.100	-.255	-.255	1.000											
NO3	-.186	-.101	-.534	-.064	-.110	-.226	-.065	-.289	-.211	-.748	-.139	-.331	-.118	-.332	-.135	-.039	-.039	-.039	1.000										
As	-.012	-.473	-.592	-.292	-.446	-.499	-.245	-.112	-.258	-.423	-.257	-.342	-.146	-.526	-.223	-.223	-.223	-.223	-.223	1.000									
Temp	-.023	-.422	-.468	-.161	-.023	-.168	-.359	-.181	-.371	-.027	-.342	-.071	-.148	-.050	-.050	-.050	-.050	-.050	-.050	-.050	1.000								
Cond	-.747	-.117	-.094	-.281	-.529	-.489	-.062	-.781	-.801	-.232	-.059	-.248	-.638	-.323	-.224	-.224	-.224	-.224	-.224	-.224	-.224	1.000							
Eh	-.039	-.581	-.518	-.642	-.848	-.620	-.370	-.042	-.273	-.420	-.109	-.093	-.133	-.476	-.379	-.016	-.250	-.176	-.130	-.130	-.299	-.247	1.000						

R 95% = 0.497 (Koch and Link 1970)

deep borehole sample RPDW 7 yielded an As(III) concentration of 53.6 µg/l (39% total As), and a concentration of 47 µg/l As(III) was recorded in RPDW1.

2.2.3.4 Major anions

Concentrations of HCO₃, NO₃, SO₄ and Cl in the shallow groundwater sample suite were recorded in the ranges 20-386 mg/l, 0.1-39.4 mg/l, 1.86-40.4 mg/l and 3.36 - 55.6 mg/l respectively (Table 11). The general spatial pattern with respect to anion dominance is analogous to that recorded in surface waters. Hence, the majority of shallow waters are HCO₃ dominated, with sites RPSW 18 and 16 showing an increased influence of Cl⁻. Sites RPSW 1, 2 and 5 are SO₄ dominated, on account of their very low HCO₃ concentrations (Figure 19).

In the deep carbonate aquifer, HCO₃, NO₃, SO₄ and Cl⁻ concentrations vary from 78 - 653, 0.1-28.2, 0.24-277 and 3.8 -132 mg/l respectively (Table 12). Levels of HCO₃ are higher in deep waters than recorded in both shallow groundwaters and surface waters on account of the increased water-rock interaction with limestone matrices. Accordingly, all deep waters are HCO₃-dominated, although the contribution to the total anion budget made by Cl⁻ is elevated at sites RPDW 8 and 11, and sulphate is a major component of RPDW 10 (Figure 20).

2.2.3.5 Major cations

Major cation abundances in shallow and deep groundwaters of the Ron Phibun area are outlined in Table 11 and Table 12 respectively. Calcium is the dominant cation at the majority of sites, with generally higher concentrations in the deep aquifer (35-103 mg/l) reflecting an increase in the dissolution of CaCO₃ from the carbonate bedrock. The close spatial relationship between high Ca and HCO₃, and the strong correlation ($R > 0.7$) between Ca and HCO₃ (Tables 14 and 15) indicate that carbonate and/or bicarbonate species are the principal carriers.

The shallow and deep aquifers show considerable 'internal' variability with respect to salinity. Sodium routinely exceeds Mg in concentration, and forms the dominant major cation in isolated instances (245 mg/l in RPSW 18, 209 mg/l in RPDW 10, Figures 19 and 20).

Relatively high K concentrations (frequently exceeding Mg) prevail in the shallow groundwaters (max. 22 mg/l in RPSW 10), but fall significantly in the deeper carbonate aquifer (max. 6.3 mg/l).

2.2.3.6 Minor and trace elements:

Minor and trace element abundances in shallow groundwaters are generally low (Table 11), with few notable features. Waters from several shallow wells (RPSW 1, 2, 3, 5, 6, 7, 9, 12, 13, 14, 15, 18, 19, 20, 21, 22, 23) do, however, contain Mn concentrations which exceed the WHO potable water guideline (100 µg/l). One anomalous sample, yielding a value of 8.06 mg/l Mn (RPSW 6) is also distinguished by its extremely high As content (>5 mg/l). The source of Mn and its solubility controls are highly uncertain. Divalent Mn is theoretically stable in solution across a wide pH-Eh range (Figure 21), but the localised reduction and dissolution of solid Mn phases required to provide an adequate supply to the shallow groundwater is difficult to envisage under the near-neutral, oxidizing conditions prevailing.

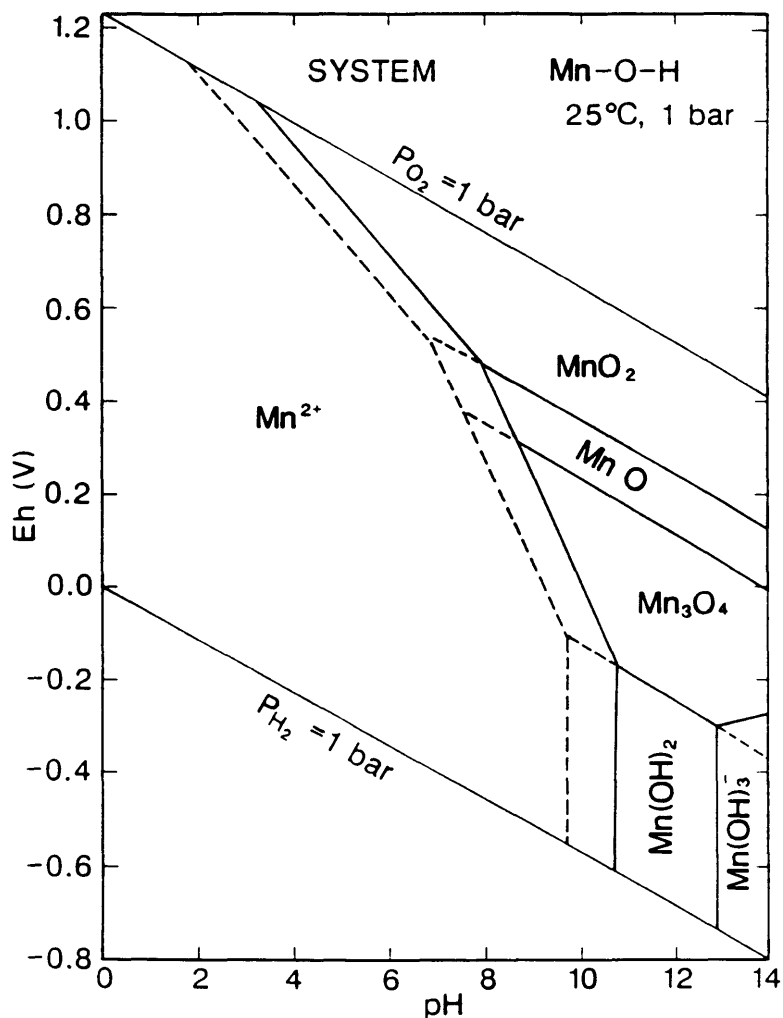


Figure 21. Eh-pH diagram for the system Mn-O-H (after Brookins 1988)

Concentrations of dissolved Fe in the shallow groundwaters are low (0.07 - 0.321 mg/l), as would be expected under the moderate pH/ Eh regime. The WHO guideline of 300 µg/l Fe is exceeded only at site 15, where locally acid conditions (pH 5.95) could account for the

increased Fe solubility. Waters from sites RPSW 1, 3, 5, 6, 7, 10, 12, 15, 16, 19 and 20 were analysed for Fe(II), of which only site 15 showed a predominance of Fe in ferrous form.

Other elements recorded at concentrations which exceed WHO thresholds include Al (>200 µg/l at sites RPSW 1, 2 and 5) and Cd (18.9 µg/l at RPSW 2). Sites RPSW 1, 2 and 5 are located in village 2, and may be affected by spring water known to carry enhanced Al concentrations (as confirmed by surface water RPW 13). The increased Cd content of RPSW 2 (also in village 2) corresponds closely with the anomalous surface water Cd detected in this area.

Minor and trace element concentrations in deep aquifer waters are generally lower than those of the shallow groundwater (despite their longer residence time), and typically lie within WHO potable water guidelines (Table 15). Manganese is sporadically enhanced, notably in conjunction with Fe (14 mg/l) and Zn (6857 µg/l) in the reducing water RPDW 7 (2.3 mg/l Mn). Sites 2, 5, 7, 8, 9, 10, 12 and 13 contain levels of Fe above the WHO guideline of 300 µg/l. Both Mn and Fe show a strong negative correlation with Eh ($R < -0.6$, Table 15). All the deep borehole samples were analysed for Fe(II) content. Waters from sites 1, 2, 5, 6, 7, 8, 9, 11, 12 and 13 were found to contain detectable levels of ferrous Fe. In contrast to the surface waters and shallow groundwaters, the contribution of this phase to total Fe ranges from 70-100%.

2.3 Geochemical modelling

2.3.1 Methodology

Equilibrium-speciation models provide a valuable tool for appraising mechanisms of metal transport and attenuation in surface and groundwater systems, and are increasingly being used for hydrochemical characterisation and toxicological risk assessment of mine-waters (Alpers and Nordstrom, 1990; Williams and Smith, 1994). The range of aqueous metal species, their stability and degree of saturation in Ron Phibun surface waters (RPW 2, 11 and 17), shallow groundwaters (RPSW 6, 7 and 10) and deep groundwaters (RPDW 1 and 7) was assessed using the equilibrium code WATEQ4F (Ball et al, 1987). Full WATEQ4F output is provided in a supplementary appendix volume A (held in BGS Overseas Geology Series archives).

From a theoretical viewpoint, the WATEQ4F model requires that (i) the aqueous system is in full chemical equilibrium (between solid, aqueous and gas phases) and (ii) kinetic constraints on speciation adjustments do not operate. In the acid regime of the headwater surface drainage at Ron Phibun and, to a lesser extent, the shallow aquifer waters with relatively low residence times, these requirements may not be met. The

slow kinetics of many oxidation-reduction reactions, coupled with the relatively rapid transport of reactants from precipitated products, creates an empirical situation in which chemical equilibrium is highly variable and largely determined by flow rates.

The WATEQ4F code facilitates the calculation of saturation indices (SI) for some 600 minerals for which data are held within the database. It should be stressed that SI values signify the extent of theoretical dis-equilibrium (in terms of under- or over-saturation). In the absence of kinetic data, SI values indicating over-saturation with respect to a given mineral phase need not imply that precipitation will actually take place. By convention, $SI = \log Q - \log K$, where $\log Q$ is the activity quotient which is equal to $\log K$, the equilibrium constant at equilibrium. Accordingly, $SI < 0$ = under-saturation; $SI = 0$ at equilibrium; $SI > 0$ = over-saturation.

The thermodynamic constants used for calculating chemical equilibria for Ron Phibun waters were unchanged from those in the original WATEQ4F dataset. Correct operation of the Fortran code was ensured by running and cross-checking results against output for standard test cases for seawater, surface water and an acidic volcanic condensate. Empirical input data included pH, Eh (temp. corrected), Ca, Mg, Na, K, Cl, HCO_3 , SO_4 , Fe, Mn, Cu, Zn, Ni and As. Sample density was assumed to be 1.00 g/cm^3 in all cases.

Charge-balance errors for the empirical input data were determined as:- RPW 2 = 7.1%, RPW 11 = 3.44%, RPW 17 = 15%, RPSW 6 = -0.53%, RPSW 7 = -2.09, RPDW 1 = -4.00, RPDW 7 = 15.86. Modelled balance errors (based on post-speciation discrepancies determined by the WATEQ4F code) were within 2% of the input errors in all cases. Calculations of total ionic strength (TIS) based on input data were within the range 0.007 - 0.12 for all samples. Estimated ionic strength (EIS) data (based on modelled speciation) were within 1% of the empirical values in all cases.

2.3.2. Modelled arsenic speciation.

Modelled equilibrium-speciation data for As confirm empirical observations of arsenate dominance throughout the surface drainage, shallow groundwater and deep groundwater systems (Figure 22). Oxyanions dominate, with the ratio of monovalent to divalent species ($\text{H}_2\text{AsO}_4^{-1}/\text{HAsO}_4^{-2}$) controlled by pH. Ratios of >1 characterise relatively low pH waters, including RPW 2 (pH 6.3, ratio 2.5), RPDW 1 (pH 6.5, ratio 1.29) and RPDW 7 (pH 6.6, ratio 1.01), rising to an infinite value (ie. zero HAsO_4^{-2}) in the strongly acid adit water RPW 17 (pH 2.99). Low ratios generally

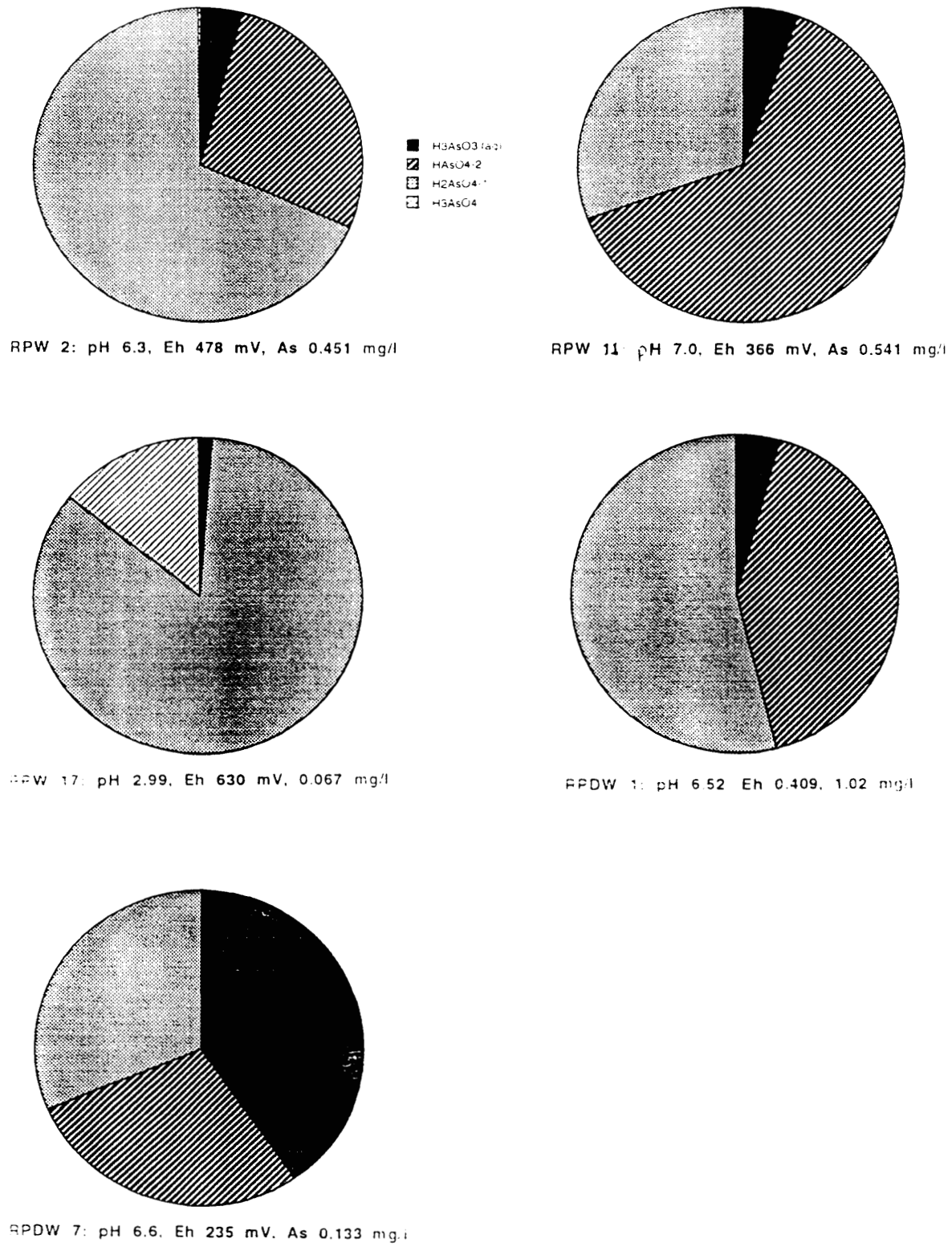


Figure 22. Modelled As speciation in surface drainage samples RPW 2, 11 and 17, and deep groundwaters RPDW 1 and 7. Arsenate dominance is indicated in surface waters and moderately oxidizing groundwater RPDW1. A substantial arsenite component is stabilised in reducing groundwater RPDW 7. Charge-partitioning of arsenate is strongly pH controlled, with divalent oxyanions dominating at highest pH values.

prevail at pH values of >6.5, exemplified by RPW 11 (pH 7.0, ratio 0.46). The 'neutral' species H_3AsO_4 is predicted as a significant component (13%) of total As only under the strongly acid regime of RPW 17. There is no systematic differentiation between the charge-partitioning of arsenate in surface drainage, shallow groundwaters and deep groundwaters.

Thermodynamic calculations favour a very small H_3AsO_3 component in all modelled surface drainage and shallow groundwaters (RPW 2: 4% total As, RPW 11: 5%, RPW 17: 1.5 %, RPSW 6: <1%, RPSW 7: 5%). A more variable arsenite component is, however, predicted in deep aquifer waters (Figure 22), ranging from 4.5% total As in RPDW 1 to 39% in RPDW 7 (in association with Eh 235 mV, Fe^{2+} dominance and probable sulphate reduction). The modelled distribution of H_3AsO_3 is closely compliant with analytical data for As speciation.

Saturation indices for a range of As phases including arsenolite, $\text{Ba}_3(\text{AsO}_4)_2$, $\text{Ca}_3(\text{AsO}_4)_2$ and scorodite signify that precipitation of discrete As minerals is strictly limited in all waters. Regulation of dissolved As loadings is thus likely to be through scavenging by non-As phases. While, saturation with respect to $\text{Ba}_3(\text{AsO}_4)_2$ (SI range 5.4 - 12.0) is indicated in all waters with the exception of the strongly acid adit sample RPW 17 (SI -8.1), the solubility-product of this phase is extremely low (7.7×10^{-51}). Saturation thus occurs at negligible ambient Ba concentrations, and precipitation of the mineral is rarely a significant constraint on overall As mobility.

2.3.3. Modelled surface water hydrochemistry.

The acidic headwater drainage of the Ron Na system (adit water RPW 17) shows a predominance of major divalent cations (Mg^{2+} and Ca^{2+}) and trace metals (e.g. Fe, Cu, Zn, Cd) in uncomplexed form (>80% total). With respect to Fe, Zn and Cd, the remaining fraction is present as MSO_4 (9-14 % total). The predicted occurrence of CdSO_4 is particularly notable as the stability field of this phase is strictly confined to very low pH. Aluminium shows a more equal partitioning between uncomplexed Al^{3+} (57%) and AlSO_4 (41%). Carbonate (or bicarbonate) species account for a minor component of total Cu.

WATEQ4F speciation calculations for stream waters RPW 2 and RPW 11 highlight a series of progressive hydrochemical adjustments with increasing distance from the Ron Na headwaters (and with increased buffering). At RPW 2, major cations and trace metals occur almost exclusively as uncomplexed mono- and divalent species (e.g. Ca^{2+} >97%, Mg^{2+} >97%, Fe^{2+} >90%, Zn^{2+} >90%), with SO_4 components depleted in the

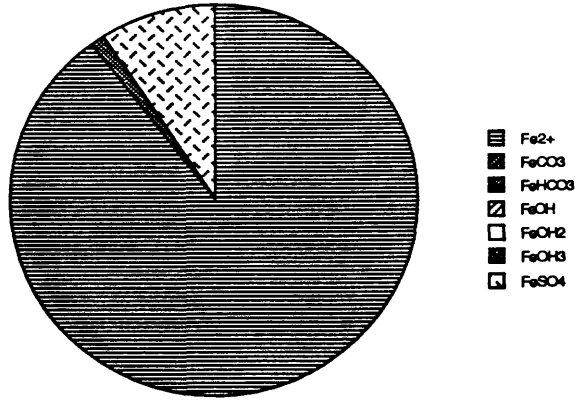
weakly acid (pH 6.3) regime. Further downstream, an adjustment involving the stabilisation of significant hydroxyl (>80 % Fe) and carbonate (12% Zn) complexes, is favoured under neutral conditions (and higher HCO₃ loading) at station RPW 11. The contrasting partitioning of Fe in surface waters with increasing distance from the upland Sn-W mining localities to the west of Ron Phibun is graphically illustrated in Figure 23.

Modelled surface waters are characteristically undersaturated with respect to their most abundant dissolved (complexed) species (e.g. MSO_4 in RPW 17, $\text{M}(\text{OH})$ and CO_3/HCO_3 species in RPW 2 and 11). The Fe and SO_4 concentrations at RPW 17 are relatively low for acid mine-water, with resultant undersaturation with respect to common precipitates such as jarosites and Fe oxy-hydroxides. This position is redressed with increasing pH downstream, as signified by positive SI values for ferrihydrite (1.5) and goethite (7.4) at RPW 11. An increasing degree of saturation with respect to CaCO_3 is also evident towards the lower sectors of the Ron Na system (SI rising from -6 at RPW 17, to -2 at RPW 2 and -0.9 at RPW 11).

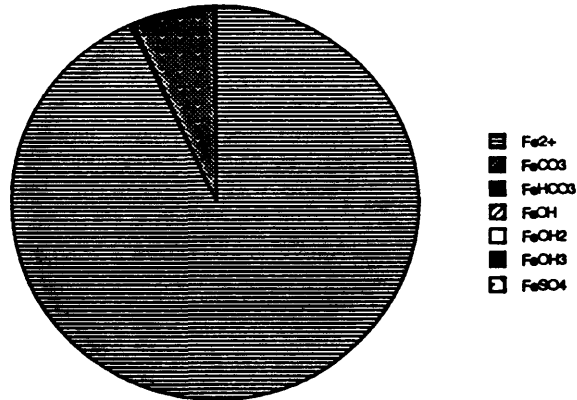
2.3.4. Modelled groundwater hydrochemistry

The shallow and deep groundwater systems have analogous equilibrium hydrochemical characteristics, with a predominance of uncomplexed major and trace cations. The significance of (bi-)carbonate and hydroxyl trace metal species is, however, considerably greater than in surface drainage. In shallow groundwater samples carbonate/bicarbonate phases account for 23-27% of total Fe, 29-40% Zn and up to 79% Ni. In the deeper groundwaters, $(\text{H})\text{CO}_3$ complexes account for up to 24% of total Fe and 29% Zn. Stabilisation of 10% total Fe as $\text{Fe}(\text{OH})$ complexes is predicted in moderately oxidizing sample RPDW 1, but such species are absent in the low Eh regime (235 mV) of RPDW7.

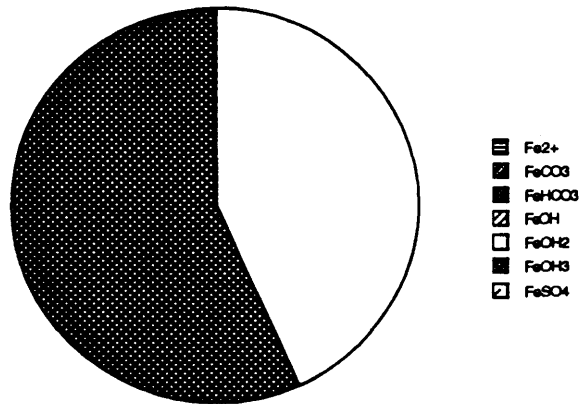
Groundwater SI calculations indicate a generally low degree of major solute equilibration (possibly influenced by short residence times) in both the shallow and deep aquifers. Surprisingly, the degree of undersaturation with respect to CaCO_3 is greater in the deep than in the shallow groundwaters (despite analogous pH conditions in the two systems). A positive SI value for this phase is recorded only in RPSW 7 (0.17). Values of -0.43 and -0.45 have been calculated for RPDW 1 and RPDW 7. The degree of Fe saturation varies significantly between oxidizing (RPDW1) and reducing (RPDW 7) sectors of the deep aquifer, exemplified by a positive SI for ferrihydrite (0.14) in the former and a negative value in the latter (-0.66).



RPW 17: pH 2.99, Eh 630 mV, Fe 4.11 mg/l



RPW 2: pH 6.3, Eh 478 mV, Fe 0.025 mg/l



RPW 11: pH 7.0, Eh 366 mV, Fe 0.087 mg/l

Figure 23. Modelled Fe speciation in surface drainage samples RPW 2, 11 and 17. A progressive downstream progression from a mine-water signature (RPW 17) in which uncomplexed Fe²⁺ and FeSO₄ dominate, towards a (saturated) hydroxyl-dominated Fe chemistry (RPW 11) is evident.

2.4 Arsenic pedogeochemistry

2.4.1 Methodology

Sequential extractive procedures formulated by Breward and Peachey (1983) were applied to 'B-horizon' soils from three sites (coded RPS 1-3), plus a comparative A and B horizon suite from a fourth sampling site (RPS 4). Samples RPS 1 and 2 were collected from village area 2, in the upper and mid catchment areas of the Hai Ron Na. The former was recovered from a pit approximately 50 m west of stream sampling site RPW 2 (near the now derelict 'upper' ore dressing plant) and comprised yellow silty clay with an abundance of quartz fragments. The latter was obtained from the central area of village 2, in an area of sandy alluvium. Samples RPS 3 and 4 (A-B) were collected from agricultural land to the east of Ron Phibun town, from thick clay-rich, variably gleyed profiles. All sampling locations are given in Figure 18.

Oxidation of sample material was avoided prior to analysis to preclude adjustments of speciation. The partitioning of As in each sample was determined by use of a three stage extractive sequence. Approximately 1g of soil (dry wt.) was initially leached with 1M NH₄OH to remove organic matter, which was subsequently separated into fulvic and humic fractions by HCl precipitation. The inorganic residuum remaining after the NH₄OH application was then leached for 1 hour with Tamm's reagent (oxalic acid and ammonium oxalate mixture) to remove Fe-oxide-bound phases. Washing of the residuum was undertaken between each stage to avoid cross-contamination and/or reduced efficiency of extractants. All leachates were analysed by a combination of hydride generation AAS and ICP-AES methods, as applied for natural waters (section 2.2.1). A semi-quantitative XRF analysis of a bulk-sub-sample of soil from each site was used to provide an indication of total As content.

2.4.2 Results

Total As concentrations showed significant variations between sample localities, with pronounced enrichment noted only at sites RPS 1 (c. 550 µg/g) and RPS 2 (>5000 µg/g). Samples RPW 3, RPW 4A and RPW 4B each yielded total As concentrations of <100 µg/g. On the basis of this limited information, the zone of soil enrichment can be assumed not to extend onto the carbonate terrain to the east of the main Nakhon si Thammarat highway.

The concentrations of As held in fulvic organic, humic organic and Fe-oxide fractions of each analysed sample are shown in Table 16. The enriched samples, RPS 1 and RPS 2 yielded only around 20% of their total As content during the leaching sequence, of which the dominant component was found to be associated with crystalline ferric

oxides. The remainder is assumed to be held as detrital sulphides, suggesting that the soils overlying the Ron Na-Suang Chan massif, and the alluvial deposits immediately adjacent to the granite terrain (in villages 2 and 12) hold a substantial reservoir of arsenopyrite. In the less As enriched soils from sites RPS 3 and RPS 4, iron oxides and fulvic organics appear to hold a negligible fraction of the total soil As content, and detrital (sulphide) phases may, again, dominate. However, a partitioning of over 39% As into humic organic matter was noted in the gleyed B horizon at site RPS 4. This suggests that arsenopyrite is rapidly dissolved in the reducing sub-surface environment, and scavenged by organics on account of a virtual absence of ferric iron.

Table 16. Results of sequential extraction of As in soils from Ron Phibun District

Sample	Fulvic As ($\mu\text{g/g}$)	% total	Humic As ($\mu\text{g/g}$)	% total	Fe-oxide As ($\mu\text{g/g}$)	% total
RPS1	10.75	1.9	12.5	2.2	88.7	16.0
RPS2	266.2	5.3	4.5	<0.01	879.0	17.5
RPS3	2	2.8	1.27	1.7	20.7	29.5
RPS4A	1.25	1.3	1.25	1.3	2.25	2.5
RPS4B	1.25	1.7	27.5	39.2	2.2	3.1

3. DISCUSSION

3.1. Mechanisms of surface and groundwater water contamination

Previous geochemical investigations by DMR in the Ron Phibun area have highlighted primary Sn-W mining activities (principally on the eastern flank of the Ron Na-Suang Chan massif), commercial alluvial Sn mining, ore-dressing and the disparate activities of small scale prospectors as potential causes of As contamination. Of these, the arsenopyrite-waste piles derived from the exploitation of Sn-W-As-rich pegmatite veins on the steep granite slopes to the west of Ron Phibun have been identified as posing the most critical hazard. These waste-piles currently form the main focus of DMR research efforts towards the design of a successful pollution mitigation strategy, and clearly warrant particular scrutiny.

3.1.1 High-grade waste piles

The significance of the As-rich waste piles at Maihom and neighbouring extractive localities of the Ron Na Suang range with respect to local or sub-regional scale surface water contamination can be appraised from the mineralogical data presented (for mine waste), in conjunction with hydrochemical data for outflow drainage from the former Sn-W-As mining area (ie. the headwaters of the Hai Ron Na). The mineralogical data depict a contaminant source enriched in both As and heavy metals (including Pb, Zn and Cd). However, the paragenetic sequences initiated by the weathering of As and heavy metal

sulphides, and hence the release rates of these elements, differ markedly. In the case of As, an in-situ process of immobilisation, involving the growth in place of relatively insoluble ferric arsenates (following arsenopyrite oxidation) restricts the proportion of water-soluble As in the weathered waste to much lower levels than reported for many other As-rich tailings sites in SE Asia and tropical Africa (e.g. Williams et al., 1994; Williams and Smith 1994). In contrast, the partitioning of heavy metals into sulphates following sulphide degradation induces high solubility, and a rapid flux of elements such as Pb, Zn and Cd into the outflow waters.

This differential mobilisation of As and heavy metals from the 'high-grade' waste exerts a corresponding influence on the hydrochemical signature of the Hai Ron Na headwaters. Hence, the Maihom adit water, and all stream water samples collected from within c. 600 m of the principal arsenopyrite piles, show enrichment of Cd, Al, Cu and Zn (by 2 orders of magnitude relative to the regional average), yet As concentrations remain below the regional median. In the case of adit water RPW 17, the reported As concentration (66 µg/l) is the fifth lowest of the entire surface water dataset. Further downstream, the aqueous behaviour of As and the contaminant metals continues to be inversely related. While Cd, Al and Zn attenuate (in response to increasing pH) in the mid-reaches of the Hai Ron Na (downstream of site RPW 8), As concentrations show a marked increase to >500 µg/l.

Given the relatively low concentrations of As (<200 µg/l) recorded in the Hai Ron Na headwaters (close to the former Maihom mine and neighbouring bedrock workings) it is difficult to envisage the As-rich waste piles of the Ron Na Suang range as the principal source of the high As concentrations (>500 µg/l) reported for surface waters of the lower catchment area. Furthermore, it is unlikely that As from these waste accumulations could exert a major effect on the shallow or deep aquifers to the east of the granite massif. The terrain on the eastern flank of the Ron Na Suang range (ie. between the bedrock mining area and stream site RPW 2) is steep, virtually devoid of overburden and underlain by granites with low fracture porosity. Surface runoff pathways therefore constitute the only plausible mechanism by which recharge water from the Maihom mining area could be carried towards the shallow or carbonate aquifers of the colluvial plain. A more detailed examination of the role of alternative As contaminant sources affecting surface- and groundwaters is thus fully warranted.

3.1.2 Alternative sources of As contamination

It would appear from the relatively high values of As (> 200 µg/l) recorded in surface and shallow groundwaters in the vicinity of the dressing plants located to the west of village 2 and in Ron Phibun town that waste from these plants (and near-by small-scale prospecting activities) probably constitute a major source of As contamination. However, the increase

in As concentration at these sites (RPW 8, 9, and 10; RPSW 15, 1, 2, 12, 11 and 10) does not correspond to increased levels of other heavy metals with the exception of Fe. The extent, distribution, mineral assemblage and weathering mechanism of waste associated with the ore dressing and panning activities must be established to fully evaluate the influence that these sources exert on local geochemical conditions.

Although the zone of high As values in surface and shallow groundwaters in the Hai Ron Na catchment is largely covered by alluvial deposits that have clearly been dredged in the past, it is uncertain whether these deposits are an active contaminant source. Certainly, the acute contamination contrasts with the relatively low As concentrations ($< 100 \mu\text{g/l}$) recorded in alluvial mining areas in adjacent catchments. Two possible scenarios could therefore be indicated: (i) alluvial mining activity exerts little control on As concentrations in waters, and the presence of other factors in the Hai Ron Na catchment account for the As contamination, or (ii) the alluvium in the Hai Ron Na catchment, which is derived from the main primary mined area, contains higher levels of As than in the surrounding deposits. The soil data presented for RPS 2 (village 2) confirm that the concentrations of As in alluvium in this area are indeed very high ($> 5000 \mu\text{g/g}$) and that much remains in detrital minerals. However, it is not known if similar As concentrations prevail in alluvial deposits in catchments to the north and south of the Hai Ron Na. It is also possible that the actual concentrations of As in alluvium are not the primary factor determining how readily As is released into the groundwater. The multi-element composition of the alluvium, notably the presence of elements which can immobilise As following the weathering of sulphides, could be equally important. Although data for other major and trace elements in soils have not been collected in this study, the clean quartzose Fe-poor nature of alluvial soil at site RPS 2 was visually noted during sampling. In studies of similarly Fe-poor soils in Zimbabwe (Williams and Smith 1994), As has been shown to be highly mobile due to the absence of hydrous oxide scavenging agents. Detailed investigations into the mineralogy and multi-element chemistry, particularly the As and Fe content, and the groundwater redox conditions and flow characteristics in the alluvium are required to quantify the influence of the alluvial deposits on As contamination

3.2: Toxicological aspects of As contamination at Ron Phibun

Evidence from numerous regions of Asia and Latin America has indicated that the dose-response relationship between human arsenism and As in drinking water is relatively simplistic at high ambient As concentrations ($>500 \mu\text{g/l}$), but becomes complex within the lower ($<200 \mu\text{g/l}$) sector of the curve. Population responses to acute, yet variable levels of As contamination have been documented for parts of Mexico (Espinoza, 1963), Taiwan (Tseng, 1968) and Chile (Borgono and Griber, 1972). These studies indicate that symptoms of arsenism (principally skin lesions and cancer) routinely affect $>50\%$ of

exposed subjects at As concentrations of 4-6 mg/l (equating to an average adult ingestion of 110-170 $\mu\text{g}/\text{kg}/\text{day}$) with a sub-linear decline in incidence as concentrations fall to c. 500 $\mu\text{g}/\text{l}$. The epidemiological data collected by Thai and Japanese authorities for the Ron Phibun District, indicating a district-wide skin lesion or hyper-pigmentation incidence of >20%, rising to over 90% in the immediate vicinity of Ron Phibun town, appear consistent with this international trend. Data obtained in this study have shown that shallow groundwater concentrations in the most contaminated wells in village areas 2 and 12 fall within the 4-6 mg/l range considered likely to induce visible arsenism symptoms in a majority of the population.

Despite the sporadically high (>1 mg/l) concentrations of As in shallow and deep groundwaters in village areas 2 and 12, the average groundwater concentration over the entire study area is approximately 350 $\mu\text{g}/\text{l}$. This value is reduced to <100 $\mu\text{g}/\text{l}$ if the five most extreme shallow well values are removed from the dataset. Considerable uncertainties exist in the interpretation of dose-response curves relating to exposures of this magnitude. For example, Chen et al (1988) have presented detailed data for skin cancer in discrete sectors of the Taiwan 'Blackfoot area' with groundwater As concentrations of <200 $\mu\text{g}/\text{l}$, 300-600 $\mu\text{g}/\text{l}$ and >600 $\mu\text{g}/\text{l}$, and confirmed a significantly increased incidence (relative to the regional mean) in all cases. In contrast, populations exposed to As burdens of up to 150 $\mu\text{g}/\text{l}$ in New Zealand and California have been reported to exhibit no obvious adverse skin effects (Abernathy, 1993). These inconsistencies attest to the influence of numerous 'secondary' factors which, although unimportant at very high (>1 mg/l) ambient As concentrations, become critical in areas with water supply concentrations of <200 $\mu\text{g}/\text{l}$ As (equating to <10 $\mu\text{g}/\text{kg}/\text{day}$ body burden). In assessing As toxicity at Ron Phibun, it is vital that these secondary influences, including As speciation, compounding effects exerted by other trace elements, population behavioural patterns and alternative (ie. non-water) exposure pathways are evaluated. At the 'average' groundwater As concentrations recorded across much of the study region, such factors may be of fundamental importance in the derivation of a toxicologically acceptable threshold value for potable water.

The US-EPA and EC threshold of 50 $\mu\text{g}/\text{l}$ for As in potable waters is widely recognised to constitute a 'compromise' value based on (i) linear downward extrapolation of clinical and epidemiological dose-response curves for a range of human and animal diseases to a point where the incidence (per 1000 subjects) approaches the national/international background and (ii) practical attainability (with respect to cost and technical capability). The 50 $\mu\text{g}/\text{l}$ concentration is deemed to impart an acceptably low human body burden, given an average daily adult water consumption of 2 litres. This consumption rate, calculated exclusively on the basis of western behavioural patterns, could differ significantly for rural populations of

southern Thailand (and may thus warrant a re-evaluation of the maximum permissible concentration).

Chen et al. (1994) have shown that human As dose-response curves for skin cancer and hyper-pigmentation in the Blackfoot area of Taiwan are systematically steepened by the presence of reduced arsenic species in groundwater, and have proposed that international water quality guidelines should be amended to account for the inherent ten-fold difference between As(III) and As(V) toxicity. Although the speciation of As in shallow groundwaters at Ron Phibun is almost exclusively dominated by HAsO_4 phases, the presence of up to 40% H_3AsO_3 in the deeper carbonate aquifer may have important implications with regard to risk-assessment of supplies from this system. Since establishing that highest total As concentrations routinely occur in the shallow groundwater system at Ron Phibun, DMR have made concerted efforts to promote the availability of water from the deeper, less contaminated, limestone aquifer. If, however, a species-compensated comparison is made, the toxicity of deep borehole water holding 133 $\mu\text{g/l}$ at RPDW 7 (80 $\mu\text{g/l}$ As(V) and 53 $\mu\text{g/l}$ As(III)) could actually exceed that of shallow groundwaters holding over 600 $\mu\text{g/l}$ total As, but with a negligible arsenite component.

Toxicological risk assessments relating to As exposure can be further complicated by the dietary and trace nutrient status of affected subjects. For example, Zaldivar and Guillier (1977) have reported that the adverse human effects of As concentrations of c. 500 $\mu\text{g/l}$ in drinking water in Antofagasta, Chile, were significantly heightened in low socio-economic groups with insufficiently varied, nutrient deficient diets. This may reflect deficiencies of trace elements such as Se, which assist in human As de-toxification processes (Fergusson, 1990). Within the context of Ron Phibun, attempts to reduce the As burden derived from water supplies could potentially be combined with increased research to establish the nutritional ability of inhabitants to suppress the adverse effects of As exposure.

3.3 Mitigation potential

In contrast to many gold and base metal mining operations in tropical developing countries, Ron Phibun is not a typical acid mine drainage situation. Buffering over alluvial deposits and calcareous lithologies ensures that acid mine-waters are neutralised within a short distance of the primary mined area. Furthermore, dissolved Fe concentrations are low and, with the exception of As, heavy metal contamination is restricted to the acidic waters immediately draining the primary mined area. Dispersal of As is the primary environmental hazard. Given these circumstances and the mobility of As across a wide pH range, conventional methods for decontamination of mine waters through regulation of the pH regime (eg. limestone drains) are inappropriate. Physical removal and containment of the

arsenopyrite, biotic treatment systems and induced sorption techniques are more appropriate remediation techniques.

3.3.1 Physical removal of arsenopyrite waste

As discussed in section 1.4.3., mitigation measures currently employed at Ron Phibun centre on the removal of the arsenopyrite piles from the primary mined area for containment in a sealed landfill on the mid-slopes of the Ron Na-Suang Chan range. Although this measure may partly eliminate one of the potential As sources, results of this study suggest that the arsenopyrite piles may not constitute the most important source of As contamination in the area. Therefore, other remediation measures will have to be implemented to fully alleviate the problem.

3.3.2. Bioremediation

The role of microbial processes in accelerating rates of sulphide oxidation beyond the theoretical kinetic maximum has been recognised for several decades (eg. Singer and Stumm 1970). In addition, the use of *Thiobacilli* for degrading refractory ores is becoming an increasingly widespread aspect of mineral processing technology (eg. Suzuki et al 1993). Similar technology has attracted widespread interest as a possible mechanism for the rapid degradation or 'in situ' removal of sulphide waste. However, in areas of arsenical waste, the identification of microbial species which do not suffer from the effects of As toxicity has been problematic. One microbe with possible application is the arsenate reducing species MIT13. The species has been found to utilise energy from arsenopyrite oxidation and subsequent arsenate reduction. Although potentially causing increased short-term toxicity problems through the generation of arsenites, long-term hazards associated with FeAsS and arsenate wastes could potentially be solved by the carefully managed culture of MIT13 populations in affected areas such as Ron Phibun. The system has the considerable advantage that long-term imbalances to microbial populations do not occur. Once the energy source (ie arsenopyrite) is depleted, the MIT13 population dies out. Further research into the applicability of this technology at Ron Phibun is required.

3.3.3 Chemical removal

The induced precipitation of metal hydroxides, which subsequently act as heavy metal/ metalloid sorption sites, offers considerable potential for the decontamination of As polluted water at low discharge (< 2 m³ /s). In Fe-poor waters (such as prevail in the mid - lower reaches of the Hai Ron Na), synthetic oxides or resins may be utilised for sorption. The efficiency of the process is determined by the charge characteristics of the oxide/ resin surface. For the removal of oxyanions of As, positively charged surfactants are required. A predictive model based on the equilibrium-speciation model MINTEQ and a GTLM sorption code (Smith et al. 1993) facilitates prediction of gross metal/ metalloid retrieval by

the above process. The application of the model to a mine site in Colorado predicted that the precipitation of 100% Fe (total 310 mg/l) as hydrous ferric oxide would induce significant recovery of As at pH 2.0 and total recovery at pH > 6. The weakly acid - neutral pH regime encountered in waters at Ron Phibun may facilitate good recovery by this method.

4. CONCLUSIONS AND FUTURE PRIORITIES

The principal conclusions to be drawn from this study can be summarised as follows:

1. **Surface water, shallow and deep groundwater and soil As contamination presents a serious health problem in Ron Phibun. Levels of As over 500 times the WHO guideline level of 10 µg/l were recorded in waters in the area. The high incidence of skin lesions amongst the local population makes remediation of the problem a priority.**
2. **Initial investigations point to three potential sources of contamination: (i) arsenopyrite rich waste piles in the primary mining area; (ii) ore dressing plants and small scale mining by local villagers and (iii) alluvial dredging.**
3. **Previously, the 'arsenopyrite' rich waste piles had been identified as the main source of As contamination. Measures to physically remove the As piles for containment have been initiated. However, results of this study suggest that the waste piles are substantially composed of weathered secondary As minerals such as scorodite. These secondary minerals appear relatively insoluble, and the amount of As in waters draining the piles is actually quite low. Accordingly, it is hard to envisage a mechanism whereby the waste piles constitute the primary contaminant source of surface waters and groundwaters further downstream.**
4. **It is likely that the ore dressing plants, small scale mining and alluvial mining activities contribute significantly to the As problem. Further detailed investigations are required to determine the extent to which these factors affect water and soil quality in the area.**
5. **Hydrogeochemical investigations founded on a single sampling exercise are inherently limited by a failure to account for short- and long- term fluctuations of hydrology and hydrogeochemistry. While some information regarding surface and groundwater quality has been provided, both the water and soil sampling**

campaign carried out in August 1994 were limited in their spatial extent. A detailed evaluation of the pH, Eh and dissolved metal characteristics of pore-water in the waste material from the alluvial mining area; the ore dressing plants and the secondary alluvial deposits; the full extent of contaminant plumes in groundwaters and further investigations into groundwater flow paths using tracer studies should form part of a more detailed investigation. Further studies into the pathways of As in the food chain should also be carried out in close collaboration with epidemiologists in order to fully isolate the As sources.

6. In addition to the current removal and containment of the arsenopyrite piles, other potential remediation methods could include biological and chemical decontamination. The investigations proposed by DMR and BGS are of vital importance to the design, pilot testing and implementation of a full remediation programme in at Ron Phibun and should be undertaken as a matter of priority.

5. ACKNOWLEDGEMENTS

Sincere thanks are extended to the Department of Mineral Resources for the provision of local expertise, field staff, vehicles and related logistical support for the duration of fieldwork at Ron Phibun. The enthusiastic response given by Dr Gawee Permpoon and Dr Nopadon Mantajit (Deputy Director Generals, DMR) and Dr Prakmard Suwanasing (Director, Environment Division, DMR) is much appreciated by all BGS staff involved in the project. Valuable field guidance was provided by DMR staff Ms Nuchanad Juntavises, Mr Suppachai Tongnamhaen, Mr Chakawal Homwanta and Mr Chaiyaporn Lohsakul. Sincere thanks are due to Mr Apinun Suethanuwong (District Commissioner, Ron Phibun) and the Forest Service Department, Ron Phibun for facilitating access to the primary mined area and to Dr Thada Piamphongsant (Institute of Dermatology) and Dr Chanpen Choprapawon (National Epidemiological Board) for very useful epidemiological information.

6. REFERENCES

- Abernathy, C.O. 1993: Draft drinking water criteria document on arsenic. US-EPA Science Advisory Board report. Contract 68-C8-0033.
- Adriano, D.C. 1986: Trace Elements in the Terrestrial Environment. Springer Verlag.
- Alpers, C.N. and Nordstrom, D.K. 1990: Stoichiometry of mineral reactions from mass balance computations for acid waters: Iron Mountain, California. In: Gadsby, Mallick and Day (eds). Acid Mine Drainage-Designing for Closure. Bi-tech. Pub. Ltd, B.C. Canada.
- Andreae, M.O. 1986: Chemical species in seawater and marine pesticides. In: Bernhard, Brinkman and Sadler (eds). Speciation in Environmental Processes. Springer Verlag, 301-335.
- Borogno, J.M. and Greiber, R. 1972: Epidemiological study of arsenism in the city of Antofagasta. In: Hemphill, D.D. (ed). Trace Substances in Human Health V. University of Missouri, Columbia MO, 13-24.
- Borgono J.M., Venturino, H. and Vicent, P. 1980: Clinical and epidemiological study of arsenism in northern Chile. Rev. Med. Chile, 108. 1039-1048.
- Bowell, R.J. 1993: Mineralogy and geochemistry of tropical rain-forest soils., Ashanti, Ghana. Chem. Geol., 106, 345-358.
- Bowell, R.J. 1994: Sorption of arsenic by iron oxides and oxyhydroxides in soils. Applied Geochem., 9, 279-286.
- Boyle, R.W. and Jonasson, I.R. 1973: The geochemistry of arsenic and its use as an indicator element in geochemical prospecting. Journal of Geochemical Exploration, 2. 251-296.
- Breward, N. and Peachey, D. 1983: The development of a rapid scheme for the elucidation of the chemical speciation of elements in sediments. Science of the Total Environment, 29, 155-162.
- Breward, N. and Williams, T.M. 1994: Environmental geochemistry of the Bau mining area, Sarawak, Malaysia. British Geological Survey Overseas Geology Series Technical Report WC/94/67R.
- Brookins, D.G. 1988: pH-Eh Diagrams for Geochemistry. Springer Verlag.
- Buchet J.P. and Lauwerys, M.D. 1993: Inorganic arsenic metabolism in humans. In Proceedings of 1st International Conference on Arsenic Exposure and Health Effects (New Orleans, 1993). 20.
- Cebrian, M.E. Albores, A. Aquilar, M. and Blakely, E. 1983: Chronic arsenic poisoning in the north of Mexico. Human Toxicol. 2. 121-133.
- Chakraborty, A.K. and Saha, K.C. 1987: Arsenical dermatosis from tubewell water in west Bengal. Indian Jn. Med. Res. 85, 326-334.
- Chaney, R.L., Freeman, G.B., Seawright, A. and Johnson, J.B. 1993: Bioavailability of soil arsenic. In Proceedings of 1st International Conference on Arsenic Exposure and Health effects (New Orleans, 1993). 6.

Chen, C.J., Kuo, T.L. and Wu, M.M. 1988: Arsenic and cancers. *Lancet* 1 (8575/6), 414-415.

Chen, C.J. 1992: Cancer potential in liver, lung, bladder and kidney due to ingested inorganic arsenic in drinking water. *British Jn. of Cancer*, 66, 888-892.

Chen, S.L., Dzung, S.R. and Yang, M.H. 1994: Arsenic species in the Blackfoot disease area, Taiwan. *Environ. Sci. Tech.* 28, 877-881.

Cobbing, E.L., Pitfield, P.E.J., Darbyshire, D.P.F. and Mallick, D.I.J. 1992: The Granites of the South-east Asian Tin Belt. *British Geological Survey Overseas Memoir* 10. HMSO. London.

Crounce, R.G., Pories, W.J., Bray, J. T. and Mauger, R.L. 1983: Geochemistry and man: health and disease 2. Elements possibly essential, those toxic and others. In: Thornton, I. (ed) *Applied Environmental Geochemistry*. Academic Press. London. 309-330.

Davis A. and Ruby, M.V. 1993: Mineralogical constraints on the bioavailability of arsenic in smelter impacted soils. In *Proceedings of 1st International Conference on Arsenic Exposure and Health Effects (New Orleans, 1993)*. 53.

Espinoza, E. 1963: Intoxicacion colectiva por arsenico en Torreon, Coah. Mexico. 1. *Bol. Epidemiol (Mexico)*. 4. 213-220.

Farmer, J. G., and M. A. Lovell. 1986: Natural enrichment of arsenic in Loch Lomond sediments: *Geochim. et Cosmochim. Acta*, 50, 2059-2067.

Fergusson, J.E. 1990: *The Heavy Elements: Chemistry, Environmental Impact and Health Effects*. Pergamon press.

Greenwood, N.N. and Earnshaw, A. 1984: *Chemistry of the Elements*. Pergamon Press.

Mertz, W. (ed) 1987: *Trace Elements in Human and Animal Nutrition*. Academic Press Inc. London.

Nakashima, S. 1979: Selective determination of arsenic (iii) and arsenic (v) by atomic absorption spectrophotometry following arsene generation. *Analyst*, 10, 172-173.

Piamphongsant, T. and Udomnitikul, P. 1989: Arsenic levels in hair and nail samples of normal adolescents in Amphoe Ron Phiboon. *Bulletin of the Department of Medical Services (Thailand)*, 14, 225 - 229

Pierce, M.L. and Moore, C.B. 1982: Adsorption of arsenite and arsenate on amorphous iron oxides. *Water Res.* 16, 1247-1253.

Porter, E.K. and Peterson P.J. 1975: Arsenic accumulation by plants on mine waste (UK). *The Science of the Total Environment*, 4, 365-371.

Royal Society of Chemistry. 1982: *Environmental Chemistry Volume 2. Specialist Periodical Reports*. The Royal Society of Chemistry. London.

Sasieni, P. and Cuzick, J. 1993: Long-term follow-up of patients treated with medicinal arsenic. In *Proceedings of 1st International Conference on Arsenic Exposure and Health Effects (New Orleans, 1993)*. 13.

Singer, P.C. and Stumm, W. 1970: Acid mine drainage: the rate-determining step. *Science*, 142, 1121-1123.

Smith, K.S., Ficklin, W.H., Plumlee, G.S. and Mejer, A.L. 1993: Computer simulations of the influence of Fe-rich particulates on trace-metal removal from mine drainage waters. In: Plumlee and Longsdon (eds). *Reviews in Economic Geology*, Vol. 6, Society of Economic Geologists.

Suzuki, I., Chan, C.W. and Takeuchi, T.L. 1993: Oxidation of sulphide by Thiobacilli. In Alpers and Blowes (eds). *The Environmental Geochemistry of Sulphide Oxidation*. American Chemical Society, Washington DC.

Tseng, W.P., Chu, H.M., How, S.W., Fong, J.M., Lin, C.S. and Yeh, S. 1968: Prevalence of skin cancer in an endemic area of chronic arsenism in Taiwan. *J. Nat. Cancer Inst.* 40, 453-463.

Tsuji, J.S. 1993: Effects of chemical and physical form on the bioavailability of arsenic in the environment. In *Proceedings of 1st International Conference on Arsenic Exposure and Health Effects (New Orleans, 1993)*. 52.

Ure, A.M. and Berrow, M.L. 1982. The elemental constituents of soils. In *Environmental Chemistry*. Bowen, H.J.M. (ed) Royal Society of Chemistry Special Report Series. London.

US-EPA. 1993: Science Advisory Board Report. Contract 68-C8-0033.

Vahter, M.E. 1993: Species differences in the metabolism of arsenic. In *Proceedings of 1st International Conference on Arsenic Exposure and Health Effects (New Orleans, 1993)*. 19.

Van Leeuwen, F.X.R. 1993: The new WHO guideline value for arsenic in drinking water. In *Proceedings of 1st International Conference on Arsenic Exposure and Health Effects (New Orleans, 1993)*. 38.

Warren, H.V., Delavault, R.E. and Barakso, J. 1964: *Econ. Geol.*, 59, 1381.

Williams, T.M., Breward, N., Gunn, A.G. and Cummins, C. 1994: Environmental geochemistry of the Penjom Mine area, Kuala Lipis, Pahang, Malaysia: Preliminary results with particular reference to arsenic. *British Geological Survey Overseas Geology Series Technical Report WC/94/20R*.

Williams, T.M. and Smith, B. 1994: Supergene geochemistry of arsenic, antimony and associated elements at Globe Phoenix Mine, Kwekwe, Zimbabwe. *British Geological Survey Overseas Geology Series Technical Report WC/94/65R*.

Zaldivar, R. and Gullier, A. 1977: Environmental and clinical investigation of epidemic chronic arsenic poisoning in infants and children. *Zentralb. Bakteriol. Parasitenkd. Infektionskr. Hyg. Abt. 1 Orig. Reihe. B*.

APPENDIX 1. List of arsenic minerals

Mineralogy of arsenic

Environments of formation of arsenic minerals

The main primary arsenic-bearing mineral, arsenopyrite, is found in all the types of mineral deposit listed below. Other arsenic minerals which are generally of primary origin and found only in some of the deposits listed below are enargite, luzonite, tennantite, gersdorffite, nickeline, cobaltite, lollingite, orpiment and realgar:

Sn and W skarns;
exhalative Sn or replacement Sn;
W and Sn veins and Sn greisen;
porphyry Sn and Sn polymetallic veins;
Cu, Pb and Zn skarns;
Volcanic-hosted Cu-As-Sb and polymetallic veins;
Sb veins;
sedimentary exhalative Zn-Pb;
Mississippi valley type Pb-Zn;
Kipushi-type Cu-Pb-Zn;
hot spring Au-Ag and epithermal veins;
Carlin-type or carbonate-hosted Au-Ag;
Low-sulphide Au-quartz veins;
Iron-formation hosted Au;
unconformity U.

In addition to these types of mineral deposit where the arsenic occurs as essential constituents of discrete minerals, there are many types of deposit where arsenic is present in trace amounts, generally in other metal sulphides or sulpharsenides as it exhibits mostly chalcophilic character in the primary natural environment.

Deposit types with geochemically high anomalies for arsenic other than those given above (proximal unless stated):

Limassol Forest type Co-Ni;
Alaskan Platinum Group Elements;
porphyry Cu and porphyry Mo (distal);
Kuroko massive sulphide;
placer Au-Platinum Group Elements.

(using the deposit types recognized by the USGS in Cox and Singer, 1986; Bliss, 1992)

In oxidation zones of these deposits the number of minerals identified increases dramatically with a range of oxides, hydroxides, silicates, arsenites, and more than 200 arsenates. In addition arsenic can also substitute in minute amounts in many of the other minerals of such oxidation assemblages. A full list of known arsenic and arsenic-bearing mineral species is attached, those shown in bold being of most importance.

References

- Bliss, J.D. 1992, (editor) Developments in Mineral Deposit Modeling. *Bulletin of the United States Geological Survey* **2004**. 168pp.
- Cox, D.P. and Singer, D.A. 1986, (editors) Mineral Deposit Models. *Bulletin of the United States Geological Survey* **1693**. 379pp.

Mineralogy of arsenic

Elements and alloys

Arsenic

Arsenolamprite
Paxite
Koutekite
Domeykite
 β -Domeykite
Algodonite
Novakite
Kutinaite
Stibarsen
Paradocrasite

As

As
CuAs₂
Cu₅As₂
Cu₃As
Cu₃As
Cu₆As
Cu₂₀AgAs₁₀
Cu₂AgAs
AsSb
Sb₂(Sb,As)₂

Sulphides, sulpharsenides, arsenides etc

Lautite
Mgriite
Chameanite
Dervillite
Duranusite
Realgar
Pararealgar
Alacranite
Uzonite
Orpiment
Jeromite
Laphamite
Getchellite
Wakabayashilite
Paakkonenite
Lollingite
Arsenopyrite
Modderite
Safflorite
Clinosafflorite
Skutterudite
Cobaltite
Alloclasite
Glaucodot
Dienerite
Orcelite
Maucherite
Nickeline
Rammelsbergite
Pararammelsbergite
Nickel skutterudite
Oregonite
Westerveldite
Langisite
Gerardorfite
Jolliffeite
Seinajokite
Ruthenarsenite
Anduoite
Ruarsite

CuAsS
Cu₃AsSe₃
(Cu,Fe)₄As(Se,S)₅
Ag₂AsS₂
As₄S
AsS
AsS
As₈S₉
As₄S₅
As₂S₃
As(S,Se)₂
As₂(Se,S)₃
AsSbS₃
(As,Sb)₁₁S₁₈
Sb₂AsS₂
FeAs₂
FeAsS
(Co,Fe)As
(Co,Fe,Ni)As₂
(Co,Fe,Ni)As₂
(Co,Fe,Ni)As₂₋₃
CoAsS
(Co,Fe)AsS
(Co,Fe)AsS
Ni₃As
Ni_{5-x}As₂
Ni₁₁As₈
NiAs
NiAs₂
NiAs₂
NiAs₂₋₃
Ni₂FeAs₂
(Fe,Ni)As
(Co,Ni)As
NiAsS
NiAsSe
(Fe,Ni)(Sb,As)₂
(Ru,Ni)As
(Ru,Os)As₂
(Ru,Os)AsS

Cherepanovite	RhAs
Hollingworthite	(Rh,Pt,Pd)AsS
Palladoarsenide	Pd ₂ As
Stillwaterite	Pd ₈ As ₃
Atheneite	(Pd,Hg) ₃ As
Majakite	PdNiAs
Palarstanide	Pd ₈ (As,Sn) ₃
Arsenopalladinite	Pd ₈ (As,Sb) ₃
Vincentite	(Pd,Pt) ₃ (As,Sb,Te)
Palladobismutharsenide	Pd ₂ (As,Bi)
Isomertieite	Pd ₁₁ Sb ₂ As ₂
Mertieite-I	Pd ₁₁ (Sb,As) ₄
Mertieite-II	Pd ₈ (Sb,As) ₃
Sperrylite	PtAs ₂
Platarsite	(Pt,Rh,Ru)AsS
Daomanite	CuPtAsS ₂
Omeiite	(Os,Ru)As ₂
Osarsite	(OsRu)AsS
Iridarsenite	(Ir,Ru)As ₂
Irarsite	(Ir,Ru,Rh,Pt)AsS

Sulphosalts etc

Gerstleyite	Na ₄ As ₂ Sb ₈ S ₁₇ ·6H ₂ O
Sinnerite	Cu ₆ As ₄ S ₉
Tennantite	(Cu,Fe)₁₂As₄S₁₃
Goldfieldite	Cu ₁₂ (Te,Sb,As) ₄ S ₁₃
Giraudite	(Cu,Zn,Ag) ₁₂ (As,Sb) ₄ (Se,S) ₁₃
Smithite	AgAsS ₂
Trechmannite	AgAsS ₂
Proustite	Ag ₃ AsS ₃
Xanthoconite	Ag ₃ AsS ₃
Pearceite	Ag ₁₆ As ₂ S ₁₁
Arsenopolybasite	(Ag,Cu) ₁₆ (As,Sb) ₂ S ₁₁
Argentotennantite	(Ag,Cu) ₁₀ (Zn,Fe) ₂ (As,Sb) ₄ S ₁₃
Benleonardite	Ag ₈ (Sb,As)Te ₂ S ₃
Nowackiite	Cu ₆ Zn ₃ As ₄ S ₁₂
Aktashite	Cu ₆ Hg ₃ As ₄ S ₁₂
Laffittite	AgHgAsS ₃
Galkhaite	(Cs,Tl)(Hg,Cu,Zn) ₆ (As,Sb) ₄ S ₁₂
Tvalchrelizeite	Hg ₃ (Sb,As) ₂ S ₃
Lorandite	TlAsS ₂
Ellisite	Tl ₃ AsS ₃
Imhofite	Tl ₆ CuAs ₁₆ S ₄₀
Simonite	TlHgAs ₃ S ₆
Christite	TlHgAsS ₃
Routhierite	TlHgAsS ₃
Hutchinsonite	(Tl,Pb) ₂ As ₅ S ₉
Wallisite	(Cu,Ag)TlPbAs ₂ S ₅
Bernardite	Tl(As,Sb) ₅ S ₈
Vrbaite	Tl ₄ Hg ₃ Sb ₂ As ₈ S ₂₀
Rebulite	Tl ₅ Sb ₅ As ₈ S ₂₂
Gillulyite	Tl ₃ (As,Sb) ₈ S ₁₃
Pierrotite	Tl ₂ Sb ₆ As ₄ S ₁₆
Parapierrrotite	Tl(Sb,As) ₅ S ₈
Chabourmeite	(Tl,Pb) ₅ (Sb,As) ₂₁ S ₃₄
Sartorite	PbAs ₂ S ₄

Dufrenoyite
 Liveingite
 Baumhauerite
 Gratonite
 Jordanite
 Guettardite
 Twinnite
 Veenite
 Sorbyite
 Geocronite
 Kirkiite
 Seligmannite
 Marrite
 Baumhauerite-2A
 Sterryite
 Lengenbachite
 Rathite
 Hatchite
 Arsenohauchecomite
 Vozhminite
 Vincienneite
 Renierite
Enargite
Luzonite
 Arsenosulvanite
 Colusite
 Nekrasovite

$Pb_2As_2S_5$
 $Pb_9As_{13}S_{28}$
 $Pb_3As_4S_9$
 $Pb_9As_4S_{15}$
 $Pb_{14}(As,Sb)_6S_{23}$
 $Pb(Sb,As)_2S_4$
 $Pb(Sb,As)_2S_4$
 $Pb_2(Sb,As)_2S_5$
 $Pb_{17}(Sb,As)_{22}S_{50}$
 $Pb_{14}(Sb,As)_6S_{23}$
 $Pb_{10}Bi_3As_3S_{19}$
 $PbCuAsS_3$
 $PbAgAsS_3$
 $Pb_{11}Ag(As,Sb)_{18}S_{36}$
 $Pb_{10}Ag_2(Sb,As)_{12}S_{29}$
 $(Ag,Cu)_2Pb_6As_4S_{13}$
 $(Pb,II)_3As_5S_{10}$
 $(Pb,II)_2AgAs_2S_5$
 Ni_9BiAsS_8
 $(Ni,Co)_4(As,Sb)S_2$
 $Cu_{10}Fe_4Sn(As,Sb)S_{16}$
 $(Cu,Zn)_{11}(Ge,As)_2Fe_4S_{16}$
 Cu_3AsS_4
 Cu_3AsS_4
 $Cu_3(As,V)S_4$
 $Cu_{26}V_2(As,Sn,Sb)_6S_{32}$
 $Cu_{26}V_2(Sn,As,Sb)_6S_{32}$

Oxides and hydroxides

Arsenolite
 Claudetite

As_2O_3
 As_2O_3

Borates

Cahnite
 Teruggite

$Ca_2BaSO_4(OH)_4$
 $Ca_4MgB_{12}O_{20}(AsO_4)_2 \cdot 18H_2O$

Silicates

Ardennite
 Medaite
 Johnninsite
 Tiragalloite
 Dixenite
 Asbecasite
 Mergovernite
 Kraisslite
 Schallerite
 Nelenite
 Kolicite
 Parwelite
 Cervandonite-(Ce)

$Mn_4(Al,Mg)_6(SiO_4)_2(Si_3O_{10})[(As,V)O_4](OH)_6$
 $(Mn,Ca)_6(V,As)Si_5O_{18}OH$
 $Na_2Mg_4Mn_{12}As_2Si_{12}O_{43}(OH)_6$
 $Mn_4AsSi_3O_{12}(OH)$
 $CuMn_{14}Fe(AsO_3)_5(SiO_4)_2AsO_4(OH)_6$
 $Ca_3(Ti,Sn)As_6Si_2Be_2O_{20}$
 $Mn_9Mg_4Zn_2As_2Si_2O_{17}(OH)_{14}$
 $(Mn,Mg)_2Zn_4(AsO_4)_4(SiO_4)_8(OH)_{12}$
 $(Mn,Fe)_{16}Si_{12}As_3O_{36}(OH)_{17}$
 $(Mn,Fe)_{16}Si_{12}As_3O_{36}(OH)_{17}$
 $Mn_7Zn_4(AsO_4)_2(SiO_4)_2(OH)_8$
 $(Mn,Mg,Ca)_5Sb(As,Si)_2O_{12}$
 $(Ce,Nd,La)(Fe,Ti,Al)_3(Si,As)_3O_{13}$

Arsenates

Lammerite	$\text{Cu}_3[(\text{As},\text{P})\text{O}_4]_2$
Olivenite	$\text{Cu}_2\text{AsO}_4 \cdot \text{OH}$
Clinoclase	$\text{Cu}_3\text{AsO}_4(\text{OH})_3$
Cornwallite	$\text{Cu}_5(\text{AsO}_4)_2(\text{OH})_4$
Cornubite	$\text{Cu}_5(\text{AsO}_4)_2(\text{OH})_4$
Geminite	$\text{Cu}_2\text{As}_2\text{O}_7 \cdot 3\text{H}_2\text{O}$
Euchroite	$\text{Cu}_2\text{AsO}_4 \cdot \text{OH} \cdot 3\text{H}_2\text{O}$
Strashimirite	$\text{Cu}_8(\text{AsO}_4)_4(\text{OH})_4 \cdot 5\text{H}_2\text{O}$
Arhbarite	$\text{Cu}_2\text{AsO}_4(\text{OH}) \cdot 6\text{H}_2\text{O}$
Lindackerite	$\text{Cu}_5\text{H}_2(\text{AsO}_4)_4 \cdot 8\text{H}_2\text{O}$
Conichalcite	$\text{CaCuAsO}_4 \cdot \text{OH}$
Liroconite	$\text{Cu}_2\text{AlAsO}_4(\text{OH})_4$
Ceruleite	$\text{Cu}_2\text{Al}_7(\text{AsO}_4)_4(\text{OH})_{13} \cdot 11.5\text{H}_2\text{O}$
Chenevixite	$\text{Cu}_2\text{Fe}_2(\text{AsO}_4)_2(\text{OH})_4 \cdot \text{H}_2\text{O}$
Arthurite	$\text{CuFe}_2(\text{AsO}_4\text{PO}_4\text{SO}_4)_2(\text{O},\text{OH})_2 \cdot 4\text{H}_2\text{O}$
Bearsite	$\text{Be}_2\text{AsO}_4 \cdot \text{OH} \cdot 4\text{H}_2\text{O}$
Brassite	$\text{MgHAsO}_4 \cdot 4\text{H}_2\text{O}$
Roslerite	$\text{MgHAsO}_4 \cdot 7\text{H}_2\text{O}$
Homesite	$\text{Mg}_3(\text{AsO}_4)_2 \cdot 8\text{H}_2\text{O}$
Weilite	CaHAsO_4
Johnbaumite	$\text{Ca}_5(\text{AsO}_4)_3\text{OH}$
Haidingerite	$\text{CaHAsO}_4 \cdot \text{H}_2\text{O}$
Pharmacolite	$\text{CaHAsO}_4 \cdot 2\text{H}_2\text{O}$
Sainfeldite	$\text{Ca}_5\text{H}_2(\text{AsO}_4)_4 \cdot 4\text{H}_2\text{O}$
Vladimirit	$\text{Ca}_5\text{H}_2(\text{AsO}_4)_4 \cdot 5\text{H}_2\text{O}$
Guerinite	$\text{Ca}_5\text{H}_2(\text{AsO}_4)_4 \cdot 9\text{H}_2\text{O}$
Ferrarisite	$\text{Ca}_5\text{H}_2(\text{AsO}_4)_4 \cdot \text{H}_2\text{O}$
Rauenthalite	$\text{Ca}_3(\text{AsO}_4)_2 \cdot 10\text{H}_2\text{O}$
Phaunouxite	$\text{Ca}_3(\text{AsO}_4)_2 \cdot 11\text{H}_2\text{O}$
Mcnearite	$\text{NaCa}_5\text{H}_4(\text{AsO}_4)_5 \cdot 4\text{H}_2\text{O}$
Nickenichite	$\text{Na}_x\text{Ca}_y\text{Cu}_z(\text{Mg},\text{Fe},\text{Al})_3(\text{AsO}_4)_3$
Bergslagite	$\text{CaBeAsO}_4 \cdot \text{OH}$
Adelite	$\text{CaMg}(\text{AsO}_4)\text{OH}$
Talmessite	$\text{Ca}_2\text{Mg}(\text{AsO}_4)_2 \cdot 2\text{H}_2\text{O}$
Irhtemite	$\text{Ca}_4\text{MgH}_2\text{O}$
Camgasite	$\text{CaMg}(\text{AsO}_4)\text{OH} \cdot 5\text{H}_2\text{O}$
Picroparmacolite	$(\text{Ca},\text{Mg})_3(\text{AsO}_4)_2 \cdot 6\text{H}_2\text{O}$
Barium-pharmacosiderite	$\text{BaFe}_8(\text{AsO}_4)_6(\text{OH})_8 \cdot 14\text{H}_2\text{O}$
Adamite	$\text{Zn}_2\text{AsO}_4(\text{OH})$
Paradamite	$\text{Zn}_2\text{AsO}_4(\text{OH})$
Koritnigite	$\text{ZnHAsO}_4 \cdot \text{H}_2\text{O}$
Legrandite	$\text{Zn}_2\text{AsO}_4(\text{OH}) \cdot \text{H}_2\text{O}$
Warikahnite	$\text{Zn}_3(\text{AsO}_4)_2 \cdot 2\text{H}_2\text{O}$
Kottigite	$\text{Zn}_3(\text{AsO}_4)_2 \cdot 8\text{H}_2\text{O}$
Stranskiite	$(\text{Zn},\text{Cu})_3(\text{AsO}_4)_2$
Philipsburgite	$(\text{Cu},\text{Zn})_6(\text{As},\text{P})\text{O}_4)_2(\text{OH})_6 \cdot \text{H}_2\text{O}$
Austinite	$\text{CaZn}(\text{AsO}_4)\text{OH}$
Prosperite	$\text{HCaZn}_2(\text{AsO}_4)_2\text{OH}$
Gaitite	$\text{Ca}_2\text{Zn}(\text{AsO}_4)_2 \cdot 2\text{H}_2\text{O}$
Zincroselite	$\text{Ca}_2\text{Zn}(\text{AsO}_4)_2 \cdot 2\text{H}_2\text{O}$
O'Danielite	$\text{Na}(\text{Zn},\text{Mg})_3\text{H}_2(\text{AsO}_4)_3$
Johillerite	$\text{Na}(\text{Mg},\text{Zn})_3\text{Cu}(\text{AsO}_4)_3$
Holdenite	$(\text{Mn},\text{Mg})_6\text{Zn}_3(\text{AsO}_4)_2(\text{SiO}_4)(\text{OH})_8$
Chudobaite	$(\text{Na},\text{K})(\text{Mg},\text{Zn})_2\text{H}(\text{AsO}_4)_2 \cdot 4\text{H}_2\text{O}$

Chlorophoenicite	$(\text{Mn,Mg})_3\text{Zn}_2(\text{AsO}_4)(\text{OH},\text{O})_6$
Lotharmeyerite	$\text{CaMnZn}(\text{AsO}_4)_2\text{OH}\cdot 2\text{H}_2\text{O}$
Metakottigite	$(\text{Zn,Fe})_3(\text{AsO}_4)_2\cdot 8(\text{H}_2\text{O},\text{OH})$
Ojuelaite	$\text{ZnFe}_2(\text{AsO}_4)_2(\text{OH})_2\cdot 4\text{H}_2\text{O}$
Fahleite	$\text{Zn}_5\text{CaFe}_2(\text{AsO}_4)_6\cdot 14\text{H}_2\text{O}$
Keyite	$(\text{Cu,Zn,Cd})_3(\text{AsO}_4)_2$
Chursinite	Hg_2AsO_4
Mansfieldite	$\text{AlAsO}_4\cdot 2\text{H}_2\text{O}$
Bulachite	$\text{Al}_2\text{AsO}_4(\text{OH})_3\cdot 3\text{H}_2\text{O}$
Alumopharmacosiderite	$\text{KAl}_4(\text{AsO}_4)_3(\text{OH})_4\cdot 6.5\text{H}_2\text{O}$
Luetheite	$\text{Cu}_2\text{Al}_2(\text{AsO}_4)_2(\text{OH})_4\cdot \text{H}_2\text{O}$
Arsenogoyazite	$\text{SrAl}_3(\text{AsO}_4)_2(\text{OH})_5\cdot \text{H}_2\text{O}$
Arsenocrandallite	$(\text{Ca,Sr})\text{Al}_3(\text{As,P})\text{O}_4(\text{OH})_5\cdot \text{H}_2\text{O}$
Arsenoflorencite-(Ce,Nd,La)	$(\text{Ce,La,Nd})\text{Al}_3(\text{AsO}_4)_2(\text{PO}_4)(\text{OH})_6$
Gerdremmelite	$(\text{Zn,Fe})(\text{AlFe})_2\text{AsO}_4(\text{OH})_5$
Gasparite-(Ce)	$(\text{Ce,REE})\text{AsO}_4$
Chernovite-(Y)	YAsO_4
Agardite-(Y,La)	$(\text{Y,La,Ca})\text{Cu}_6(\text{AsO}_4)_3(\text{OH})_6\cdot 3\text{H}_2\text{O}$
Goudeyite	$\text{Cu}_6(\text{Al,Y})(\text{AsO}_4)_3(\text{OH})_6\cdot 3\text{H}_2\text{O}$
Retzian-(Ce,La,Nd)	$\text{Mn}_2(\text{Ce,La,Nd})\text{AsO}_4(\text{OH})_4$
Cafarsite	$\text{Ca}_8(\text{Ti,Fe,Mn})_6\cdot 7(\text{AsO}_4)_3\cdot 12\cdot 4\text{H}_2\text{O}$
Schultenite	PbHAsO_4
Duftite	$\text{PbCuAsO}_4\text{OH}$
Bayldonite	$\text{Cu}_3\text{Pb}(\text{AsO}_4)_2(\text{OH})_2$
Philipsbornite	$\text{PbAl}_3(\text{AsO}_4)_2(\text{OH})_5\cdot \text{H}_2\text{O}$
Arsendescloizite	$\text{PbZbAsO}_4\text{OH}$
Helmutwinklerite	$\text{PbZb}_2(\text{AsO}_4)_2\cdot 2\text{H}_2\text{O}$
Thometzekite	$\text{Pb}(\text{Cu,Zn})_2(\text{AsO}_4)_2\cdot 2\text{H}_2\text{O}$
Caryinite	$(\text{Ca,Na,Pb})_3(\text{Mn,Mg,Fe})_4(\text{AsO}_4)_4$
Ludlockite	$(\text{Fe,Pb})\text{As}_2\text{O}_6$
Gabrielsonite	$\text{PbFeAsO}_4\text{OH}$
Carminite	$\text{PbFe}(\text{AsO}_4)_2(\text{OH})_2$
Segnitite	$\text{PbFe}_3\text{H}(\text{AsO}_4)_2(\text{OH})_6$
Tsumconite	$\text{PbZnFe}(\text{AsO}_4)_2\cdot \text{H}_2\text{O}$
Jamesite	$\text{Pb}_2\text{Zn}_2\text{Fe}_5(\text{AsO}_4)_5\text{O}_4$
Mawbyite	$\text{Pb}(\text{Fe}_{1.5}\text{Zn}_{0.5})(\text{AsO}_4)_2(\text{OH})_{1.5}(\text{H}_2\text{O})_{0.5}$
Arsenbrackebuschite	$\text{Pb}_2(\text{Fe,Zn})(\text{AsO}_4)_2\cdot \text{H}_2\text{O}$
Rooseveltite	BiAsO_4
Preisingerite	$\text{Bi}_3(\text{AsO}_4)_2\text{O}(\text{OH})$
Arsenobismite	$\text{Bi}_2\text{AsO}_4(\text{OH})_3$
Atelestite	$\text{Bi}_8(\text{AsO}_4)_3\text{O}_5(\text{OH})_5$
Mixite	$\text{BiCu}_6(\text{AsO}_4)_3(\text{OH})_6\cdot 3\text{H}_2\text{O}$
Walpurgite	$(\text{BiO})_4\text{UO}_2(\text{AsO}_4)_2\cdot \text{H}_2\text{O}$
Trogerite	$(\text{UO}_2)_3(\text{AsO}_4)_2\cdot 12\text{H}_2\text{O}$
Sodium-uranospinite	$(\text{Na}_2\text{Ca})(\text{UO}_2)_2(\text{AsO}_4)_2\cdot 5\text{H}_2\text{O}$
Abernathyite	$\text{K}(\text{UO}_2\text{AsO}_4)\cdot 4\text{H}_2\text{O}$
Metazeunerite	$\text{Cu}(\text{UO}_2)_2(\text{AsO}_4)_2\cdot 8\text{H}_2\text{O}$
Zeunerite	$\text{Cu}(\text{UO}_2)_2(\text{AsO}_4)_2\cdot 10\text{-}16\text{H}_2\text{O}$
Metanovacekite	$\text{Mg}(\text{UO}_2)_2(\text{AsO}_4)_2\cdot 4\text{-}8\text{H}_2\text{O}$
Novacekite	$\text{Mg}(\text{UO}_2)_2(\text{AsO}_4)_2\cdot 12\text{H}_2\text{O}$
Arsenuranylite	$\text{Ca}(\text{UO}_2)_4(\text{AsO}_4)(\text{OH})_4\cdot 6\text{H}_2\text{O}$
Metauranospinite	$\text{Ca}(\text{UO}_2)(\text{AsO}_4)_2\cdot 8\text{H}_2\text{O}$
Uranospinite	$\text{Ca}(\text{UO}_2)(\text{AsO}_4)_2\cdot 10\text{H}_2\text{O}$
Metaheinrichite	$\text{Ba}(\text{UO}_2)_2(\text{AsO}_4)_2\cdot 8\text{H}_2\text{O}$

Heinrichite $\text{Ba}(\text{UO}_2)_2(\text{AsO}_4)_2 \cdot 10\text{-}12\text{H}_2\text{O}$
 Metalodevite $\text{Zn}(\text{UO}_2)(\text{AsO}_4) \cdot 2\text{H}_2\text{O}$
 Arsenuranospathite $\text{HAl}(\text{UO}_2)_4(\text{AsO}_4)_4 \cdot 40\text{H}_2\text{O}$
 Hallimondite $\text{Pb}_2\text{UO}_2(\text{AsO}_4)_2$
 Hugelite $\text{Pb}_2(\text{UO}_2)_3(\text{AsO}_4)_2(\text{OH})_4 \cdot 5\text{H}_2\text{O}$
 Asselbornite $(\text{Pb},\text{Ba})(\text{UO}_2)_6(\text{BiO}_4)[(\text{As},\text{P})\text{O}_4]_2(\text{OH})_{12} \cdot 3\text{H}_2\text{O}$
 Metakahlerite $\text{Fe}(\text{UO}_2)_2(\text{AsO}_4)_2 \cdot 8\text{H}_2\text{O}$
 Kahlerite $\text{Fe}(\text{UO}_2)_2(\text{AsO}_4)_2 \cdot 12\text{H}_2\text{O}$
 Metakirchheimerite $\text{Co}(\text{UO}_2)_2(\text{AsO}_4)_2 \cdot 8\text{H}_2\text{O}$

Sarkinite $\text{Mn}_2\text{AsO}_4\text{OH}$
 Eveite $\text{Mn}_2\text{AsO}_4\text{OH}$
 Arsenoclasite $\text{Mn}_5(\text{AsO}_4)_2(\text{OH})_4$
 Flinkite $\text{Mn}_3\text{AsO}_4(\text{OH})_4$
 Jarosewichite $\text{Mn}_3\text{AsO}_4(\text{OH})_6$
 Allactite $\text{Mn}_7(\text{AsO}_4)_2(\text{OH})_8$
 Krautite $\text{MnHAsO}_4 \cdot \text{H}_2\text{O}$
 Synadelphite $\text{Mn}_9(\text{AsO}_3)(\text{AsO}_4)_2(\text{OH})_9 \cdot 2\text{H}_2\text{O}$
 Sterlinghillite $\text{Mn}_3(\text{AsO}_4)_2 \cdot 4\text{H}_2\text{O}$
 Geigerite $\text{Mn}_5(\text{AsO}_4)_2(\text{AsO}_3\text{OH})_2 \cdot 10\text{H}_2\text{O}$
 Akrochordite $\text{Mn}_4\text{Mg}(\text{AsO}_4)_2(\text{OH})_4 \cdot 4\text{H}_2\text{O}$
 Manganese-hornesite $(\text{Mn},\text{Mg})_3(\text{AsO}_4)_2 \cdot 8\text{H}_2\text{O}$
 Fluckite $\text{CaMnH}_2(\text{AsO}_4)_2 \cdot 2\text{H}_2\text{O}$
 Brandite $\text{Ca}_2(\text{Mn},\text{Mg})(\text{AsO}_4)_2 \cdot 2\text{H}_2\text{O}$
 Parabrandite $\text{Ca}_2\text{Mn}(\text{AsO}_4)_2 \cdot 2\text{H}_2\text{O}$
 Wallkilldellite $\text{Ca}_2\text{Mn}_3(\text{AsO}_4)_2(\text{OH})_4 \cdot 9\text{H}_2\text{O}$
 Berzeliite $(\text{Ca},\text{Na})_3(\text{Mg},\text{Mn})_2(\text{AsO}_4)_3$
 Manganberzeliite $(\text{Ca},\text{Na})_3(\text{Mn},\text{Mg})_2(\text{AsO}_4)_3$
 Magnesium-chlorophoenicite $(\text{Mg},\text{Mn})_3\text{Zn}_2(\text{AsO}_4)(\text{OH},\text{O})_6$
 Villyaellenite $(\text{Mn},\text{Ca},\text{Zn})_5(\text{AsO}_4)_2[\text{AsO}_3(\text{OH})]_2 \cdot 4\text{H}_2\text{O}$
 Hematolite $(\text{Mn},\text{Mg},\text{Al})_{15}(\text{AsO}_3)(\text{AsO}_4)_2(\text{OH})_{23}$
 Grischunite $(\text{Ca},\text{Na})(\text{Mn},\text{Fe})_2(\text{AsO}_4)_2$

Angelellite $\text{Fe}_4\text{As}_2\text{O}_{11}$
Scorodite **$\text{FeAsO}_4 \cdot 2\text{H}_2\text{O}$**
 Kankite $\text{FeAsO}_4 \cdot 3.5\text{H}_2\text{O}$
 Ferrisymplectite $\text{Fe}_3(\text{AsO}_4)_2(\text{OH})_3 \cdot 5\text{H}_2\text{O}$
 Kaatialaite $\text{Fe}(\text{H}_2\text{AsO}_4)_3 \cdot 5\text{H}_2\text{O}$
 Symplectite $\text{Fe}_3(\text{AsO}_4)_2 \cdot 8\text{H}_2\text{O}$
 Parasymplectite $\text{Fe}_3(\text{AsO}_4)_2 \cdot 8\text{H}_2\text{O}$
 Sodium-pharmacosiderite $(\text{Na},\text{K})_2\text{Fe}_4(\text{AsO}_4)_3(\text{OH})_4 \cdot 7\text{H}_2\text{O}$
 Pharmacosiderite $\text{KFe}_4(\text{AsO}_4)_3(\text{OH})_4 \cdot 6\text{-}7\text{H}_2\text{O}$
 Kolfanite $\text{Ca}_2\text{Fe}_2(\text{AsO}_4)_3\text{O}_2 \cdot 2\text{H}_2\text{O}$
 Arseniosiderite $\text{Ca}_3\text{Fe}_4(\text{AsO}_4)_4(\text{OH})_6 \cdot 3\text{H}_2\text{O}$
 Yukonite $(\text{Cu}_3,\text{Fe}_2)_2(\text{AsO}_4)_2(\text{OH})_6 \cdot 5\text{H}_2\text{O}$
 Dussertite $\text{BaFe}_3(\text{AsO}_4)_2(\text{OH})_5$
 Liskardite $(\text{Al},\text{Fe})_3\text{AsO}_4(\text{OH})_6 \cdot 5\text{H}_2\text{O}$
 Mapimite $\text{Zn}_2\text{Fe}_3(\text{AsO}_4)_3(\text{OH})_4 \cdot 10\text{H}_2\text{O}$
 Ogdensbergite $\text{Ca}_2\text{Fe}_4(\text{Zn},\text{Mn})(\text{AsO}_4)_4(\text{OH})_6 \cdot 6\text{H}_2\text{O}$
 Walentaite $\text{H}(\text{Ca},\text{Mn},\text{Fe})\text{Fe}_3(\text{AsO}_4)_4\text{PO}_4 \cdot 7\text{H}_2\text{O}$

Erythrite **$\text{Co}_3(\text{AsO}_4)_2 \cdot 8\text{H}_2\text{O}$**
 Cobaltaustinitite $\text{CaCoAsO}_4(\text{OH})$
 Roselite $\text{Ca}_2(\text{Co},\text{Mg})(\text{AsO}_4)_2 \cdot 2\text{H}_2\text{O}$
 β -Roselite $\text{Ca}_2(\text{Co},\text{Mg})(\text{AsO}_4)_2 \cdot 2\text{H}_2\text{O}$
 Wendwilsonite $\text{Ca}_2(\text{Mg},\text{Co})(\text{AsO}_4)_2 \cdot 2\text{H}_2\text{O}$
 Cobaltkoritnigite $(\text{Co},\text{Zn})(\text{AsO}_3)(\text{OH}) \cdot \text{H}_2\text{O}$
 Aerugite $\text{Ni}_9\text{As}_3\text{O}_{16}$

Xanthiosite	$\text{Ni}_3(\text{AsO}_4)_2$
Annabergite	$\text{Ni}_3(\text{AsO}_4)_2 \cdot 8\text{H}_2\text{O}$
Smolyaninovite	$(\text{Co}, \text{Ni}, \text{Mg}, \text{Ca})_2(\text{Fe}, \text{Al})(\text{AsO}_4)_2(\text{OH}) \cdot 5\text{H}_2\text{O}$
Nickelaustinite	$\text{Ca}(\text{Ni}, \text{Zn})\text{AsO}_4\text{OH}$

Vanadates

Schumacherite	$\text{Bi}_3[(\text{V}, \text{As}, \text{P})\text{O}_4]_2\text{O}(\text{OH})$
Santafeite	$\text{NaMn}_3(\text{Ca}, \text{Sr})(\text{V}, \text{As})_3\text{O}_{13} \cdot 4\text{H}_2\text{O}$

Arsenates with other anions

Maxwellite	$\text{NaFe}(\text{AsO}_4)\text{F}$
Svabite	$\text{Ca}_5(\text{AsO}_4)_3(\text{F}, \text{Cl}, \text{OH})$
Tilasite	$\text{CaMgAsO}_4\text{F}$
Fermorite	$(\text{Ca}, \text{Sr})_5[(\text{P}, \text{As})\text{O}_4]_3(\text{F}, \text{OH})$
Durangite	$\text{NaAlAsO}_4\text{F}$
Lavendulan	$\text{NaCaCu}_5(\text{AsO}_4)_4\text{Cl} \cdot 5\text{H}_2\text{O}$
Turneauroite	$\text{Ca}_5[(\text{As}, \text{P})\text{O}_4]_3\text{Cl}$
Shubnikovite	$\text{Ca}_2\text{Cu}_8(\text{AsO}_4)_6\text{ClOH} \cdot 7\text{H}_2\text{O}$
Richelsdorffite	$\text{Ca}_2\text{Cu}_5\text{Sb}(\text{AsO}_4)_4(\text{OH})_6\text{Cl} \cdot 6\text{H}_2\text{O}$
Morelandite	$(\text{Ba}, \text{Ca}, \text{Pb})_5(\text{AsO}_4)_4\text{PO}_4\text{Cl}$
Mimetite	$\text{Pb}_5(\text{AsO}_4)_3\text{Cl}$
Clinomimetite	$\text{Pb}_5(\text{AsO}_4)_3\text{Cl}$
Sahlinite	$\text{Pb}_{14}(\text{AsO}_4)_2\text{O}_9\text{Cl}_4$
Georgiadesite	$\text{Pb}_{16}(\text{AsO}_4)_4\text{Cl}_{14}(\text{OH})_6$
Hedyphane	$\text{Pb}_3\text{Ca}_2(\text{AsO}_4)_3\text{Cl}$
Nealite	$\text{Pb}_4\text{Fe}(\text{AsO}_4)_2\text{Cl}_4$
Parnauite	$\text{Cu}_6(\text{AsO}_4)_2\text{SO}_4(\text{OH})_{10} \cdot 7\text{H}_2\text{O}$
Machatschkiite	$(\text{Ca}, \text{Na})_6\text{AsO}_4(\text{AsO}_3\text{OH})_3\text{PO}_4\text{SO}_4 \cdot 15\text{H}_2\text{O}$
Clinotyrolite	$\text{Cu}_9\text{Ca}_2(\text{As}, \text{S})\text{O}_4(\text{OH}, \text{O})_{10} \cdot 10\text{H}_2\text{O}$
Chalcopyllite	$\text{Cu}_{18}\text{Al}_2(\text{AsO}_4)_3(\text{SO}_4)_3(\text{OH})_{27} \cdot 33\text{H}_2\text{O}$
Schlossmacherite	$(\text{H}_3\text{O}, \text{Ca})\text{Al}_3\text{SO}_4\text{AsO}_4(\text{OH})_6$
Kemmlitzite	$(\text{Sr}, \text{Ce})\text{Al}_3\text{AsO}_4\text{SO}_4(\text{OH})_6$
Weilerite	$\text{BaAl}_3\text{AsO}_4\text{SO}_4(\text{OH})_6$
Arsentsumebite	$\text{Pb}_2\text{Cu}(\text{AsO}_4)(\text{SO}_4)\text{OH}$
Hidalgoite	$\text{PbAl}_3\text{AsO}_4\text{SO}_4(\text{OH})_6$
Beudantite	$\text{PbFe}_3(\text{AsO}_4)(\text{SO}_4)(\text{OH})_6$
Sarmientite	$\text{Fe}_2\text{AsO}_4\text{SO}_4 \cdot \text{H}_2\text{O}$
Bukovskiyite	$\text{Fe}_2(\text{AsO}_4)(\text{SO}_4)\text{OH} \cdot 7\text{H}_2\text{O}$
Zykaite	$\text{Fe}_4(\text{AsO}_4)_3\text{SO}_4\text{OH} \cdot 15\text{H}_2\text{O}$
Tooeleite	$\text{Fe}_{8-2x}[(\text{As}_{1-x}\text{S}_x)\text{O}_{3+x}(\text{OH})_{1-x}]_6(\text{OH})_{12}$
Pitticite	<i>Arsenate and sulphate of iron</i>
Tyrolite	$\text{CaCu}_5(\text{AsO}_4)_2\text{CO}_3(\text{OH})_4 \cdot 6\text{H}_2\text{O}$
Gartrellite	$\text{Pb}(\text{Cu}, \text{Fe})_2(\text{AsO}_4)_2\text{SO}_4(\text{CO}_3 \cdot \text{H}_2\text{O})_{0.7}$
Fornacite	$\text{Pb}_2\text{CuCrO}_4(\text{As}, \text{P})\text{O}_4\text{OH}$
Molybdoformacite	$\text{Pb}_2\text{CuOH}(\text{As}, \text{P})\text{O}_4(\text{Mo}, \text{Cr})\text{O}_4$
Betpakdalite	$\text{KCa}_2\text{Fe}_3\text{As}_2\text{Mo}_8\text{O}_{36}(\text{OH})_2$
Sodium betpakdalite	$(\text{Na}_2\text{Ca})\text{Fe}_2(\text{As}_2\text{Mo}_6\text{O}_{28}) \cdot 15\text{H}_2\text{O}$
Obradovicite	$\text{H}_4(\text{K}, \text{Na})\text{CuFe}_2\text{AsO}_4(\text{MoO}_4)_5 \cdot 12\text{H}_2\text{O}$

Arsenites

Trippkeite	CuAs_2O_4
Nanlingite	$\text{CaMg}_4(\text{AsO}_3)_2\text{F}_4$
Leiteite	ZnAs_2O_4
Reinerite	$\text{Zn}_3(\text{AsO}_3)_2$

Kuznetsovite	$\text{Hg}_6\text{As}_2\text{Cl}_2\text{O}_9$
Paulmooreite	$\text{Pb}_2\text{As}_2\text{O}_5$
Ekdemite	$\text{Pb}_6\text{As}_2\text{O}_7\text{Cl}_4$
Heliophyllite	$\text{Pb}_6\text{As}_2\text{O}_7\text{Cl}_4$
Finnemanite	$\text{Pb}_5(\text{AsO}_3)_3\text{Cl}$
Gebhardtite	$\text{Pb}_8(\text{As}_2\text{O}_5)_2\text{OCl}_6$
Zimbabweite	$(\text{Na,K})_2\text{PbAs}_4(\text{Ta,Nb,Ti})_4\text{O}_{18}$
Trigonite	$\text{Pb}_3\text{MnH}(\text{AsO}_3)_3$
Rouseite	$\text{Pb}_2\text{Mn}(\text{AsO}_3)_2 \cdot 2\text{H}_2\text{O}$
Freedite	$\text{Pb}_{15}(\text{Cu,Fe})_3\text{As}_4\text{O}_{19}\text{Cl}_{10}$
Manganarsite	$\text{Mn}_3\text{As}_2\text{O}_4(\text{OH})_4$
Magnussonite	$\text{Mn}_5\text{As}_3\text{O}_9(\text{OH,Cl})$
Armangite	$\text{Mn}_{26}\text{As}_{18}\text{O}_{50}(\text{OH})_4(\text{CO}_3)$
Karibibite	$\text{Fe}_2\text{As}_4\text{O}_9$
Schneiderhohnite	$\text{Fe}_4\text{As}_5\text{O}_{13}$
Lazarenkoite	$(\text{Ca,Fe})\text{FeAs}_3\text{O}_7 \cdot 3\text{H}_2\text{O}$
Stenhuggarite	$\text{CaFeSbO}(\text{AsO}_3)_2$
Tomichite	$(\text{V,Fe})_4\text{Ti}_3\text{AsO}_{13}\text{OH}$

Antimonates and antimonites

Theisite	$\text{Cu}_5\text{Zn}_5(\text{As,Sb}_2\text{O}_8(\text{OH}))_{14}$
Hemloite	$(\text{As,Sb})_2(\text{Ti,V,Fe,Al})_{12}\text{O}_{23}\text{OH}$
Thorikosite	$\text{Pb}_3(\text{Sb,As})\text{O}_3(\text{OH})\text{Cl}_2$
Manganostibite	$(\text{Mn,Fe})_7\text{SbAsO}_{12}$

Tellurate

Dugganite	$\text{Pb}_3\text{Zn}_3(\text{TeO}_6)_x(\text{AsO}_4)_{2-x}(\text{OH})_{6-3x}$
-----------	--